Quantitative controls on the routing of supraglacial meltwater to the bed of glaciers and ice sheets

Caroline Clason

BSc (hons) Geography and Environmental Science, University of Dundee

April 2012

A thesis presented for the degree of Doctor of Philosophy (Geography)
at the University of Aberdeen

Author's declaration

I declare that this thesis has been composed by myself, and that it has not been accepted in any other application for a degree. The work has been done by myself, with contributions from Dave Burgess, Martin Sharp and Julian Dowdeswell who provided data for the Croker Bay catchment of Devon Ice Cap, and from Ian Bartholomew, Andrew Sole, Steven Palmer and Ian Joughin, who provided data sets with which to run the model for Leverett Glacier in Greenland. Wolfgang Schwanghart contributed towards one component of the modelling routine, and all other model development and data analyses were carried out by me alone. Chapter 4 of this thesis has been published in a peer-reviewed Journal, and chapter 5 has been submitted as a manuscript. I hereby acknowledge contributions from my co-authors towards these manuscripts. All quotations have been distinguished by quotation marks and the sources of information specifically acknowledged.

Caroline Clason, 13th February 2012

Summary

The influence of seasonal influx of supraglacial meltwater on basal water pressures and consequent changes in ice surface velocity has been a focus of research spanning over three decades, particularly focussing on alpine glaciers. Now, with increased recognition for a need to better include glacial hydrology within models of ice dynamics and ice sheet evolution, the ability to predict where and when meltwater is delivered to the subglacial system is paramount, both for understanding the dynamics of alpine glaciers, and of large Arctic ice masses. Studies of the dynamics of outlet glaciers on the Greenland Ice Sheet have received particular attention in recent years, as links between ice acceleration and increased surface melt production are explored. Responses of horizontal and vertical ice velocities to meltwater generated suggest efficient transmission of meltwater from the supraglacial to subglacial hydrological systems. Indeed, in the case of meltwater transfer through the drainage of supraglacial lakes, it has been shown that such build-ups of stored meltwater can force crevasse penetration through many hundreds of metres of ice. This thesis presents a new modelling routine for the prediction of moulin formation and delivery of meltwater to the ice-bed interface. Temporal and spatial patterns of moulin formation through propagation of crevasses and drainage of supraglacial lakes are presented, and quantitative controls on water-driven crevasse propagation are investigated through a series of sensitivity tests.

The model is applied to two glacial catchments: the Croker Bay catchment of Devon Ice Cap in High Arctic Canada; and Leverett Glacier catchment of the southwest Greenland Ice Sheet. Through model application to these sites, sensitivities to crevasse surface dimensions, ice tensile strength, ice fracture toughness and enhanced production of surface meltwater are investigated. Model predictions of moulin formation are compared with field observations and remotely sensed data, including ice surface velocities, dynamic flow regimes, and visible surface features. Additionally, model quantification of meltwater delivered to the ice-bed interface of Leverett Glacier is compared with profiles of measured proglacial discharge. Moulin formation is predicted at increasingly high elevation with time into the ablation season in both

catchments, and furthermore, the model predicts an increase in both the number of moulins and the number of lake drainages in response to increased melt scenarios. Sensitivity testing confirms that the model is most sensitive to factors influencing the rate at which meltwater fills a crevasse, and results highlight the importance of accurate parameterisation of crevasse surface dimensions and the tensile strength of the ice.

Further applications of the model are discussed, with a focus on incorporation into coupled models of glacial hydrology and dynamics, including larger scale ice sheet modelling. The inclusion of spatially distributed points of temporally varying meltwater delivery to the subglacial system is imperative to fully understand the behaviour of the subglacial drainage system. Furthermore, dynamic response to future climatic change and increased melt scenarios, and the consequent evolution of ice masses, including those in the Canadian Arctic and Greenland, cannot be fully understood without first understanding the glacial hydrological processes driving many of these changes.

Acknowledgements

Completing the research for this thesis, particularly during its final stages, has been a challenge in many respects. Without the support of those whom I acknowledge below, this task would have been infinitely more difficult.

Firstly, I wish to thank my principal supervisor, Doug Mair, for his advice, endless flow of good ideas, and for giving me support when I needed it. His initial thoughts on this project helped to steer the direction that my research took, whilst he was consistently supportive in the decisions I made on expanding and communicating my work. Pete Nienow, in his capacity as second supervisor, has also contributed notably to the project, particularly with regards to in-field observations in Greenland, and has provided valuable advice on communicating this work through presentations and within papers. In addition to my supervisors, I have appreciated the advice and support of a number of my academic colleagues and fellow researchers, including Brice Rea, Kevin Edwards, Al Gemmell, Matteo Spagnolo, Ed Schofield, Nick Spedding and Lorna Philip at the University of Aberdeen, who have also provided a friendly and supportive atmosphere during my time there. I would like to thank my examiners, Rob Bingham and Neil Arnold, for making my PhD viva a pleasant experience, and for their words of encouragement on furthering my research.

On travelling to Simon Fraser University for the 3rd year of my research, I was welcomed by and enjoyed the company of all members of the glaciology research group and of other staff and students. Notably, Mauro Werder has been a good friend and wonderful help in all matters 'Matlab', whilst Gwenn Flowers was the best support I could have hoped for, both personally and professionally, and I really cannot thank her enough. Additionally, I would like to thank Dave Burgess, Wolfgang Schwanghart and Christian Schoof for their valued input to this research, to Andrew Sole and Ian Bartholomew for their much appreciated data contributions to this research, and to John Clague for his time, thoughts and advice on the crazy world of academia. Furthermore, I would like to acknowledge the financial support of the University of

Aberdeen, College of Physical Sciences, and the Leverhulme Trust for providing me with funding to conduct my 3rd year of research in Canada. I would like to thank Jean Cater for her much appreciated help in organising this trip.

In addition to the academic staff from whom I have had support, I would like to note my full appreciation for the technical and administrative staff who have made this journey run as smoothly as possible, and have been a source of friendship, including, but not limited to, Jackie Brown, Rona Kennedy, Kim Paterson, Alison Sandison, Matthew Norrie, Matt Plotnikoff and Glenda Pauls. Furthermore, I would not have made it this far without the inspiration provided by John Martindale at Larbert High School, and Ben Brock and Martin Kirkbride at Dundee University, who have turned me into the geography geek I am today. Of all the people I wish to thank, perhaps the most important are my friends, without whom I would be a miserable, unsociable, academic lost-cause by now. Angela Curl, Marie Porter, Sue Heard, Kate Pangbourne, Ed Loffill, Nicky Millar, Michael Woods, Graeme Brown, Matthiew Sturzenegger, Corinne Griffing and Dan Shugar all deserve some particularly big shout outs. But, I thank all of my fellow students and friends at Aberdeen, Dundee and SFU, who really have enhanced my enjoyment of my time as a student, with all its highs and lows. I especially wish to thank Peter Schön for his patience, encouragement, for providing me with a reason to have a work desk in many different countries, and for seeing through the most difficult time. I also thank I thank Monika and Jürgen Schön for their hospitality, good company and for always making me feel welcome.

My family have been of constant encouragement throughout my studies, and never more so than during the years of my PhD research. I thank my Mum and sister for their love, for being my shoulders to cry on, putting up with my frustrations, and for making me laugh in the limited time I've spent at home recently, and also thank my Dad and Deborah for their love, support and patience, for being a great source of fun, and perhaps most importantly, for providing a good 'local' in Wales! My Gran, Grandad and Auntie Christine have also always been very good to me, and make coming home to visit even more enjoyable. I especially appreciate the supply of carrot cake... Finally, I want to thank my uncle, John Wilson, who was always supportive, without exception,

of whatever I wanted to do with my life, and who is missed so very much. This thesis is dedicated to him.

Table of contents

List of figures

List of tables

Chapter 1. Introduction

1.1 Glacial response to a changing climate

Anthropogenic climatic warming of today is likely to be directly influencing the mass loss of ice globally, and improving our understanding of the mechanisms by which mass loss occurs is imperative if we are to predict how climatic warming of the future will influence the evolution of global land ice. Indeed, highlighting the importance of this, Chapter 4 of "Climate Change 2007: The Physical Science Basis" (IPCC 2007, Chapter 4, pg 377) concludes,

> *"The geographically widespread nature of these snow and ice changes suggests that widespread warming is the cause of the Earth's overall loss of ice."*

Ablation processes such as direct runoff and calving are well established within scientific literature and are known to contribute directly to mass loss. We do not yet fully understand the extent to which meltwater accessing the beds of ice sheets and glaciers can enhance ice velocities, and hence, contribute to the mass loss of glaciated areas. Zwally et al. (2002) initiated debate regarding the significance of this for the Greenland Ice Sheet (GrIS) when they presented data to support a correlation between increased surface melting and ice acceleration at an area of the west-central GrIS. The proposed mechanism for the observed velocity response to changes in meltwater production was a direct coupling between the hydrology on the ice surface and at the bed, via moulins or fully-propagated crevasses. This is a process that has also been used previously to explain spring and summer speed-up on Alpine valley glaciers (Iken & Bindschadler, 1986; Hooke et al., 1989; Mair et al., 2001). Supraglacial meltwater can enter the englacial drainage system in very large volumes, particularly during periods of increased melt in response to warmer air temperatures, or following the drainage of supraglacial lakes. Where sufficient water enters moulins or surface crevasses, fractures are able to propagate through the entire ice-thickness, allowing supraglacial meltwater to be delivered to the ice-bed interface where it may lubricate the bed and influence subglacial water pressure, thus contributing to basal sliding.

Given evidence for dynamic response to meltwater generation through such direct englacial coupling from surface to bed, and in light of a warming global climate (Figure 1.1.1), it is crucial that the temporal and spatial formation of moulins are explored further.

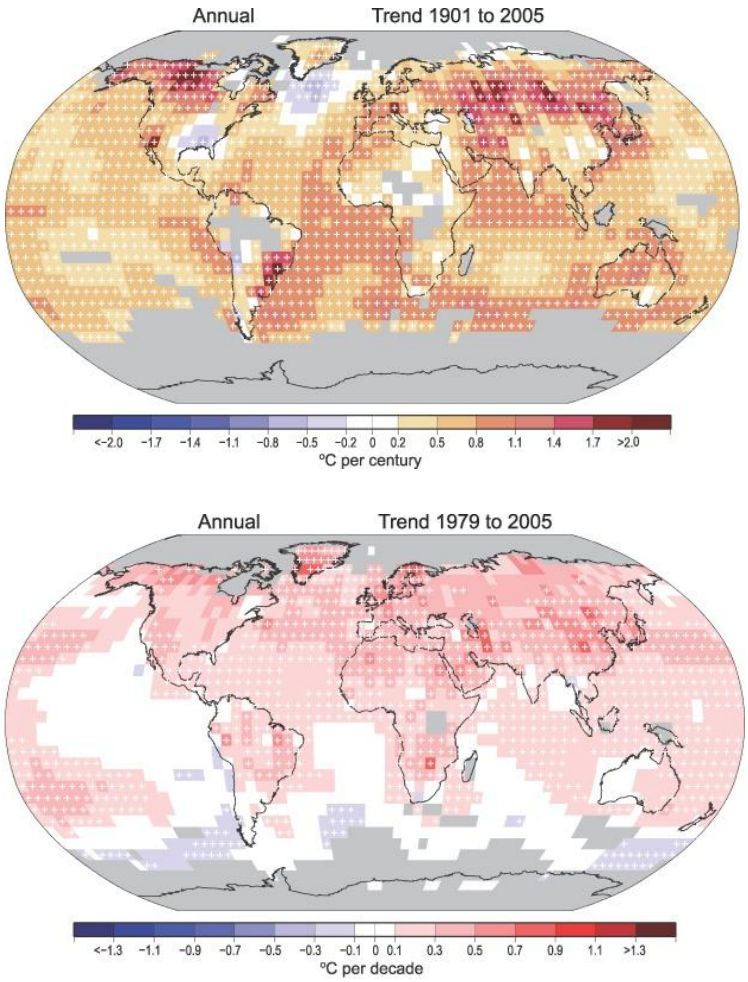

Figure 1.1.1. Global annual surface temperature trends for 1901 to 2005 (°C/century) and 1979 to 2005 (°C/decade). Reproduced from IPCC (2007).

Global annual mean air temperatures have been shown to be increasing, notably so over the past c.30 years. The monitoring of air temperatures and mass balance for glaciated regions is, therefore, becoming increasingly significant. Parts of south-western Greenland have been estimated to have undergone over 0.7°C increase in surface temperature (Figure 1.1.1) per decade between 1979 and 2005 (IPCC, 2007),

an increase that is likely to have affected mass balance either directly or indirectly. Combined, the GrIS and Antarctic Ice Sheet (AIS) have the potential to generate a 70 m rise in sea level (Bamber et al., 2007), and a series of estimates of their mass balance and thus contribution to eustatic sea level change have been made (Figure 1.1.2). However, there is considerable variation and uncertainty in these estimates, partly down to limited understanding of the dynamic controls on mass loss.

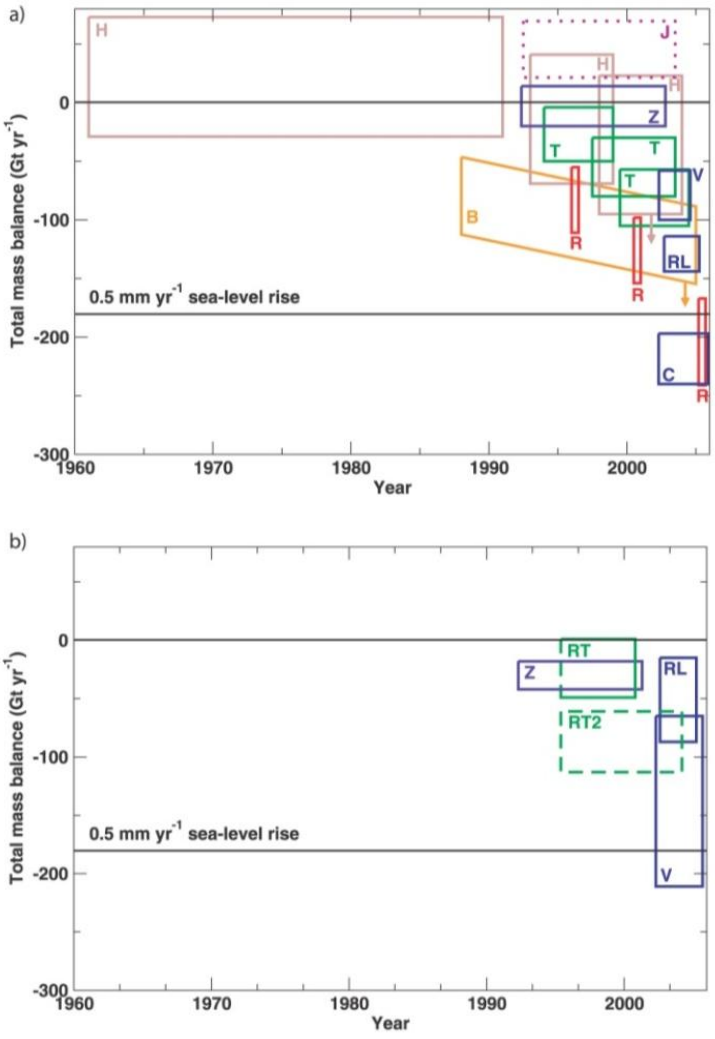

Figure 1.1.2. Mass balance estimates for a) the Greenland Ice Sheet and b) Antarctic grounded ice, where each coloured box represents a different estimate. The width of each box is the time span for which measurements apply and the height represents the mean +/- uncertainty. Reproduced from IPCC (2007).

Numerous studies (Zwally et al., 2005; Rignot et al., 2004; Alley et al., 2005a) have proposed that ice dynamics may contribute more substantially towards future eustatic

sea level rise than is currently considered within modelling. This may be of particular significance if acceleration of glaciers in some regions is to continue or intensify in line with a warming future climate (Alley et al., 2005a). Acceleration of Greenland's glaciers has been observed to be extending to the north (Rignot & Kanagaratnam, 2006), a trend which may result in mass loss which exceeds previous predictions. Furthermore, as outlined in the 2010 NOAA Arctic Report Card, record high temperatures and duration of melting (Figure 1.1.3) were recorded in Greenland for 2010, particularly in the west (Box et al., 2010). This resulted in the highest melt rate since 1958, and provided strong further evidence that the rate of ice mass loss during the past decade is greater than that before 2000. Given that record melting is being recorded in Greenland, direct access of supraglacially-generated meltwater to the bed should not be discounted as an increasingly significant mechanism for ice dynamic response, and thus mass loss, from outlet glaciers of the GrIS.

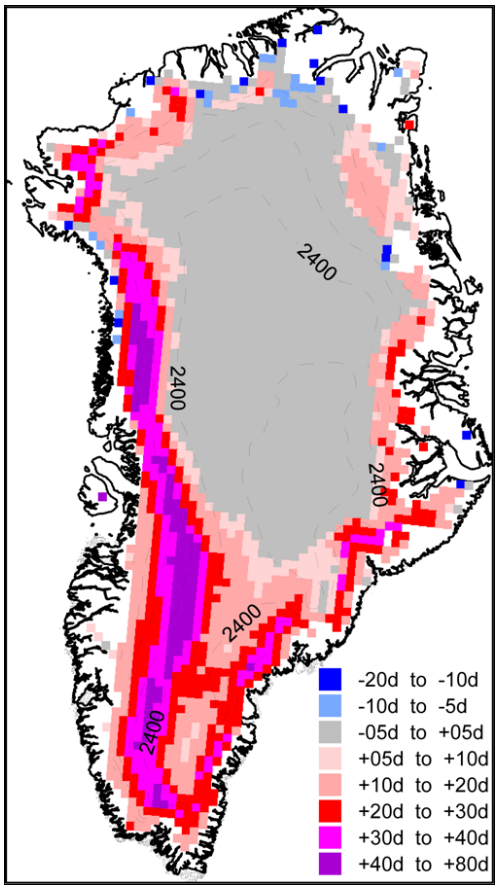

Figure 1.1.3. Change (number of days) in melt duration in summer 2010 compared to the 1979-2007 mean. Reproduced from Box et al. (2010).

1.2 Research rationale and aims

Despite increasing recognition of the potential significance of transfer of supraglacially-derived melt to the bed, the physical controls on where and when meltwater reaches the ice-bed interface of glaciers and ice sheets remain poorly understood, with a relative dearth of focus on this topic within current glaciological literature. It is, therefore, imperative that we improve our understanding of surface-to-bed connections between the supraglacial and subglacial hydrological systems if we are to better couple models of glacier hydrology and dynamics within glacier and ice sheet models, particularly if their future response to a warming climate is to be fully evaluated. The overall aim of this research is, therefore,

to develop a predictive model of moulin formation and quantification of meltwater delivery to the ice bed.

The following objectives have been set to address this research aim:

1. To model the generation and routing of meltwater across the ice surface, including storage in supraglacial lakes.
2. To predict the spatial distribution of surface crevassing from ice velocity-derived tensile stresses.
3. To calculate penetration depths of water-filled crevasses over time to establish the timing and spatial distribution of moulin formation.
4. To quantify the timing and discharge of meltwater delivery to the ice-bed interface through moulins and supraglacial lake drainages.

The methodology applied to meet these objectives, and how the modelling routine, developed using these methods, performed when applied to real glacial catchments is described within this thesis. The structure of the thesis is now outlined.

1.3 Chapter outline

In the following six chapters, model development and operation are described, followed by an account of model application to both the Croker Bay glacial catchment of Devon Ice Cap in High Arctic Canada and to Leverett outlet glacier of southwest Greenland. This thesis also includes model sensitivity analyses, comparison of model outputs against field and remotely sensed observations, and a discussion of potential model applications and future development. To begin, chapter 2 will introduce the existing literature and scientific background to the main considerations of this modelling study. This includes the coupling of glacial dynamics and hydrology, elements of the supraglacial hydrological system, and the formation and propagation of ice surface crevasses. Chapter 3 describes the methodology behind model development and application. The model components of ice surface melt modelling, supraglacial meltwater routing, the surface tensile stress regime, and the formation of moulins through water-driven crevasse propagation and drainage of supraglacial lakes are discussed, followed by a description of the primary model outputs. Model application to the Croker Bay catchment of Devon Ice Cap is considered in chapter 4, where the results of modelling moulin formation for two meteorologically-differing years, and of a thorough sensitivity analysis, are presented. Chapter 4 has been adapted for this thesis from Clason et al. (2012). Following model application to Devon Ice Cap, application to Leverett outlet glacier of the southwest Greenland Ice Sheet is described in chapter 5, also based upon a paper in preparation. As well as results of modelling for two ablation seasons, comparisons between model predictions of melt delivery to the bed against field-measured proglacial discharge, and of moulin densities against GPS velocities are presented. The thesis discussion, chapter 6, includes a consideration of model performance, including sensitivities and differences between application to the two study sites. Furthermore, model transferability between sites and models of varying spatial resolution is examined, followed by a discussion of potential future applications of the modelling routine. Finally, chapter 7 completes this thesis with the overall conclusions of the research.

The IPCC report of 2007 largely discounted the potential contribution of the GrIS to future sea level rise, partly because current uncertainties in the processes controlling ice mass loss are too large, and thus, model predictions of ice sheet evolution too speculative. This research directly aims to quantitatively predict one of the key processes controlling ice sheet dynamic thinning, and therefore contributes towards the larger challenge facing glaciological science today: improving our ability to predict the future evolution of the GrIS and other large ice masses, and their consequent contribution to global eustatic sea level, within a future warming climate.

Chapter 2. Literature review

2.1 Coupling glacial hydrology and ice dynamics

2.1.1 Subglacial hydrology

This chapter provides a background to how our knowledge of glacier hydrology has evolved and introduces the key themes contributing to the understanding of and application of the model, beginning with the important link between hydrology and ice dynamics. Investigation of the links between the hydrology and the dynamics of glaciers has resulted in varied research spanning many decades. Studies including Müller & Iken (1973) were some of the first to clarify the influence of water inputs on ice surface velocities in the context of the Arctic, followed closely by numerous papers debating the significance of water pressure and discharge as controls on consequent ice flow velocities. Seminal papers such as Iken & Bindschadler (1986), which concluded that sufficient basal water pressures could locally hydraulically jack a glacier from its bed, producing significantly enhanced ice velocities, have been central to the development of the theory of drainage system structure and evolution. Kamb (1987) concluded from observations of the 1982-83 surge of Variegated Glacier that subglacial switch from a low pressure, tunnel system, or channelized, efficient, 'fast' drainage, to a high-pressure linked-cavity system, or distributed, inefficient, 'slow' drainage, may act as a trigger mechanism for surging. This again highlighted the ability of changes in hydrological configuration to precipitate significant changes to ice dynamics. More recent studies (e.g. Jansson, 1995; Sugiyama & Gudmundsson, 2004) continued to strengthen links between glacier hydrology and dynamics using new technologies to further understand the role of subglacial water pressure and subglacial pathways. These studies were conducted largely on temperate valley glaciers; however ongoing research suggests that land-terminating outlet glaciers on the GrIS may exhibit similar dynamic response to changes in subglacial water pressure and configuration as previously documented in an Alpine setting (e.g. Bartholomew et al., 2010).

Prior to those described here, many studies did not recognise the potential for such a relationship between water influx and dynamics to translate warming air temperatures into a mechanism for climatically-enhanced mass loss. This may be partially down to there being inherently less interest in "climate change" pre-1980, despite a much lengthier knowledge of the science surrounding global warming (Corfee-Morlot et al., 2007). The establishment of the Intergovernmental Panel on Climate Change (IPCC) by the World Meteorological Organisation and the United Nations Environment Programme in 1988 and the publication of the IPCC First Assessment Report in 1990 was a significant turning point for climate research. Recent research has increasingly recognised the relationship between increased melt production and ice dynamics as likely to become progressively more important if global temperatures continue to rise, resulting in accelerated transfer of ice to lower, warmer elevations. Nevertheless, to truly understand how changing glacial hydrology may translate to a dynamic response, the spatial dimension of subglacial hydrological systems must be further considered. This is highlighted by the search for the yet elusive universal sliding law, through numerous studies on temperate valley glaciers. The response of such temperate glaciers to melt production is described below, focussing on alpine settings.

2.1.2 Glacial hydrology of temperate and polythermal glaciers

Whilst glacial research has been undertaken on many temperate alpine glaciers, Haut Glacier d'Arolla in Valais, Switzerland, has been subject to particularly numerous studies of glacial hydrology and dynamics. "Spring events", a product of increased water influx producing short-lived periods of increased surface ice velocity, have been observed on a number of occasions. In early June, 1994, a velocity stake field was constructed in a staggered formation to allow surface strain triangles to be inferred from measured motion (Mair et al. 2001). Enhanced surface velocities of up to 500% of average annual surface velocity were recorded within the stake field between the 23rd and 29th of June (Mair et al., 2002). Analysis of horizontal velocity data twinned with vertical uplift measurements, where high vertical uplift was associated with enlarged subglacial cavities, suggested that cavities opened or expanded following the onset of

spring events, and highest cavity growth rates were observed down-glacier from moulins. A later study by Mair et al. (2003) further investigated these high velocity events during the ablation seasons of 1998 and 1999, recording three such events: two in June, 1998 and one in early July, 1999. In contrast to earlier work, this study included a more thorough examination of internal deformation, basal motion and subglacial hydrology. Conclusions suggested that events producing a widespread area of basal high water pressure resulted in complex patterns of surface motion and stress, partially due to the particularly high water pressure concentrated along the preferential drainage axis, with consequent high rates of basal motion in that area. Events which produced a more concentrated area of high water pressure resulted in more localised ice-bed decoupling, and as the highest velocities were concentrated on the glacier centre line, a less complex pattern of motion was observed at the ice surface.

Whilst ice dynamic response to meltwater influx is especially well understood on Haut Glacier d'Arolla, numerous studies have reported such dynamic feedbacks on other alpine glaciers. In a North American context, Raymond et al. (1995) identified coupled weather-related hydrological and ice motion events on both the Black Rapids and Fels glaciers of Alaska, and motion events linked to release of melt stored in marginal lakes on the Black Rapids glacier. Anderson et al. (2004), in agreement with Raymond et al. (1995) also concluded from observations of the Alaskan Bench glacier that high meltwater input and coupled motion associated with weather events in spring and autumn was operative in the evolution of the subglacial drainage system. Furthermore, research conducted on the Kennicott Glacier by Bartholomaus et al. (2011) emphasised how the sensitivity of dynamic responses to increased meltwater input varies significantly throughout the melt season, and indeed the importance of whether this melt is stored subglacially or englacially. The study stressed the importance of knowledge of the meltwater input history for full models of glacier sliding. The drainage of ice-dammed lakes has also been observed in European alpine environments, including the drainage of one lake on Gornergletscher in Switzerland, which triggered a 50% increase in ice flow speed and a clear ice-bed decoupling (Sugiyama et al., 2007).

Deviating from alpine glaciers, Bingham et al. (2003) was a study of particular significance, as it proposed a direct link between drainage of supraglacially-ponded meltwater and springtime velocity increases of up to 50%, resulting from enhanced basal water pressures and basal motion on an Arctic polythermal glacier, John Evans Glacier on Ellesmere Island. Furthermore the study produced results that supported the work of Zwally et al. (2002) on Greenland, suggesting that meltwater-induced velocity responses were not restricted to temperate glaciers, and could indeed be a important mechanism within Arctic ice masses, prompting a new generation of research in a different, non-alpine, setting, as described in section 2.1.3. Irvine-Fynn et al. (2011) presented a review of polythermal glacier hydrology, highlighting that non-temperate valley glaciers are likely more representative of the hydrological processes occurring on ice sheets. Furthermore, given that a large proportion of global ice masses are non-temperate, it is important to understand as much about polythermal hydrology as we go about temperate valley glacier hydrology. While reduced flow velocities and deformation on non-temperate glaciers do not always give rise to the extent of crevasse formation more often seen on temperate glaciers, englacial drainage systems are present, and provide an important link to the subglacial system and to consequent dynamic response. In crevasse-free areas of polythermal glaciers mechanisms including meltwater channel incision can contribute to englacial conduit evolution. This was explored by Gulley et al. (2009) from mapping studies on both clean and debris-covered polythermal glaciers in Svalbard and the Khumbu Himal, where “cut and closure” channels were described.

Water flow into existing fractures on polythermal glaciers has also been observed to contribute to the formation of englacial conduits and moulins, which can act as pathways for localised meltwater delivery to the subglacial system, and thus influence dynamic response. Holmlund (1988) documented moulins on the non-temperate Storglaciären in northern Sweden, formed where meltwater channels running across the gently-sloping ice surface intersected crevasses. The presence of cold ice on Storglaciären limits the spatial extent of moulins due to the low permeability of ice below pressure-melting point, with a large central area of the glacier characterised by uninterrupted meltwater stream-flow across the surface (Per Holmlund, personal

communication). Where the cold ice layer thins in the lower ablation zone, and where crevasses are also present due to increased strain-rates as the ice flows over a riegel, moulins have been seen to open in the same locations annually. In addition to the constraints imposed by a surface cold ice layer, the occurrence of refreezing and percolation of meltwater within the snowpack on non-temperate glaciers can produce superimposed ice. This increases the low primary permeability of these glaciers, and can result in significant meltwater storage within supraglacial lakes, slush zones, and subsequent weathering crusts following snowpack removal (Irvine-Fynn et al., 2011). Importantly for potential moulin formation, this storage can delay or dampen runoff, hindering the ability of crevasses to be driven through the ice by hydrofracture. The importance of continuous water influx for maintaining connections to the bed of non-temperate glaciers was highlighted by Boon & Sharp (2003) in their study of ice fracture driven by meltwater on John Evans Glacier, where refreezing and plugging or cessation of further downwards fracture is more likely to due low ice temperatures. Temperate and polythermal glaciers, although often smaller in scale, provide important analogues for hydrological and dynamic processes occurring on the outlet glaciers of the GrIS, studies of which are described below.

2.1.3 Coupling hydrology and dynamics on the Greenland Ice Sheet

Glaciological research is increasingly focussing on the behaviour of Earth's ice sheets where around 80% of Earth's freshwater is stored (Bamber et al., 2007), c.8% of which within the GrIS. Unlike the Antarctic Ice Sheet where surface ablation does not contribute so substantially to mass balance change, the GrIS loses around half its mass via surface melt and runoff (IPCC, 2007), whilst much of the remaining proportion is lost via calving and enhanced thinning of tidewater glaciers. Debate surrounds the relative significance of meltwater-enhanced dynamic response in comparison to that of marine outlet glacier response to warming sea temperatures. Zwally et al. (2002) concluded from velocity and melt observations on western Greenland that enhanced basal sliding could provide a mechanism for fast response of ice sheets to increased production and delivery of meltwater to the bed through moulins (Figure 2.1.3.1).

Following the publication of that study, the significance of the coupling between supraglacial meltwater and enhanced basal sliding for parts of the GrIS under a warming climate has been equivocal within subsequent research. Thomas et al. (2009) concluded that warming of oceanic water was likely to be a significant control on the thinning of many of the GrIS outlet glaciers, particularly those with deep beds terminating in water, due to the removal of the buttressing effect provided by floating tongues. The study also concluded that outlet glaciers without deep beds were not thinning as significantly, suggesting that the role of surface-meltwater induced basal lubrication was not as significant a mechanism of mass loss as that of warming deep-ocean water. Sole et al. (2008) conducted a comparison of elevation change data for a sample of marine-terminating and land-terminating outlet glaciers around the GrIS. Results indicated that marine-terminating glaciers were thinning significantly more than land-terminating glaciers. Additionally, as thinning of land-terminating glaciers did not statistically differ from that which would be expected from patterns of ablation, the study suggested that meltwater accessing the bed of Greenland's land-terminating glaciers may not be influencing thinning rates significantly. What these studies do not consider is the influence of a future increased melt scenario on the dynamics of land-terminating glaciers, particularly their relative contribution to mass loss when marine-terminating glaciers become grounded.

Figure 2.1.3.1. Moulin on Leverett Glacier, southwest Greenland. Photo credit: Caroline Clason.

A study by Price et al. (2008) suggested that the propagation of fractures due to water filling is unlikely to operate near to the equilibrium line altitude (ELA) of the GrIS, but instead water reaching the ice-bed interface nearer the margin may affect flow velocities further inland through longitudinal coupling. As such, Price et al. concluded that acceleration caused by an increased water-flux at the bed may not translate to the magnitude of impact on mass-balance suggested by studies such as Zwally et al. (2002). McMillan et al. (2007) had also stated that the transfer of meltwater from the ice surface to the bed was affecting the faster flowing downstream ice of outlet glaciers through longitudinal coupling, but (conversely to Price et al. (2008)) concluded that this may provide a mechanism for rapid response of the ice sheet to climatic forcing. Catania et al. (2008) supported the conclusions of Price et al. (2008) based on ice penetrating radar profiles, with almost all 'moulins' inferred from radar profiles having been observed within the lower elevation region downstream of Swiss Camp. The area was, notably, deemed by the authors to have been under-sampled. Das et al. (2008), contrary to the results by Catania et al. (2008), recorded the drainage of a large

supraglacial lake, with corresponding increased horizontal velocities and vertical uplift, supporting the presence of a surface-to-bed connection of almost 1 km depth in that area of the western ice sheet. Catania et al. (2008) had suggested that the volume of water held within supraglacial lakes alone may not be sufficient to initiate ice surface fracture due to the compressive nature of the ice in the depressions within which lakes typically form. However, lake drainage would provide a means for crevasses in close proximity to propagate should supraglacial meltwater from the lake flow into them, or similarly may result in propagation of crevasses which have migrated with ice flow to intersect lakes. Although relatively few real-time observations of lake drainages or ground surveys of moulins have been made on the GrIS, there is no evidence to suggest that formation of supra-to-subglacial connections should not occur at or even above the present ELA, as has been included in modelling studies of the deglaciation of past ice sheets (Arnold & Sharp 1992; 2002). Furthermore, Alley et al. (2005b) concluded that meltwater can drive a crevasse through up to 1 km of ice, suggesting that melt-induced dynamic response may indeed operate above the present ELA in the future.

Two studies of velocity change in the ablation zone of the western GrIS (Joughin et al., 2008; van de Wal et al. 2008) concluded that seasonal melt induced dynamic speedup is limited in its contribution to overall ice sheet response. Van de Wal et al. (2008) presented a study of simultaneous ablation and surface GPS velocity measurements along the K-transect of the western GrIS which suggested that at an annual timescale, velocities remain fairly constant in response to changing meltwater input, due to the adaptation of the drainage system. Joughin et al. (2008) investigated an assemblage of GPS and InSAR-derived velocity data for a number of outlet glaciers of the western ice sheet. They concluded that the glaciers within their study area were limited in their sensitivity, and thus dynamic response, to melt input. However, these glaciers were all marine-terminating, and impacted substantially by ocean-ice interaction processes, and therefore cannot be said to be representative of other glaciers of the western ice sheet. As such there are clear spatial and temporal limitations to both of these studies, and moreover, they preclude a proper understanding of the hydro-mechanical coupling process. In addition, a study by Sole et al. (2011) of a marine-terminating

glacier in southwest Greenland suggests that observed seasonal and short-term velocity response to surface meltwater production is similar to that of land-terminating glaciers when sufficiently far from the terminus.

Sundal et al. (2011) investigated velocity changes in outlet glaciers of the southwest GrIS from synthetic aperture radar (SAR) data. They concluded that increased surface melt could result in decreased summer ice flow in the lower ablation zone due to response of the subglacial drainage system. However, the data despite their relatively high spatial resolution were limited in spatial extent to only the very margins of the ice sheet and thus do not consider melt input or indeed the drainage system configuration further inland. Through the use of GPS for velocity measurements of high temporal resolution, Bartholomew et al. (2011a) investigated ice surface motion extending from c.450 m elevation on the land-terminating Leverett Glacier, up to c.1700 m during the 2009 melt season. Results of contemporaneous measurements of velocity, air temperature and ablation show a strong positive correlation between melt and annual ice surface motion, with sites below 1000 m elevation having a much stronger response than those above 1000 m due to fewer melt days and delayed formation of moulins at higher elevation. Measurements also recorded a decreased sensitivity of velocities to melt production as the season progressed, explained by Bartholomew (2011b) as an increase in subglacial drainage system efficiency caused surface to bed connections forming further upglacier. Enhanced ice surface velocities on the GrIS as a feedback from increased melt production and bed lubrication under a warmer climate may result in an increase in longitudinal strain rates, leading to a higher frequency of crevassing. In addition, resultant thinning stemming from accelerated flow may then produce more frequent occurrence of meltwater reaching the ice-bed interface, as decreasing ice thicknesses make it easier for crevasses to propagate from the surface to the bed (Benn et al., 2007a). With potential for inward migration of the ELA over the course of warmer ablation seasons, and as marine-terminating glaciers threaten to retreat until grounded, moulins may yet play a highly significant role in possible future shrinkage of the GrIS, and indeed many other ice masses within high-northerly latitudes. In order to fully understand and *predict* how this process may relate to ice

mass change, it must be implemented within a modelling framework, as the following section discusses.

2.1.4 Modelling studies

The coupling of hydrology and dynamics has been limited within glaciological modelling, but some glacier dynamic models have been developed to include a meltwater component, both for deriving the evolution of past ice sheets in response to climatic change, and for modelling of current glaciers. Parizek & Alley (2004) investigated the influence of enhanced lubrication of the bed by surface-derived meltwater on the sensitivity of the GrIS to future climatic scenarios. Using a transect across the centre of Greenland (passing through the GRIP coring site), the study employed a thermomechanical flowline model to assess evolution of the transect under mean temperatures resulting from carbon dioxide levels of 2, 4 and 8 times higher than at present. Results inferred that enhanced melt, and hence basal lubrication, would eventually result in an increase in mass transfer from accumulation to ablation zones and a decrease in ice surface elevation leading to inland extension of the zone affected by surface ablation. Field observations of increased velocities succeeding periods of increased surface melt on the GrIS suggest that water can penetrate through at least 1000 m of ice (Shepherd et al., 2009). Consequently, it is possible that meltwater-induced velocity increases could occur well above the equilibrium line under conditions of thinning ice and an inland-migrating zone of surface melt. Parizek & Alley (2004) also highlighted that alongside the Arnold & Sharp papers of 1992 and 2002, it was the only other paper to the knowledge of the authors that truly included surface meltwater within ice sheet modelling.

Arnold & Sharp (1992) explored the influence of hydrology on the dynamics and evolution of the Weichselian Scandinavian ice sheet via one-dimensional flow modelling. Results inferred that during the period of deglaciation, access of meltwater to the bed of the southern area of the ice sheet was highly significant, most probably occurring over an area extending beyond the ablation zone. The study also suggested

that climatic warming had a particularly significant effect on the ice sheet, with increasing ablation and consequent meltwater discharge leading to a feedback effect where both the extent of the area affected as well as the rates of sliding were increased. This in turn led to a drawdown of ice mass from the ice sheet interior, acting to decrease elevation and further expand the area of the ablation zone. Arnold & Sharp (2002), building on the 1992 study, described a new two-dimensional version of their model for time-dependent modelling of the dynamics of the Weichselian Scandinavian ice sheet. It applied a water pressure-dependent sliding law to derive velocity changes in response to varying meltwater inputs and subglacial flow pathways. The mechanism of fracture penetration as a means to transfer meltwater to the bed was applied, with water routed to the bed where discharge reached a predefined critical value. In addition, meltwater was only added to basal melt provided the bed temperature was at pressure melting point. Results suggested that the prescribed value of critical discharge, and hence the frequency at which water was routed to the bed, had a highly significant effect on the dynamics and geometry of the ice sheet. Additionally, the study emphasised that even if meltwater were to refreeze at the bed where ice is “cold”, the transfer of latent heat from the meltwater into the basal ice could still promote sliding due to a consequent warming of the bed.

The same is true for modern glaciers and ice sheets, where such a transfer of heat energy may alter the thermal properties of both englacial and basal ice, contributing both to the presence of water at the ice-bed interface which may influence the dynamics of the ice mass, and the temperature-related physical properties of the ice including viscosity and tensile strength. The importance of such ‘cryo-hydrologic warming’ was highlighted by Phillips et al. (2010), where a parameterisation of heat exchange between the cryo-hydrological system, the englacial network of moulins, crevasses, conduits and fractures (Figure 2.1.4.1), and ice was described for implementation in ice sheet models. Under a warming climate, the authors propose an expansion of the cryo-hydrological system as the ELA increases, resulting in sustained warming of ice temperature from the water within the englacial system that does not refreeze during winter. There has been a renewed interest in inclusion of supraglacially-forced hydrology within recent modelling studies. This has been typified

in an ice dynamic modelling study coupled with hydrology, presented by Pimentel et al. (2010), which highlighted the importance of coupling hydrology and dynamics through modelling hydraulically-forced ice acceleration scenarios. Schoof (2010) presented a model of switching between channelised and cavity-based subglacial drainage in response to meltwater input. He concluded that short-term increases in melt input to the subglacial system, through lake drainages, rain events, and strong diurnal melt variation drive ice acceleration, whilst a steady increased melt supply may actually result in deceleration through channelisation once a critical discharge has been reached. Despite significant progress in coupling of hydrology and dynamics, and in modelling of subglacial drainage system evolution in response to meltwater forcing, there remains a need for observed or modelled distributed point-surface meltwater inputs, rather than prescribed inputs with little physical basis. Phillips et al. (2011) employed the remote sensing image classification method, fuzzy set theory, which allows for both partial and multiple pixel class membership, to model the spatial distribution of moulins on Sermeq Avannarleq glacier on the western GrIS. With 88% of moulin locations successfully predicted, this is an important step towards inclusion of meltwater input points within ice sheet models coupled with hydrology. The importance of moulins in this glacial catchment was explored further by McGrath et al. (2011), where the ability of moulins to transfer surface melt to the bed and overwhelm the subglacial system, resulting in enhanced basal motion was highlighted. Furthermore, the storage of meltwater in crevasses was identified as having a dampening effect on the transmission of surface melt generation. For the englacial transfer of melt to the bed to be assessed accurately, the melt generated at the surface must first be quantified accurately. The following section discusses the modelling of supraglacial melt and the pros and cons of differing approaches.

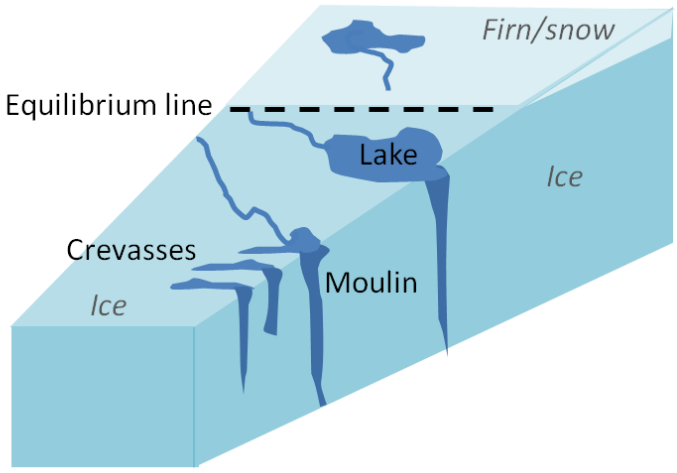

Figure 2.1.4.1. Schematic illustrating major features of the supraglacial and englacial systems.

2.2 Supraglacial hydrology

2.2.1 Melt modelling

The modelling of generated melt at the ice surface is an area of glaciological modelling within which debate abounds to the appropriate use of various modelling approaches. A review of these approaches, plus the physical processes contributing to melt and how these are represented within modelling, was written by Hock (2005). The two main approaches adopted are degree-day models and energy balance melt models, the latter of which is designed to model melt based on the energy fluxes to and from the ice surface. Hock (2005) highlighted that while this approach can produce accurate estimates of melt due to better representation of the physical processes, the data requirements to adopt this approach are often unavailable, and our ability to measure the surface albedo and turbulent heat fluxes, particularly their temporal and spatial variation, remains a source of significant uncertainty. Brock & Arnold (2000) described a point surface energy balance model, run based on knowledge of local site characteristics and the hourly outputs of an automated weather station. Non-distributed models such as this produce energy flux values for a single point, while distributed models have been developed to compute values of temporal melt across

the entire glacier surface, requiring the additional input of a DEM. Arnold et al. (1996) produced one such model to calculate melt values across Haut Glacier d'Arolla. From comparison with measured ablation values the importance of topographic data of a sufficient resolution was confirmed, in order to accurately represent the receipt of incoming shortwave radiation. The importance of accounting for albedo variation due to transient debris coverings was also highlighted. Willis et al. (2002) investigated the effect that the removal of snowpack has on distributed melt through distributed energy balance modelling. When coupled with a meltwater routing model, the results of the study drew particular attention to the dampening effect of the snowpack on diurnal discharge cycles. A study by Brock et al. (2000), introducing an update to the distributed model described by Arnold et al. (1996), also drew attention to the influence of migration of the snowline through the ablation season. Consequent changes in aerodynamic roughness and albedo were shown to exert a significant influence on energy fluxes at the ice surface, confirming the complexities of the energy balance approach.

The degree-day approach is often favoured for its simple approach, and since of all meteorological variables air temperature is most readily available. Whilst this approach may be appropriate for many applications, including this study; its suitability falters when modelling is carried out in a predictive capacity. When looking at future climate scenarios for the Greenland Ice Sheet, for example, due to degree-day factors being calibrated for a single site during one period in time they are unlikely to be transferable in space and time for melt modelling at a large spatial scale under future conditions, particularly when diurnal fluctuations are considered. The spatial and temporal limitations imposed by classical degree-day modelling were discussed by Hock (2003), a study which explored degree-day model application to a number of mountain regions and glaciers around the world. The paper highlighted how a number of variables can significantly affect degree-day factors in space and time, including the effect of those factors summarised in figure 2.2.1.1, where increasing elevation and solar radiation result in an increase in the degree day factor, whilst the opposite is true for albedo and the portion of the sensible heat flux. Despite the limitations of the degree-day approach, the minimal meteorological data requirements for this method

mean that it remains popular. Furthermore, with recent improvements in spatially distributed degree-day modelling, particularly through accounting for incoming solar radiation in what is referred to as the *enhanced temperature-index* approach (Huintjes et al., 2010; Pellicciotti et al., 2005), the simple data requirements of the degree-day approach can be maintained whilst allowing for more physically-representative spatial variation in melt. With accurate quantification of distributed generation of melt, the routing of this melt across the ice surface can then be modelled when twinned with ice surface digital elevation models, as discussed in the next section.

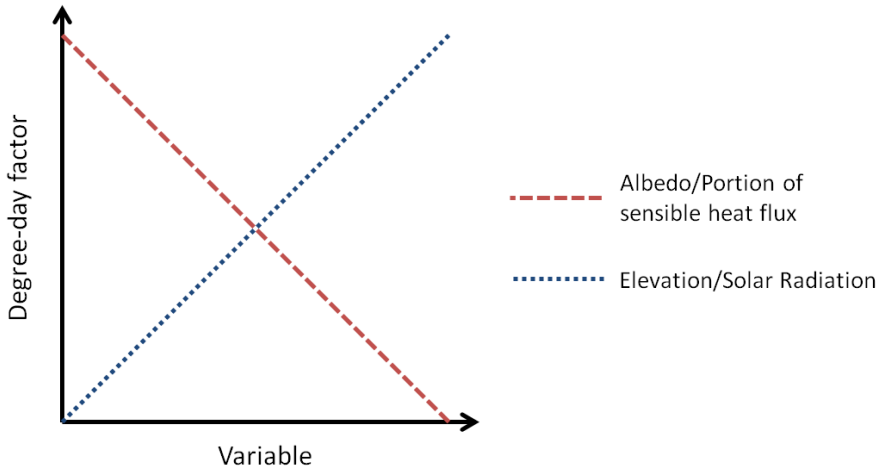

Figure 2.2.1.1. Quantitative representation of how increasing or decreasing variables affects the value of the degree-day factor. After Figure 1 of Hock (2003).

2.2.2 Modelling meltwater flow pathways

Modelling of meltwater flow pathways across the ice surface may be achieved through GIS-based flow routing from digital elevation models (DEMs) of glacier surfaces. The resultant supraglacial pathways may then be used to predict where streams intersect crevassed areas, promoting moulin formation. It is, therefore, important that the best practice for accurate flow routing across ice surfaces is achieved. This includes ensuring satisfactory spatial resolution and vertical error of DEMs, and the use of appropriate flow routing algorithms. DEMs have often been produced directly from ground surveys, although more recent advances in the acquisition of remotely sensed

imagery have led to increased utilisation of technology such as interferometric synthetic aperture radar (InSAR) and digital image correlation (orthophotos). Orthophotos are an example of a product of passive remote sensing systems, where both airborne and satellite high resolution imagery can subsequently be used as an input for DEMs (Lillesand et al., 2004). Although cost-effective in comparison to ground survey, production of DEMs via photogrammetry is constrained by light availability and weather conditions at the time of data acquisition (Molander, 2001). InSAR (Interferometric Synthetic Aperture Radar) and topographic LiDAR (Light Detection And Ranging) are not limited by such constraints. Both are examples of active remote sensing systems which emit their own source of electromagnetic radiation, the quantity of that which is consequently reflected from the surface below is measured when returned to the sensor. The distance between the sensor and the ground can be measured based on knowledge of the speed of the transmitted pulse of energy, and the time taken for the pulse to be reflected from the ground and received by the sensor. Thomas et al. (2009) is one example of a study which made use of LiDAR altimetry data to measure changes in ice thickness across parts of the GrIS. Results of these LiDAR surveys of the GrIS suggest a vertical measurement accuracy bettering 20 cm, improving on the accuracy of SAR-acquired elevation data which can be influenced by reflectance off surface slopes in excess of 1° within the large radar footprint (Krabill et al., 1995). SAR elevation measurements can also be affected by emitted radar penetrating layers of snow or firn, producing what can be significantly unrealistic elevations for those areas that are snow-covered for all, or at least part, of the year.

Using the output of a melt model, values of distributed melt across an ice surface can be interpolated from measured air temperature and other meteorological variables. Surface meltwater will most often flow down the steepest path over the ice surface, forming supraglacial streams where sufficient meltwater is produced. Therefore, by using distributed melt as an input to an ice surface DEM meltwater flow model, supraglacial meltwater pathways can be calculated and discharge can be determined from melt-weighted flow accumulation. Arnold et al. (1998) described a surface routing submodel, as part of a larger model of the hydrology of Haut Glacier d'Arolla, which assumed that water would flow directly down the steepest plane between one

grid cell and the next. A model such as this is known as a single-flow-direction model, where, in a typical square cell grid, water has a choice of eight flow directions and will choose the steepest path between itself and one of its eight neighbours (Figure 2.2.2.1).

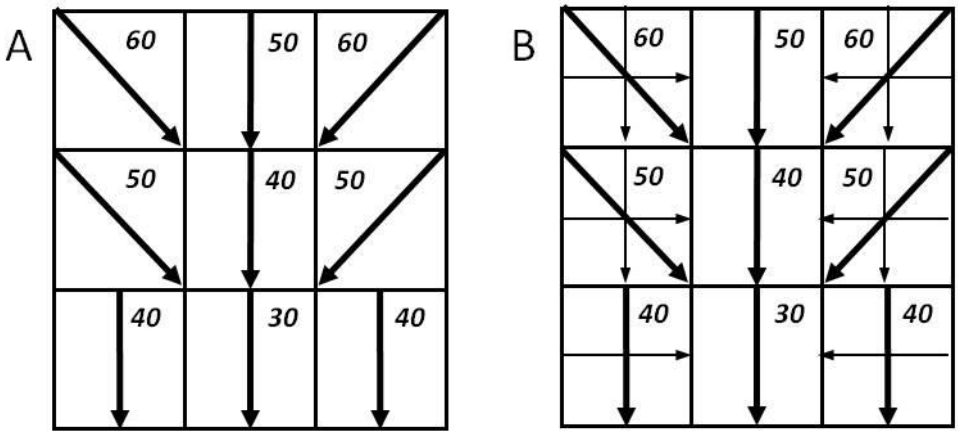

Figure 2.2.2.1. Single (A) and multiple (B) flow routing algorithm approaches on a DEM surface with numbers representing elevation.

Huggel et al. (2003) used both single and multiple-flow-direction models for hazard assessment of glacial lake outbursts in the Swiss Alps. Multiple-flow-direction models weight flow in proportion to surface slope between each cell and its eight neighbours, routing a percentage of total flow to each downhill neighbouring cell (Figure 2.2.2.1). This may be a useful tool for stream prediction in glacial catchments where the ice surface is highly transient and will not conform to the topography of a static DEM, and also for consideration of debris flow for glacial lake outburst flooding. One further aspect of flow routing algorithms which deserves consideration is their ability to maintain reliable performance when negotiating varying landscape classes, i.e. cells classified by land cover, or cells classified by slope. Wilson et al. (2007) compared performance of algorithms over a 10 m USGS DEM of the Santa Monica Mountains, California. The study classified the landscape into six classes based largely on aspect and slope, and found that the D8 (single-flow-direction) algorithm too frequently predicted cells unlikely to produce overland flow in the wrong parts of the landscape.

This supported conclusions of previous studies which endorsed preferential use of algorithms that route flow to two or three neighbouring cells (i.e. flow bifurcation). However, this has not been tested fully for ice surfaces, and may not be representative of the often limited width of supraglacial streams due to down-cutting. Flow routing, easily applied within GIS environments, can also be applied within a modelling framework such as "Matlab". Schwanghart & Kuhn (2010) described one such toolbox of "Matlab" functions for topographic analysis, including the spatial variability of water, and allowing for both single and multiple flow routing and for flow accumulation. Additionally, with supraglacial lakes being an important component of supraglacial meltwater storage and routing, it is important that they are included where necessary within such routing models. The next section highlights the importance of these lakes, and the increasing significance ascribed to them within the glacial literature.

2.2.3 Supraglacial lakes

For some glaciated areas, particularly large ice caps and ice sheets, it is imperative that recurring supraglacial lakes are mapped and included within the routing and storage of supraglacial melt due to their potential for initiating ice fracture and propagation. Meltwater ponding and subsequent drainage is observed frequently in Greenland, and particularly so in the south-west sector of the GrIS (Selmes et al., 2011), where lake drainages may affect outlet glacier dynamics. Storage of large quantities of meltwater in supraglacial lakes acts to increase pressure at crevasse tips, aiding penetration through the ice thickness (Boon & Sharp, 2003). The periodical release of substantial volumes of water from these lakes and ponds into the englacial system may help to maintain moulins, even in cold ice, through heat transfer from the meltwater to the ice walls, allowing prolonged access of supraglacial water to the ice-bed interface. Studies, including Sneed & Hamilton (2007) and Box & Ski (2007), have presented remote sensing techniques for estimation of the volumes of melt stored within supraglacial lakes. The aforementioned studies applied ASTER and MODIS imagery respectively, and although both studies were limited in their spatial coverage, they were important

in introducing innovative techniques for monitoring of lake melt content and evolution. Luthje et al. (2006) took a different approach by employing melt modelling to simulate the evolution of lakes, the locations of which were determined through the topography of a DEM. Importantly, Luthje et al. (2006) identified that surface area covered by lakes was overestimated until the inclusion of randomly placed drainage holes, highlighting the role of drainage through moulins. McMillan et al. (2007) also used a melt modelling (degree-day) approach, twinned with satellite imagery surveys, to investigate the evolution of lakes on the western GrIS. They identified that latitude, elevation and time are crucial controlling factors on lake distribution due to their influence on air temperature and melt generation. As lakes were typically shown to drain in later stages of development, the 2007 study hinted towards the subsequently observed pattern of drainage from low to high elevation with time as the area experiencing melt expands during the melt season.

The significance of supraglacial lake drainages for ice dynamics was described by Das et al. (2008) when they presented results showing increased seismicity, increased horizontal ice surface velocities and vertical uplift in response to the drainage of a large lake on the GrIS which produced discharge in the order of the Niagara Falls' c.8700 $m^3 s^{-1}$. The ice thickness beneath the lake was c.1000 m, highlighting the ability of meltwater to be transferred through the full ice thickness in a short period of time. Krawczynski et al. (2009) applied a model of linear elastic fracture mechanics (LEFM) to investigate both the importance of the geometry of cracks draining supraglacial lakes, and how much meltwater is needed to drive a fracture through 1 km of subfreezing ice. For their study area of the western GrIS, they concluded that 98% of meltwater stored within lakes had the ability to be transferred to the bed due to the sufficient size of more than 1000 lakes to drive a fracture through the full ice thickness. Sundal et al. (2009), through automated classification of supraglacial lakes from MODIS imagery, found that lakes both formed and drained at progressively high elevation in their study sites on the GrIS. Due to calculating a positive correlation between lake area and annual runoff, and since high lake extent years are characterised by high summer temperatures, they inferred from their results that in a future warming climate lakes may form earlier and at higher elevation, increasing both the time frame for, and

spatial extent of surface-to-bed connections. In investigating the relationship between supraglacial melt pathways and seasonal speed-up of ice flow for a region of the western GrIS, Palmer et al. (2011) ascertain a close correspondence between spatial patterns of ice surface motion and both modelled runoff pathways and topographic sinks in the InSAR-derived DEM identified as supraglacial lakes (Figure 2.2.3.1). This close correspondence may be representative of direct supra-subglacial coupling, and certainly suggests that further investigation into the spatial and temporal delivery of melt to the bed through moulins is necessary if we are to fully understand glacier dynamic response to future melt generation, routing and ponding. To achieve this, the surface openings through which melt can be routed to the bed must be quantifiable as must the penetration rate and depth of these englacial fractures, which will now be explained.

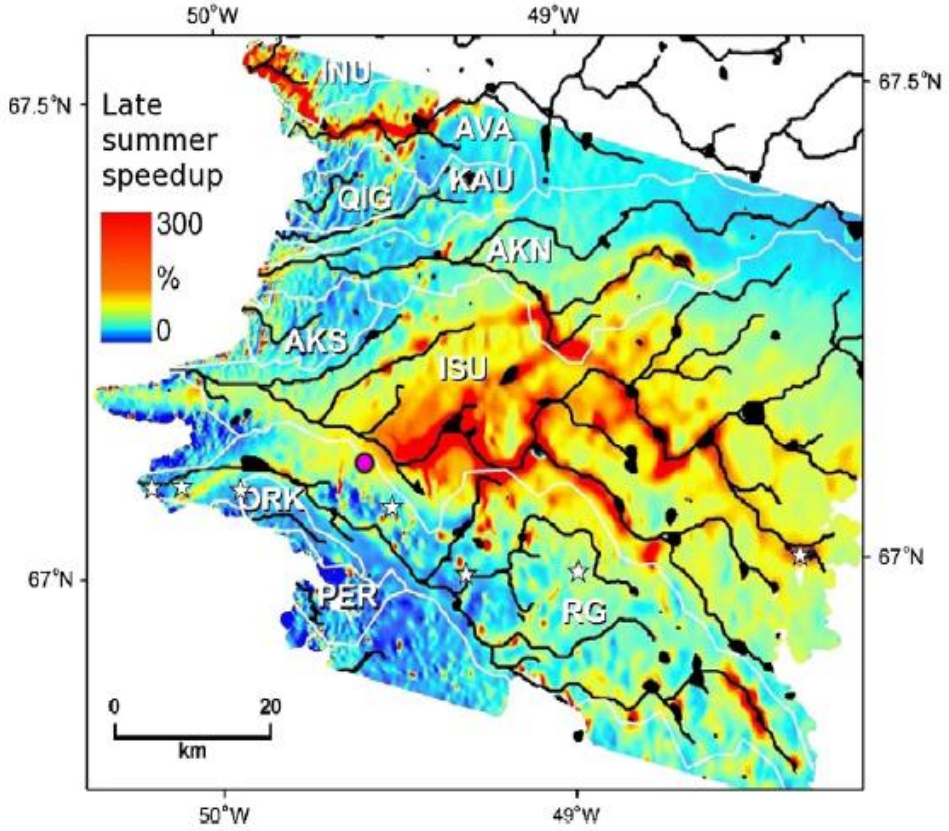

Figure 2.2.3.1. Meltwater streams and topographic sinks (black) on a map of seasonal velocity change. Reproduced from Palmer et al. (2011).

2.3 Ice surface crevassing and fracture propagation

2.3.1 Modelling the spatial distribution of surface crevassing

A variety of past studies have focussed on spatially-distributed modelling of surface crevasse formation and across the ice surface (e.g. Hubbard & Hubbard, 2002; Vaughan, 1993). This can be achieved through mapping of flow velocities and strain patterns across the ice surface, derived from both measured displacement of velocity stakes and from patterns of motion identified from remote sensing techniques combined with satellite imagery such as Interferometric Synthetic Aperture Radar (InSAR). Crevasses are predicted where the tensile strength, a failure criterion representing the maximum tensile stress that can be applied to the ice before failure, is exceeded. The value of tensile strength may be affected by the spacing of crevasses due to blunting at crevasse tips, and by the thermal regime of the ice. As such, the tensile strength will vary for temperate and cold glacial ice (Figure 2.3.1.1). Vaughan (1993) tested failure envelopes based on measured strain rates against theoretical failure envelopes predicted using, among others, the 'von Mises' and 'Coulomb' failure criteria. These criteria were initially developed for ductile yield and shear failure in rock, respectively, but have since been used to predict crevasse formation. Vaughan's paper highlighted the significance of crystal structure, impurities and density profiles as controlling variables on the tensile strength through the vertical ice profile. Furthermore, the study concluded that mechanisms responsible for creep, namely the activation energy, may also be responsible for crevasse formation at the microscopic level as the two processes display a similar Arrhenius temperature-dependence. That is, the flow parameter of ice will vary with temperature in accordance with the 'Arrhenius relation', such that strain rates produced by an applied stress will increase with temperature (Paterson, 1994). However, Vaughan did not find a clear relationship between temperature and tensile strength from the data collated in his 1993 paper. Without limitations on differentiation between the formation of crevasses within different facies of snow, firn and ice, made difficult by the lack of a good stress/strain rheology for low density ice (David Vaughan, personal communication), it cannot be

assumed that tensile strength of glacier ice is temperature-independent. Indeed, if we include tensile strength estimates calculated during researching for this thesis alongside a sample of estimates from Vaughan (1993), a negative relationship of tensile strength with temperature is evident, with an R^2 value of 0.73 (Figure 2.3.1.1).

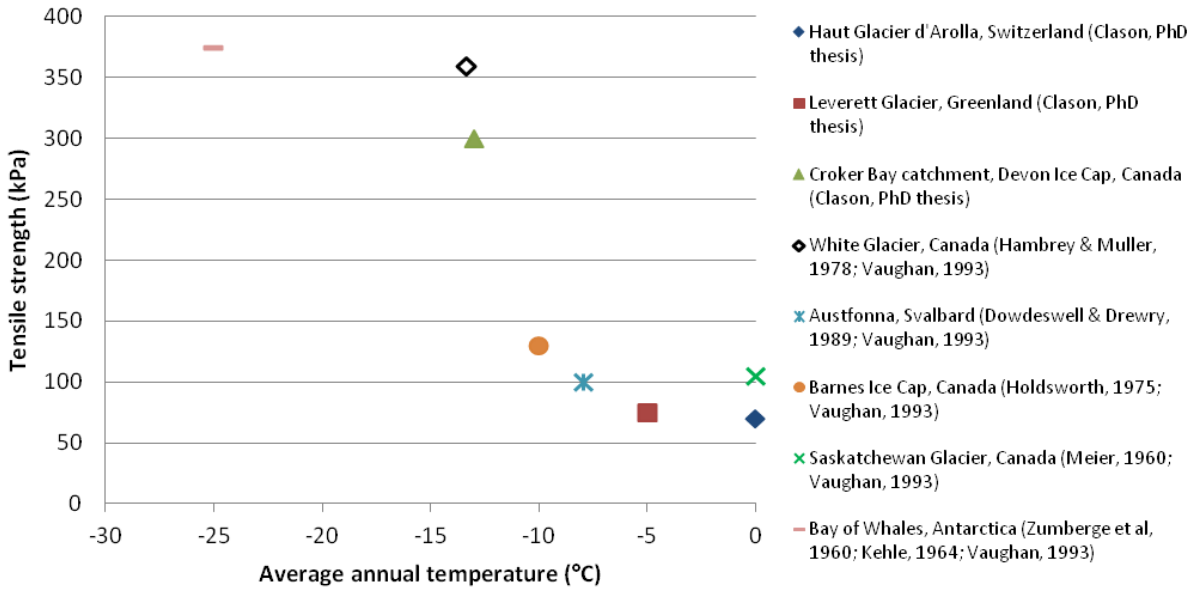

Figure 2.3.1.1. Estimated ice tensile strengths for various sites, adapted from Table 1 in Vaughan (1993).

Hubbard & Hubbard (2002) used three-dimensional stress and strain fields to predict the formation of crevasses for Haut Glacier d'Arolla using boundary conditions of glacier geometry, ice viscosity and distribution of basal sliding. Both the location of crevasse fields and the orientation of crevasses were determined. Crevasse opening was predicted to occur when a tensile stress failure criterion, in this case the maximum 10% of values calculated, was reached, based on the von Mises criterion of an octahedral stress threshold. The results of applying this approach produced both a good match between predicted failure locations and actual crevassed areas, and also between the orientation of actual crevasses and principal stress directionality. The study also highlighted the potential for the use of remotely sensed data to approximate basal motion from ice surface motion and the ice stiffness parameter, and to provide an indicator of thermal structural glaciology. Integration of such information would allow three-dimensional ice flow models, and hence stress and

strain fields, to be generated using only remotely sensed imagery. Harper et al. (1998) similarly found that values of the strain-rate tensor were able to account for distribution and orientation of crevasses for the Worthington Glacier in Alaska. Their findings concluded that crevasses were normal to the trajectories of the dominant, i.e. most tensile, strain rate. Hence, crevasses parallel to the direction of ice flow (splaying) occurred where longitudinal strain rate was compressional or ≤0, and transverse crevasses were found where there was longitudinally extending flow, ≥0. Where such relatively basic information can be inferred from measured values of strain, such predictions of crevassing can provide an adequate basis for moulin prediction in conjunction with stream pathways and modelling of crevasse propagation through the ice column, as described below.

2.3.2 Propagation of water-filled fractures

The ability of a fracture to propagate and be maintained such that it will reach the bed is determined by numerous controlling factors. These controls are of the utmost significance to prediction of moulins as they will determine whether or not a moulin can reach the bed to deliver meltwater to the ice-bedrock/sediment interface and as an input to the subglacial hydrological system. A significant body of literature exists concerning fracture mechanics and propagation of initiated surface cracks. This work, which has subsequently been applied to glacial ice, stems from theory of fracture mechanics, originally grounded in engineering and geological applications. Following early deliberation regarding the depth to which crevasses may penetrate through glacial ice by Nye (1955), Weertman (1973) expanded on the theory and applied it to the propagation of water-filled crevasses, proposing that crevasse depth would increase with depth of water-filling. The study concluded that full propagation to the bed would be possible provided that an isolated crevasse was water-filled to at least 97.4% of its depth, as the water pressure at the bottom of the crevasse would equal or exceed ice overburden pressure which would otherwise act to close the crevasse. This study was succeeded by Smith (1976), where the application of fracture mechanics produced a value of 94.6% depth of water filling for full crevasse propagation,

corresponding closely to Weertman's value. In addition, the latter study also investigated in more detail the effect of crevasse spacing on penetration depth. A crevasse within a field of crevasses will experience an effect known as 'blunting' whereby less stress is applied to the tip of the crevasse as tensile stress cannot exist within slabs of ice between closely spaced crevasses. As such, it was theorised that closely spaced crevasses would not propagate as deeply as isolated crevasses due to the compressive strain existent between them.

The stresses applied to crevasse tips are critical in determining the ability of a surface fracture to propagate, and can be described by the stress intensity factor. Van der Veen (1998) expanded on the earlier work of Smith (1976) on linear elastic fracture mechanics to calculate net stress intensity factors based on tensile stress, lithostatic stress and water pressure (assuming a crevasse is water-filled). These stress intensity factors were then used as a comparison against the ice fracture toughness, that is the threshold stress at which an existing flaw in the ice will propagate, to estimate probable penetration depths. Van der Veen (1998) concluded that penetration depth would be significantly reduced for crevasses within a relatively closely-spaced crevasse field, as the stress intensity factor for each crevasse within a field would be reduced in comparison to that of an isolated crevasse, and thus a greater tensile stress would be necessary to allow crevasses to penetrate. The study also highlighted the importance of accounting for lower density and firn layers when calculating probable crevasse depths: as firn is less dense, crevasses will penetrate more deeply where firn is present than was previously accounted for by Weertman (1973) and Smith (1976). Indeed, the presence of subsurface crevasse initiation from starter cracks in exceptional density layers at 10-30 m depth has been documented (e.g. Nath & Vaughan, 2003; Scott et al., 2010), emphasising the influence of changing tensile stresses with depth, even if the tensile strain profile remains constant. On reviewing models of crevasse penetration depth, Benn et al. (2007b) concluded from observations in the field at Breiðamerkurjökull, an outlet of Vatnajökull, that crevasse depth prediction from measured values of strain rate work adequately for both the Nye and van der Veen methods, but are significantly underestimated by the Weertman method due to its development solely for isolated crevasses.

A number of factors have been identified as having a controlling influence on the ability of a crevasse to penetrate through a full ice thickness once propagation has initiated. Van der Veen (2007) stated that the rate at which a single crevasse is filled with water is the most important factor controlling the speed and depth of fracture propagation, and that after crack initiation both the tensile stress and fracture toughness have very little effect on the propagation rate. It is important to note that not insignificant confusion is evident within the scientific literature regarding both appropriate differentiation between and quantification of the terms *tensile strength* and *fracture toughness*. Whilst Petrovic (2003) provided a review of these ice properties and was one of few studies to explicitly define the differences between the two terms, the quoted range of values of tensile strength by Petrovic, 0.7-3.1 MPa, and indeed other studies, is an order of magnitude different to those quoted by Vaughan (1993), 90-400 kPa, among others. Furthermore, quantification of fracture toughness remains largely based in laboratory testing of ice (e.g. Fischer et al., 1995; Rist et al., 1996). Alley et al. (2005b) highlighted that high stresses combined with water influx sufficient to offset refreezing via energy loss into the cold ice found in ice sheets is a necessary condition for crevasse propagation. This condition is the third of three summarised within their study of crevasse initiation and propagation through cold ice. The first two conditions reaffirm the earlier work of Weertman (1973) and van der Veen (1998): tensile stress must exceed the stress intensity at a crack tip for surface crevasse initiation, and maintained propagation will only be achieved if a crevasse is sufficiently water filled due to the inadequacy of deviatoric stress alone to offset local hydrostatic stress. Each of the studies grounded in LEFM described here assume critical failure as the mechanism for crevasse growth. Whilst Weiss (2004) explored the possibility of subcritical failure as a mechanism for crevasse formation from crystal-scale microcracks and the slow growth of crevasses in ice shelves, a lack of evidence for this exists either from field observation and measurement or from laboratory testing of glacier ice.

Alley et al. (2005b), through analytical modelling of water-driven fracture propagation, stated that supraglacial lakes are particularly important mechanisms for initiation and maintenance of surface-bed connections through large polar ice masses, due to their

ability to supply heat, increase water pressure, and thus preserve open moulins. From observations of moulin diameters on the GrIS, Box & Ski (2007) concluded that a moulin with a cross-sectional area of 10 m^2 penetrating through an 800 m ice thickness would only be able to hold around 0.1% of the water from a typical lake outburst at any one time. As such, the high discharge produced by these outbursts could potentially allow high pressure to be maintained in the subglacial system for days, resulting in prolonged uplift and enhanced surface velocities. The study backed this conclusion further by stating that the $97.4x10^6$ m^3 volume of water that was observed to drain simultaneously from two lakes in July 2003 could spread across an area of 97 km^2 of the bed if subglacial voids were 1 m in height. In a catchment constrained by bed topography this may then be sufficient to maintain high basal water pressures over prolonged periods. Connections such as this may be maintained throughout the ablation season by subsequent heat transfer by turbulent flow of water into the moulins following initial formation, allowing continual transfer of surface meltwater to the bed for lubrication. The up-glacier extent of surface-bed connections is likely to be an important factor determining the true significance of meltwater-induced velocity response. This may be controlled by factors including ice thickness, thickness of superimposed ice and the presence of firn (Parizek & Alley, 2004). These controls, among others, must be better understood, and the areal extent of the supraglacial meltwater catchments contributing to basal lubrication established, to truly determine the relative significance of meltwater propagation as a mechanism for dynamic response. Having explored these key considerations for modelling the process of melt transfer to the ice-bed interface, the components and workings of the modelling routine developed for this research project are explained in detail in chapter 3.

Chapter 3. Model development

3.1 Modelling approach

The ultimate goal of this research project is to assess the quantitative, physical controls on the routing of supraglacially-generated meltwater to the ice-bed interface, and from this assessment produce an integrated, predictive modelling routine for the temporal and spatial formation of moulins and the meltwater they deliver from the surface to the bed. This chapter will describe how the model has been developed to achieve this. One further aim of this work is to develop the model such that it is both straightforward to run and applicable to a variety of glaciers, provided the necessary data are available and reasonable values for input variables are known. Required input data take the form of Excel spreadsheets and ASCII text files, and the modelling routine has been written in its final form in Matlab, following a process of component development using GIS and grid math techniques and data processing. This chapter describes the theory behind and the workings of each component of the modelling routine (Figure 3.1.1). The necessary data inputs to the model are described, and the outputs produced through modelling are explained.

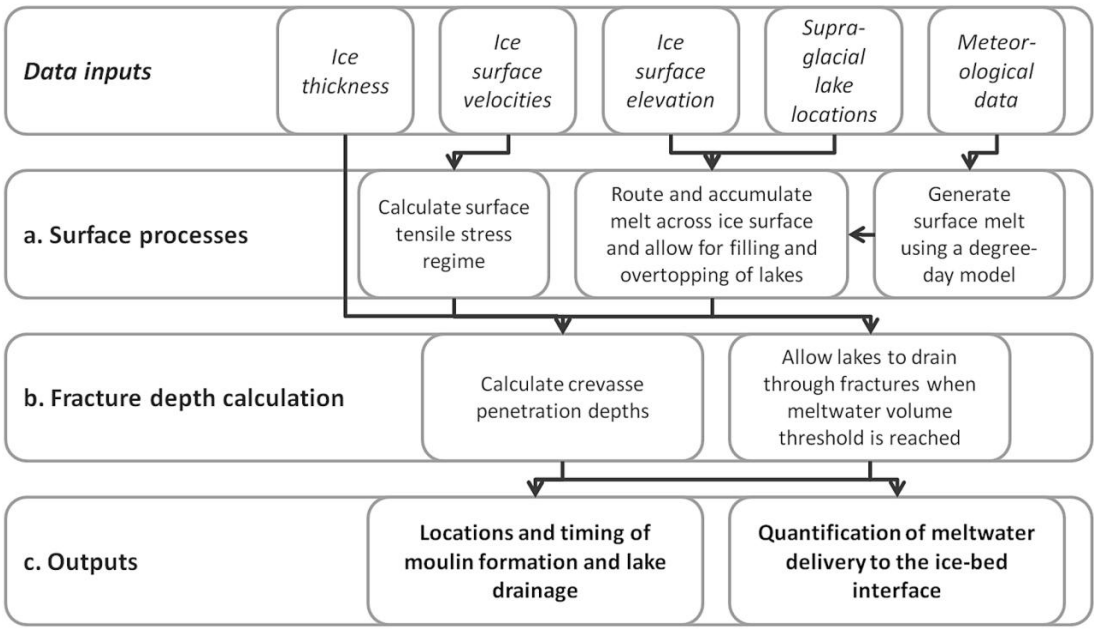

Figure 3.1.1. Model structure from data inputs to surface processes (a), fracture depth calculation (b) and outputs (c).

3.2 Ice surface melt modelling

3.2.1 Meteorological data requirements

The individual components of the modelling routine have been designed to operate based on readily available input data. As such, it was decided early on that as few meteorological input data and variables as possible should be necessary for modelled generation of surface meltwater so that model application would not be restricted only to sites where in-depth climatological studies and meteorological data collection had been carried out. This made the use of an energy balance approach redundant, given both the significantly increased necessary data requirements, and indeed the increased scope for error where data is spatially extrapolated. In light of this, and additionally due to their ability to model melt best at a lower temporal resolution due to neglecting diurnal variations (Hock, 2003), a degree-day approach was chosen to generate melt within the modelling routine. The basic data required for the melt modelling component are daily average temperatures and daily total precipitation, which are read into a "Matlab" script from an excel spreadsheet. While the modelling routine as described within the context of this thesis has been configured to run at a daily time-step, it would also be possible to generate melt and force the model at a sub-daily resolution. Data required for the degree-day modelling component are described in Table 3.2.1.1. Where multiple sites of temperature data collection are available, the air temperature lapse rate can be calculated, as was done for both sites described in chapters 4 and 5 of this thesis, otherwise a standard lapse rate for the location may be used. The density of new snow has been set at 0.3 g cm^3, but can also be altered if it can be accurately quantified in the field. Whilst the model can adjust the snowpack depth with elevation where sufficient field data are available for an accumulation gradient to be applied, the snow depth may also be kept at a constant value where a lapse rate cannot be determined due to lack of data or a weak relationship between snow depth and elevation. The data are applied to run the degree-day model, as described below.

Data/variable name	Description
“temp”	Average daily temperature data (°C)
“precip”	Daily total precipitation data (mm)
“met_elev”	Elevation (m a.s.l.) of meteorological station/temperature sensor
“temp_lapse”	Air temperature lapse rate (°C/m)
“P_s”	Density of new snow (g cm^3)
“snow_depth”	Starting snowpack depth at meteorological station (mm w.e.)
“snow_elev”	Elevation of snow depth measurement (m a.s.l.)
“accum_grad”	Snow accumulation gradient (mm w.e./m)

Table 3.2.1.1. Meteorological input data and variables for degree-day modelling in Matlab

3.2.2 Degree-day modelling

Degree-day, or *temperature index* models are a method of melt modelling based on a frequently observed correlation between air temperature and melt production (Hock, 2005). Whilst energy balance models may more fully and accurately encompass the processes relating meteorological conditions to melt production on a glacier, particularly at fine spatial and sub-daily temporal resolutions; at a catchment scale, degree-day models are often as accurate, and are used regularly for hydrological modelling studies (Hock et al., 2003; WMO, 1986). The benefits and weaknesses of each approach have been described in section 2.2.1. Degree-day factors, or the factors of proportionality between total melt and the sum of positive air temperatures for each modelled time interval, can be applied for both ice (DDF_i) and snow (DDF_s). Assigning appropriate *DDF*s is crucial to the accuracy of results from degree-day modelling, as *DDF*s vary substantially between glaciers in different regions, as was summarised by Braithwaite (1995), Braithwaite & Raper (2007) and Hock (2003), and indeed also vary within different periods of time. As such, calibration of *DDF*s with field-measured ablation is a valuable exercise. The degree-day component of the modelling routine described here calculates melt production for each cell within the spatial extent of the glacial catchment, and does this for each day of the modelled melt season. Daily average temperatures, and initial snowpack depth where possible, are

adjusted for elevation using the appropriate air temperature lapse rate and accumulation gradient. Air temperatures below 0°C are set to zero as they will be neglected within degree-day modelling which calculates melt based on only positive degree days.

Total melt produced each day, M_t, is related to mean temperature, T_t, through the application of a *DDF* for each day where T_t equals or exceeds 0°C. For a model run of '*N*' days, the total ablation, *A*, may thus be found simply as the sum of daily modelled melt values.

$$M_t = \left(DDF_{i/s} \cdot T_t\right) \qquad T_t \geq 0\ ℃ \qquad (3.1)$$

$$M_t = 0 \qquad T_t < 0\ ℃ \qquad (3.2)$$

$$A = \sum_1^N M_t \qquad (3.3)$$

The melt model component uses *DDF*s for both ice (DDF_i) and snow (DDF_s), with DDF_s applied where snowpack is present. In addition to the initial surface snowpack, any precipitation falling as snow is added to the snowpack depth. Precipitation is assumed to fall as rain when the daily average temperature is above 1°C, and to fall as snow when equal to or below 1°C (after Jóhannesson et al., 1995). In the latter case, precipitation in mm is converted to mm w.e. based on the density of new snow, and added cumulatively to the snowpack depth. As melt is calculated each day within the model and is also cumulative, DDF_s is applied until the cumulative melt exceeds the snowpack depth (initial snowpack plus falling snow), after which point DDF_i will be applied. A spatial grid of generated surface melt is produced each day within the modelling routine (Figure 3.2.2.1), and is subsequently used within the model component for weighting of meltwater flow accumulation (section 3.3.2), following calculation of the flow direction as described in the following section.

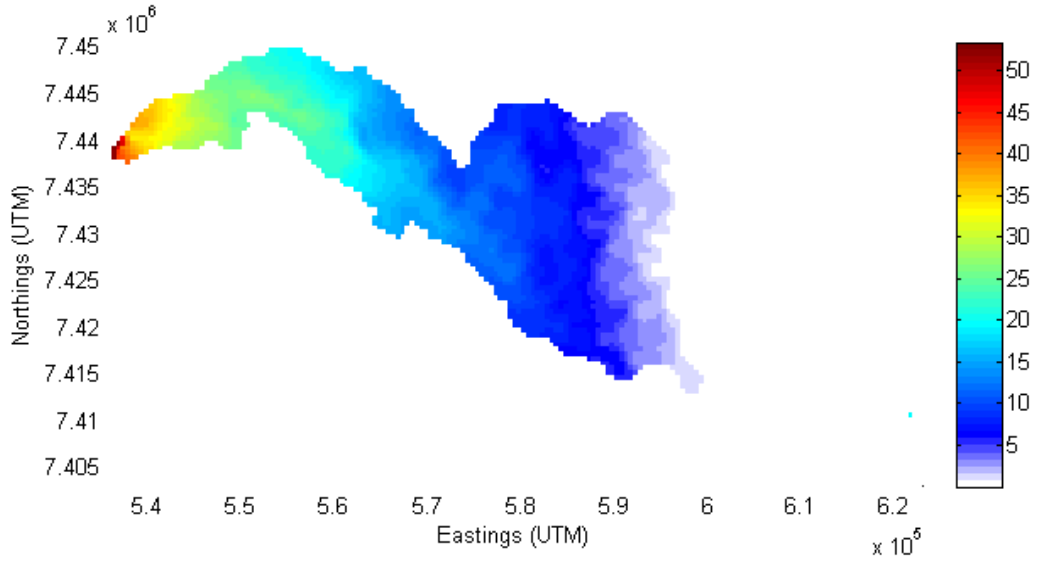

Figure 3.2.2.1. Example of a distributed melt grid output from the modelling routine for Leverett Glacier catchment (SW GrIS), JD 228, 2010. The colour bar represents mm w.e. of melt

3.3 Supraglacial meltwater routing

3.3.1 Flow direction modelling

The pathways down which water will flow across a glacial catchment can be modelled based upon the ice surface slope, as derived from surface digital elevation models (DEMs). The background to these methods is outlined in section 2.2.2. Flow direction algorithms have been developed for use in both GIS and non-GIS environments, including spatial numerical modelling (e.g. Schwanghart & Kuhn, 2010). In integrating the calculation of meltwater flow pathways within the modelling routine, initial testing with input raster format DEMs was conducted within ArcGIS. Working with commands within the 'hydrology toolbox' of ArcGIS, any sinks in the DEMs, which have an undefined direction of flow often resulting from small errors in the DEM data values, were firstly filled to ensure continuation of flow across the ice surface. The 'Flow Direction' command was used to produce an output raster of flow direction values based on the direction of flow between each raster cell and the steepest pathway to one of its eight neighbouring cells. This flow direction algorithm is known as a *single flow direction* or *D8* algorithm. Whilst *multiple flow direction* algorithms which weight

and partition flow between each neighbouring cell, can also be applied, the use of the single flow direction method and subsequent topographic analysis produced results that matched encouragingly well with supraglacial meltwater streams visible on remotely sensed imagery. Within the final modelling routine, the single flow direction algorithm is applied using a function included in TopoToolbox, a freely available set of tools for DEM analysis within Matlab (Schwanghart & Kuhn, 2010). The result of flow direction modelling is used to calculate the flow accumulation, as will now be described.

3.3.2 Meltwater-weighted flow accumulation

The modelling routine was designed to run at a daily resolution, with distributed surface melt being modelled for each day as described in section 3.2. It was thus necessary for flow routing and weighted distribution of generated meltwater across the ice surface to be calculated each day within the model. Flow accumulation is the upslope drainage area contributing flow of water into a given cell, and is controlled by the input flow direction grid. Where each upslope cell is assigned a value of melt generated from distributed melt modelling, these values can be used to weight flow accumulation such that the value of meltwater contained within an individual cell represents the total meltwater routed into that cell from above within each 24 hour period. During initial testing within ArcGIS, the 'Flow Accumulation' command within the hydrology toolbox was applied followed by extraction of a stream network through conditional analysis. By setting a threshold value above which cells in the flow accumulation grid will be included within the predicted stream network, the dendricity of the network can be controlled. Low threshold values produce highly dendritic stream networks, and higher threshold values produce less dendritic networks, as the larger the cell value, the higher the number of upstream cells necessary for contribution to stream generation. However, due to the errors associated with DEMs and the non-static nature of supraglacial streams, accurately defining such a threshold for stream locations is problematic. As such, the output of the TopoToolbox flow

accumulation function used within the Matlab modelling routine is not amended further to delineate individual stream pathways (Figure 3.3.2.1).

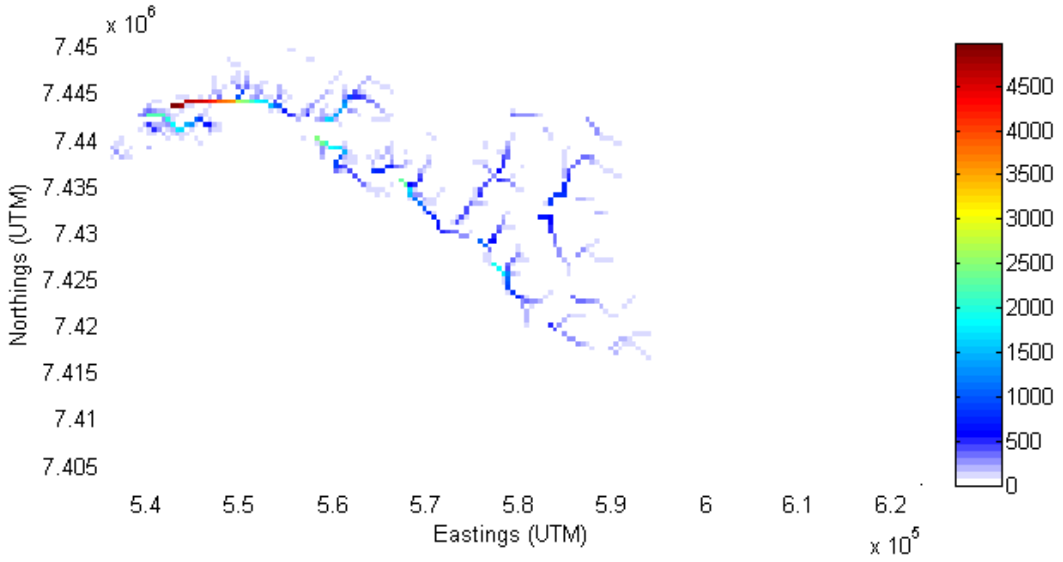

Figure 3.3.2.1. Example of a weighted flow accumulation grid output from the modelling routine for Leverett Glacier catchment (SW GrIS), JD 228, 2010. The colour bar represents mm w.e. of accumulated meltwater

Within the Matlab modelling routine, meltwater-weighted flow accumulation is interrupted when meltwater flow pathways intersect cells for which either surface crevassing has been predicted or where melt flows into a supraglacial lake. This is implemented within the model code by using a runoff ratio, such that the ratio of melt transfer from one cell to the next downstream cell is 1 when there is no obstacle to interrupt flow, and is 0 when flow meets a crevasse or lake. Thus, when water meets a cell containing a crevasse, flow must begin accumulating again downstream of the crevasse. In section 3.5.1, the usage of daily values of meltwater-weighted flow accumulation is described as an input for modelling of and primary control on the depth of water-filled crevasses. The implementation of melt storage and flow through supraglacial lakes within flow accumulation is now described, following an explanation of how lake area and storage volume are calculated.

3.3.3 Supraglacial lakes

Following initial model testing which suggested that not enough of surface-generated melt was reaching the ice-bed interface when water-filled crevasses alone were considered as surface-to-bed connections for meltwater transfer, the inclusion of supraglacial lakes within the modelling routine was investigated. With a dearth of understanding of the processes leading to lake drainage, it was acknowledged that a simplistic, conceptual approach to prediction of lake drainage events within the modelling routine would have to be taken within the context of this research project. Firstly, the outlines of supraglacial lakes within the study catchments were digitised by hand in ArcGIS (Figure 3.3.3.1, a), producing a raster representing the maximum known extent of lake surface area based on multiple images of the study regions. A script was written in Matlab to read the binary lake area raster, and assign coordinates to the centre of mass of each cluster of connected lake cells, or *connected components*, using the 'Centroid' function (Figure 3.3.3.1, b).

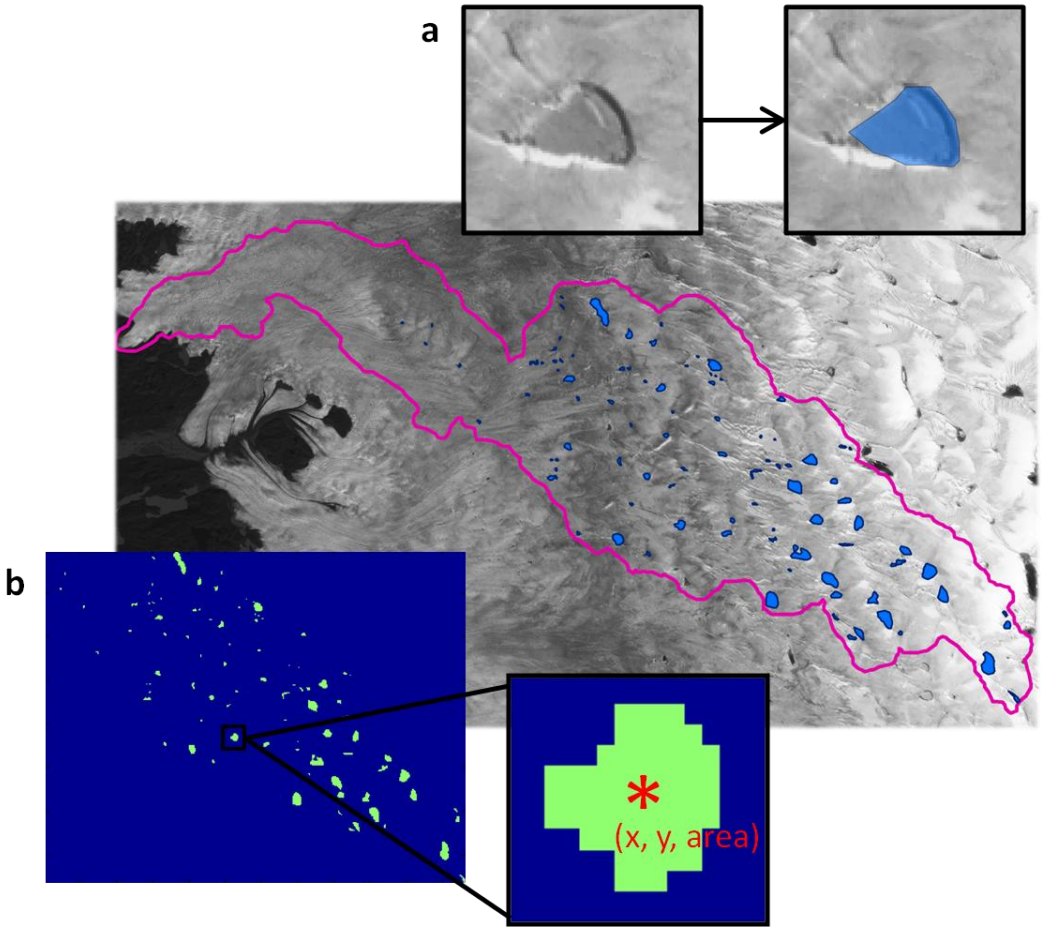

Figure 3.3.3.1. Digitisation of supraglacial lakes (a) from Landsat imagery of Leverett catchment, southwest Greenland, and allocation of the centre of mass to connected components (b).

The lake surface area, in km^2, was used to estimate lake volume, in 10^6 m^3, based on a linear equation with an R^2 value of 0.94, relating the maximum area and volume of lakes before drainage events, identified in table 6 of Box & Ski (2007). In the context of the main modelling routine, the filling of lakes is included such that within the flow accumulation function meltwater is routed into lake cells and is not transferred further downstream until the melt storage exceeds the pre-defined maximum lake volume. Thus, each day, newly generated melt routed into a lake will either be added to the water stored within that lake cell, or will continue downstream to contribute to meltwater accumulation. Additionally, cells containing supraglacial lakes begin with a runoff ratio of 0, as they act as a sink for meltwater routed across the ice surface. When the meltwater content of a lake reaches its maximum volume, unless basal

drainage occurs, the lake will overtop, and a runoff ratio of 1 will be assigned to that lake location on the grid. Another major component of the modelling routine is the tensile stress regime, which controls crevasse locations and contributes to the calculation of crevasse propagation. The calculation of the surface tensile stresses is now described.

3.4 Ice surface tensile stress regime

3.4.1 Deriving strain rates from ice surface velocities

In line with the melt modelling and flow routing components of the modelling routine, the identification of areas likely to contain surface crevassing begins with basic, readily available input data; in this case ice surface velocities. From ice surface velocity data the surface strains, and subsequently the surface stress regime, may be determined. Where velocity data is directional, for example when they have been derived using speckle tracking methods, both longitudinal and transverse components of surface velocity can be calculated. In such a case, the angle of flow can be used in conjunction with the azimuth of the data points, to resolve the measured velocity, V_u, into its longitudinal, V_x, and transverse, V_y, components based on the angle between the azimuth and average flow direction, α. On this basis, longitudinal and transverse velocities may be calculated from,

$$V_x = V_u \cos \alpha \qquad (3.4)$$

$$V_y = V_u \sin \alpha \qquad (3.5)$$

In the terrain modelling software, 'Surfer', strain rates can be calculated simply from ASCII grids of ice velocity by applying the directional derivative function of grid calculus. However, it was first necessary to calculate strain rates using a step-by-step numerical method that could be transferable between various modelling and GIS platforms including Surfer, ArcGIS and Matlab. The directional first derivative, as applied to strain rate calculation, may be defined as the change in velocity over a

distance in a single defined glacial flow direction. For the purposes of this study the specified flow direction is the average angle of flow of the glacier centreline or for distinctive sections of a glacier defined by significantly different flow trajectories. The two basic components necessary to find the directional derivative of velocity data are the velocity gradient and the velocity aspect. To calculate the gradient in Surfer the 'gradient operator' option within 'grid calculus' can be applied to a grid of surface velocity. Working with the same velocity grid, the 'terrain aspect' function of 'terrain modelling' is applied to produce a grid of aspect in degrees, based on the polar coordinate system, degrees east of north. To enable the aspect data to be applicable to calculating the directional derivative, it must first be converted into the Cartesian coordinate system. To do this, 180° must be subtracted from the grid, reversing the polarity of aspect values. As the derivative is calculated with respect to the x-axis, it is also necessary to ensure that this is in alignment with the direction of flow as specified for the section of glacier represented within a grid. This adjustment, as related to the Cartesian coordinate system, is illustrated below (Figure 3.4.1.1), where in this example the longitudinal flow direction is a polar angle, or azimuth, of 105°, and the transverse flow angle is 15°:

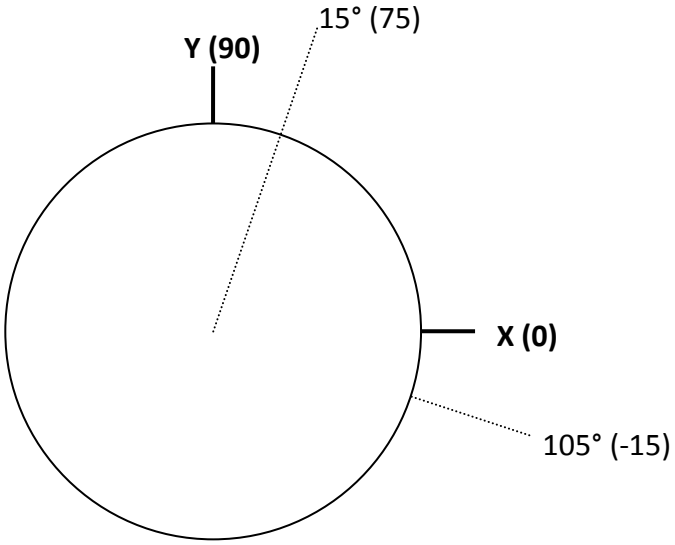

Figure 3.4.1.1. Aspect grid adjustment for ice flow direction into an x-direction, relating the polar coordinate system to the Cartesian coordinate system

From Figure 3.4.1.1, it can be inferred that for a longitudinal polar flow direction azimuth of 105°, 15 degrees should be subtracted from the grid of velocity aspect so that the direction of flow is parallel to the x-axis, or zero degrees, in the Cartesian system. If we wish to adjust transverse flow direction into the x direction, 75° should be added to the aspect grid. Thus, where the flow direction is clockwise of zero in the Cartesian system, the value of the angle between zero and the azimuth should be subtracted. When the flow direction is anticlockwise of zero (but not exceeding 90° in Cartesian) the angle between zero and the azimuth should be added to the aspect grid. Following adjustment for flow azimuth, the aspect grid must finally be converted into radians:

$$1° = 1 \cdot \frac{\pi}{180} \approx 0.0175\ rad \quad (3.6)$$

To calculate strain rates from the resultant grids of velocity gradient and aspect, the gradient of velocity between two cells (*df/dx*), must be multiplied by the sine or cosine of the aspect grid, dependent on which strain rate is being calculated:

$$\dot{\varepsilon}_{xx} = \frac{df}{dx} sin\ \alpha \quad (3.7)$$

$$\dot{\varepsilon}_{yy} = \frac{df}{dx} sin\ \alpha \quad (3.8)$$

$$Lateral\ shear = \frac{df}{dx} cos\ \alpha \quad (3.9)$$

$$Turning\ of\ flow = -\left[\frac{df}{dx} cos\ \alpha\right] \quad (3.10)$$

Both the longitudinal strain rate, $\dot{\varepsilon}_{xx}$, and the lateral shear are calculated from grids of gradient and aspect derived from data representing the longitudinal component of velocity. The aspect grid in this case should be adjusted with respect to the longitudinal flow azimuth. Where data for the transverse component of velocity is available, for example from speckle tracking data, the transverse strain rate, $\dot{\varepsilon}_{yy}$, and the turning of flow can be calculated based on the data. Aspect should be adjusted for the transverse flow azimuth which is perpendicular to the longitudinal flow azimuth.

As mentioned previously, strain rates may also be calculated quickly and simply within Surfer, using the grid calculus 'directional derivative' function. Inputting the angle of the flow within the directional derivative function produces a grid of longitudinal strain, $\dot{\varepsilon}_{xx}$, when longitudinal velocity is used as the input grid and where ∂x is the original longitudinal length, and ∂u_x is the extensional longitudinal length. The lateral shear, a component of the shear strain, can be calculated when the angle perpendicular to the flow direction is used and where ∂y is the original transverse length,

$$\dot{\varepsilon}_{xx} = \frac{\partial u_x}{\partial x} \qquad (3.11)$$

$$Lateral\ shear = \frac{\partial u_x}{\partial y} \qquad (3.12)$$

Where the transverse velocity grid is the input grid, and the angle perpendicular to the flow line is used, the transverse strain rate can be calculated using the first derivative function where $\dot{\varepsilon}_{yy}$ represents the transverse strain rate, ∂y is the original transverse length, and ∂u_y is the extensional transverse length. Finally, the other component of shear strain, turning of flow, can also be calculated from the transverse velocity grid using the flow line direction as the input angle,

$$\dot{\varepsilon}_{yy} = \frac{\partial u_y}{\partial y} \qquad (3.13)$$

$$Turning\ of\ flow = \frac{\partial u_y}{\partial x} \qquad (3.14)$$

From these resultant directional derivatives outputs, the vertical, $\dot{\varepsilon}_{zz}$, shear, $\dot{\varepsilon}_{xy}$, and effective, $\dot{\varepsilon}_e$, strain rates can be calculated within Surfer using grid math. The shear strain can be derived by combining the lateral shear and turning of flow components, whilst the effective strain rate describes the total strain acting upon the ice surface,

$$\dot{\varepsilon}_{zz} = -\dot{\varepsilon}_{xx} - \dot{\varepsilon}_{yy} \qquad (3.15)$$

$$\dot{\varepsilon}_{xy} = \frac{1}{2}\left(\frac{\partial u_x}{\partial y} + \frac{\partial u_y}{\partial x}\right) \qquad (3.16)$$

$$\dot{\varepsilon_e}^2 = \frac{1}{2}\left(\dot{\varepsilon}_{xx}{}^2 + \dot{\varepsilon}_{yy}{}^2 + \dot{\varepsilon}_{zz}{}^2\right) + \dot{\varepsilon}_{xy}{}^2 \qquad (3.17)$$

3.4.2 Ice surface tensile stress regime

From the resultant ice surface strain rate grids, the longitudinal, σ_{xx}, transverse, σ_{yy}, and shear, τ_{xy}, stresses can be determined by applying the reverse constitutive relation, either using Surfer grid math or within a Matlab script, where *n* is 3 and *B* is a stiffness parameter sensitive to temperature.

$$\sigma_{xx} = B\ \dot{\varepsilon}_e{}^{(1-n)/n}\dot{\varepsilon}_{xx} \qquad (3.18)$$

$$\sigma_{yy} = B\ \dot{\varepsilon}_e{}^{(1-n)/n}\dot{\varepsilon}_{yy} \qquad (3.19)$$

$$\tau_{xy} = B\ \dot{\varepsilon}_e{}^{(1-n)/n}\dot{\varepsilon}_{xy} \qquad (3.20)$$

Areas likely to contain surface crevassing have previously been predicted based upon calculated tensile stresses exceeding a prescribed value of tensile strength. This is discussed by Vaughan (1993), where an envelope of values of tensile stress for failure, derived from a sample of strain rates for various glaciers, was in the range predicted by both the Coulomb and von Mises failure criteria, applicable to failure of brittle materials. The von Mises stress is used to illustrate the yield strength of a material, a critical value of stress which represents the point at which a material is deemed to have begun yielding, and as such will permanently deform. The maximum and minimum, or principal stresses, are required to calculate the von Mises stress, and may be determined following:

$$\sigma_1 = \sigma_{max} = \frac{1}{2}\left(\sigma_{xx} + \sigma_{yy}\right) + \sqrt{\left[\frac{1}{2}\left(\sigma_{xx} - \sigma_{yy}\right)\right]^2 + \tau^2{}_{xy}} \qquad (3.21)$$

$$\sigma_3 = \sigma_{min} = \frac{1}{2}\left(\sigma_{xx} + \sigma_{yy}\right) - \sqrt{\left[\frac{1}{2}\left(\sigma_{xx} - \sigma_{yy}\right)\right]^2 + \tau^2{}_{xy}} \qquad (3.22)$$

The resultant grids of maximum and minimum stress are used to calculate the 'von Mises stress', σ_v, which can also be thought of as the equivalent tensile stress (Vaughan, 1993). The von Mises yield criterion is applied within the context of this modelling study, and the von Mises, or equivalent tensile, stress is calculated from,

$$\sigma_v{}^2 = (\sigma_1\sigma_1) + (\sigma_3\sigma_3) - (\sigma_1\sigma_3) \qquad (3.23)$$

The resultant grid of tensile stresses is used for calculation of the penetration of crevasses, when combined with the inflow of meltwater to these crevasses, as will now be explained.

3.5 Modelling moulin formation

3.5.1 Calculating penetration depths of water-filled crevasses

With an objective to allow for modelling of moulin formation in glacial catchments with minimal data requirements, appropriate models for calculating the penetration depth of water-filled crevasses were investigated. Modelling based on linear elastic fracture mechanics (LEFM) is one method which may be applied to penetration of surface-originating crevasses, despite the non-linear visco-elastic rheology of glacier ice when deformed under stress (van der Veen, 1998). In accordance with LEFM, fracture opening mode 'I' can satisfactorily describe cracking in ice where normal stresses are perpendicular to the tip-to-tip length of the surface fracture, resulting in an opening direction analogous to the normal stress (Figure 3.5.1.1).

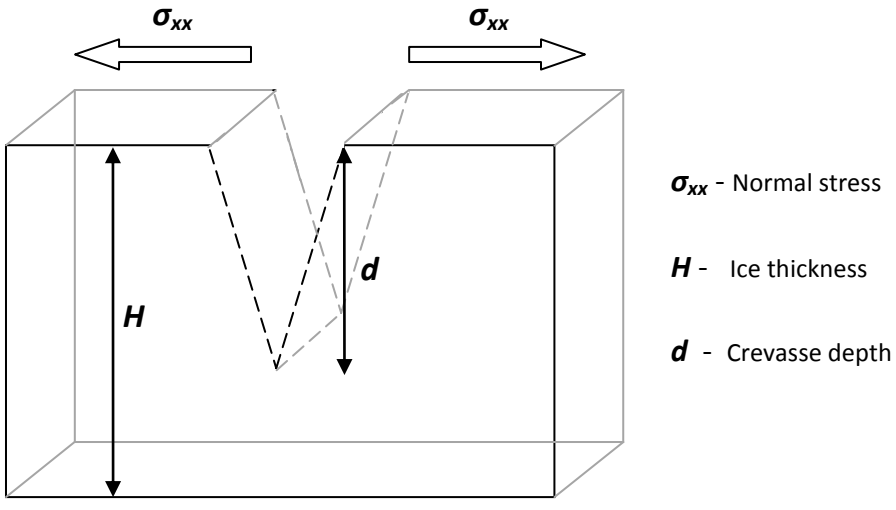

Figure 3.5.1.1. Crack propagation mode 1

To investigate mode I fracture propagation of surface crevasses, Van der Veen (1998) described calculation of the net stress intensity factor, K_I, accounting for the effects of tensile stress and the lithostatic stress of ice, offset by the effect of water pressure. For a single crevasse of depth, d, under tensile stress R_{xx}, within a glacier of ice thickness, H, the stress intensity factor relating to the tensile stress, $K_I^{(1)}$, can be found from,

$$K_I^{(1)} = F(\lambda) R_{xx} \sqrt{\pi d} \quad (3.24)$$

where:

$$F(\lambda) = 1.12 - 0.23 \cdot \lambda + 10.55 \cdot \lambda^2 - 21.72 \cdot \lambda^3 + 30.39 \cdot \lambda^4 \quad (3.25)$$

and where λ is the ratio of crevasse depth to the thickness of the ice. The lithostatic stress component, $K_I^{(2)}$, incorporating the density of ice, ρ_i, acceleration due to gravity, g, and the depth of the crevasse below the ice surface, d, represents the overburden pressure of ice as it increases with depth, and the variant shown below is a constant density solution,

$$K_I^{(2)} = \frac{2\rho_i g}{\sqrt{\pi d}} \int_0^d -b_i G(\gamma, \lambda) d b_i \quad (3.26)$$

The forces contributing to this component are integrated over crevasse depth, d, where b_i is the depth below the ice surface during integration, and as such, a depth-varying density solution can be incorporated, with a density value of surface snow defined. However, this does not accurately represent the thickness of lower density layers, assuming increasing density with depth throughout the ice column. The function $G(\gamma,\lambda)$, where $\gamma = b_i/d$ and $\lambda = d/H$, is applied to represent fitting a polynomial curve to numerical solutions, and is given by:

$$G(\gamma, \lambda) = \frac{3.52(1-\gamma)}{(1-\lambda)^{\frac{3}{2}}} - \frac{4.35 - 5.28\gamma}{(1-\lambda)^{\frac{1}{2}}} + \left[\frac{1.30 - 0.30\gamma^{3/2}}{(1-\gamma^2)^{1/2}} + 0.83 - 1.76\gamma\right] \times [1 - (1-\gamma)\lambda] \quad (3.27)$$

This method applies to propagation of a water-filled crevasse, thus, the stress intensity factor associated with water pressure inside the crevasse must also be included. Where 'a' is the depth of the water level below the ice surface, and ρ_w is the density of freshwater, the stress intensity factor is represented by:

$$K_I^{(3)} = \frac{2\rho_w g}{\sqrt{\pi d}} \int_a^d (b_i - a) G(\gamma, \lambda) db_i \quad (3.28)$$

Due to the greater density of water in comparison to ice, this component can act to offset crevasse closure due to the lithostatic stress. Thus, when $K_I^{(3)}$ equals $-K_I^{(2)}$, the water level below the crevasse is sufficiently high to offset closure. Summation of these three stress intensity factor terms produces a value of the net stress intensity factor, K_I, for a single water-filled crevasse. The penetration depth of a crevasse may, therefore, be calculated by incrementing values of d from zero, solving '$K_I = K_I^{(1)} + K_I^{(2)} + K_I^{(3)}$' until '$K_I = K_{IC}$'. K_{IC} is a prescribed value of fracture toughness, and has been quantified experimentally using glacier ice by only a limited number of studies (e.g. Fischer et al., 1995; Rist et al., 1996). Experimentally-determined fracture toughness values range from c.100 to c.400 kPa $m^{1/2}$. Where K_I at the ice surface is less than $K_{IC,}$ a crevasse cannot initiate. Thus, as the net stress intensity factor is recalculated when the model iterates through values of *d*, a crevasse can only continue to penetrate through the ice while K_I is greater than $K_{IC,}$ and may do so through the full ice-thickness as long as K_I exceeds the prescribed fracture toughness. Van der Veen (1998) also explored the effect of spacing between multiple crevasses, given that closely-spaced crevasses can undergo a blunting effect at crevasse tips caused by the lack of tensile stresses in the slabs of ice between crevasses (Weertman, 1973). The study found that the net stress intensity factor decreased as crevasse spacing decreased, but as a function of depth it was similar to a single crevasse, suggesting water can reach the bed within a field of crevasses, but the tensile stress or water level would likely need to be larger to accommodate this.

A simplified equation encompassing the three components of the net stress intensity factor, K_I, was described by van der Veen (2007), relating to the original work of Smith (1976) for penetration of single water-filled crevasses. This method neglects the blunting effect resulting from closely-spaced crevasses, but benefits from not requiring knowledge of the ice thickness as it is not a depth-integrated solution. Given that ice thickness is likely one of the largest sources of error in the datasets required for prediction of moulins within this modelling routine, and given the reduced computing expense required by taking this simplified approach, the model of crevasse depth

calculation described below has been adopted for the purposes of this study. Using the abbreviated version, K_I, the sum of $K_I^{(1)}$, $K_I^{(2)}$ and $K_I^{(3)}$, can be found, in estimation, from,

$$K_I = 1.12R_{xx}\sqrt{\pi d} - 0.683\rho_i g d^{1.5} + 0.683\rho_w g b^{1.5} \qquad (3.29)$$

The first term in this equation represents the stress intensity factor $K_I^{(1)}$ relating to tensile stress, R_{xx}. The second term represents the lithostatic stress component, $K_I^{(2)}$, and is negative as the crevasse tends towards closure due to the weight of the ice. Corresponding to the effect of water pressure, term three, $K_I^{(3)}$, is positive, where '*b*' is the water level within a crevasse, and works to offset closure by ice overburden pressure. Where crevasse depth is known, this equation may be used to estimate the net stress intensity factor. However, by setting K_I equal to ice fracture toughness, K_{IC}, crevasse depth may be calculated each day when the values of the other variables are known. Where '*Q*' is the rate at which water fills a crevasse and *'t'* is time in hours, the water level in the crevasse, *b*, is determined from

$$b = Qt \qquad (3.30)$$

In agreement with Van der Veen (2007), by setting K_I to equal K_{IC} and solving for depth for a range of values of R_{xx} and *Q*, it is apparent that *Q*, the rate at which water fills the crevasse, is the most important control on the depth to which a single crevasse will penetrate linearly with time (Figure 3.5.1.2).

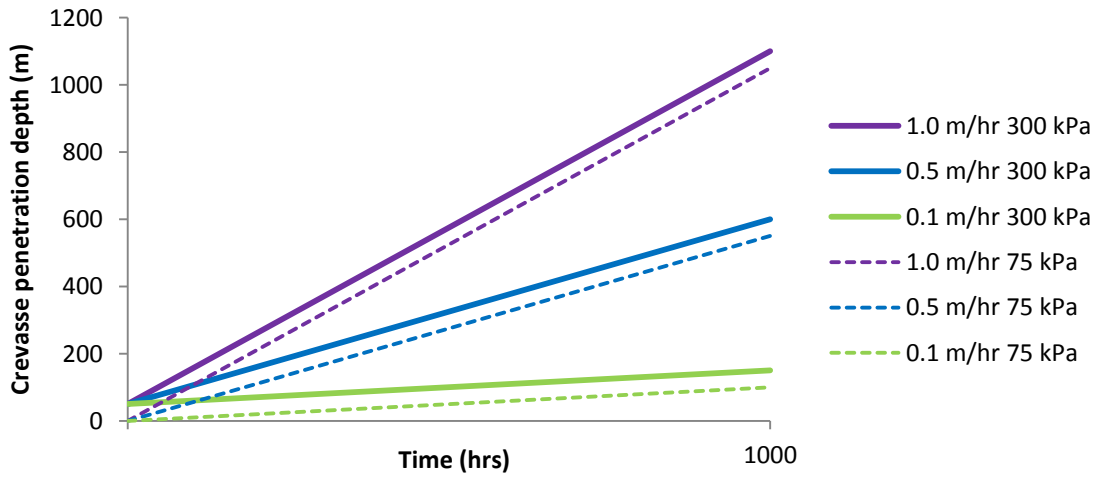

Figure 3.5.1.2. Propagation depth of a water-filled crevasse for rates of water filling of 1.0, 0.5 and 0.1 m/hr, and tensile stresses of 300 and 75 kPa, after Figure 2 of van der Veen (2007)

This method does not account for the finite thickness of ice, and thus, the ratio of crevasse depth to ice thickness ($\lambda = d/H$) is assumed to be small. This results in underestimation of term $K_I^{(1)}$ where crevasses propagate to greater than c.1/3rd of the ice thickness. However, as we are dealing with propagation of water-filled crevasses, and crevasses penetrating to great depth can only exist where the water level in the crevasse is 97.35% of crevasse depth (Weertman, 1973), term $K_I^{(3)}$, will be large enough to support propagation to the bed. This modelling routine is primarily interested in only those crevasses that reach the bed to deliver meltwater to the subglacial system, and less so on the depth of those that do not. As such, where sufficient water is routed into a crevasse, that crevasse should reach the bed regardless of small underestimation errors. In addition to the prediction of moulins, through water-driven fracture propagation of surface crevasses, the model also allows for the drainage of supraglacial lakes through lake-basal fractures. The mechanism for drainage within the modelling routine is explained in the next section.

3.5.2 Drainage of supraglacial lakes

In contrast to crevasse depth modelling of normal surface crevasses, which is only applied when the tensile stress exceeds the prescribed ice tensile strength, any lake cell may drain through a fracture regardless of the tensile stress value of that cell. The model allows for drainage of lakes through any cell since lake growth is often found in areas typified by compressive or very low tensile ice surface stresses (Catania et al., 2008). If the combined stress intensity of the tensile stress and lake water content does not meet the necessary level to drive full ice-thickness fracture, the lake may still reach its maximum prescribed volume, overtop, and contribute to water-filling of a downstream crevasse or moulin. It should be noted here that channel downcutting is not considered currently within the modelling routine, but may be a useful inclusion in future work to allow for lake drainage via overtopping and consequent formation of an exit channel.

The simplified LEFM model (van der Veen, 2007) described in section 3.5.1 is also used to predict drainage of supraglacial lakes within the modelling routine. In contrast to predicting the formation of moulins by solving for crevasse depth each day, '*d*' is set to the ice thickness at each lake cell. The meltwater content of a lake as it accumulates with each daily time-step is used to determine the rate at which water would fill a crevasse should drainage occur. This is achieved by converting the lake melt content in mm w.e. to crevasse water depth in m w.e., adjusted for crevasse width and length to produce the correct fill depth for given internal crevasse dimensions, producing a value for *b*. The equation is solved for 'K_I' each day, and when 'K_I' equals or exceeds the prescribed ice fracture toughness, and thus the accumulated meltwater content within a lake is sufficient to produce a crevasse depth equal to the ice thickness, the entire melt content of that lake is transferred to the bed within one model time-step. This allowance for fast drainage of lakes within a period of 24 hours is based on evidence of fast drainage of a large supraglacial lake by Das et al. (2008). Box and Ski (2007) also highlighted the drainage of lakes within less than 24 hours, whilst stating that the subglacial system could remain pressurised for days when moulins draining lakes reach the bed, since a single moulin may not have the capacity to store the full lake content, thus lake drainage would occur more slowly. Without knowledge of subglacial configuration to influence water pressure and englacial storage times, lake drainage is therefore assumed to occur within one day in this model. Following the drainage of a lake, or indeed the formation of a moulin, any meltwater routed into that cell will be subsequently transferred to the bed each day for the remainder of the model run, thus assuming that a surface-to-bed connection will remain open throughout the melt season.

3.5.3 Timing and locations of moulin formation and meltwater delivery to the bed

Addressing the main aim of this research, the primary outputs of the modelling routine are predicted surface-to-bed connections through moulin formation and lake drainages, and quantification of meltwater transferred to the bed through these

connections. Moulin formation and lake drainage events are recorded during each daily time step, for which spatially distributed grids of their locations within the study area are produced within the appropriate coordinate system. These outputs allow the spatial and temporal evolution of connections between the supraglacial and subglacial systems to be predicted and evaluated. Furthermore, both the total amount of water transferred from the ice surface to the bed and the amount transferred through each individual moulin are modelled. This allows for evaluation of what proportion of surface-generated melt makes it to the bed, and how meltwater delivery patterns change with each day and across the glacial catchment, dependent on surface melt production and routing. In addition to quantification of meltwater transfer from the surface to the bed in mm water equivalent, melt reaching the bed is also expressed as discharge in $m^3 s^{-1}$, or 'cumecs', which describes the number of cubic metres of water passing a point in a second. Where proglacial discharge data is available, it is possible to compare daily average modelled melt delivery with measured daily average proglacial discharge, as demonstrated by model application to Leverett Glacier in SW Greenland, described in chapter 5. Focussing on individual moulins, it would also be possible to compare the discharge entering a single, correctly-predicted, moulin with measured discharge recorded in the field.

The ability to model the formation of moulins and quantify the meltwater delivered to the ice-bed across the spatial extent of the system throughout the melt season could be of value to models of subglacial hydrology and ice dynamics, for which spatially distributed supraglacial meltwater point inputs are often currently either neglected or prescribed. Given the influence of supraglacial forcing on subglacial water pressures and the evolution of the subglacial system, and the implications this has for ice dynamics, inclusion of distributed meltwater point inputs to the ice-bed interface is an important consideration for future coupled models of glacier hydrology and dynamics, and indeed of glacier and ice sheet evolution.

The following chapters of this thesis, chapters 4 and 5, now describe model application to two real glacial catchments: The Croker Bay catchment of Devon Ice Cap, and Leverett Glacier catchment of the southwest Greenland Ice Sheet. The results of model application are illustrated for two contrasting ablation seasons in each case, and

include a thorough sensitivity analysis for the Croker Bay catchment, as well as an investigation into model predictive accuracy through comparison with field observations on Leverett Glacier.

Chapter 4. Modelling the delivery of supraglacial meltwater to the ice-bed interface: application to southwest Devon Ice Cap, Nunavut, Canada

4.1 Abstract

The transfer of surface-generated meltwater to the subglacial drainage system through full ice thickness crevassing may lead to accelerated glacier velocities, with implications for ice motion under future climatic scenarios. Accurate predictions of where surface meltwater accesses the ice-bed interface are therefore needed in fully coupled hydro-dynamic ice sheet models. In this chapter, the spatially-distributed modelling routine for predicting the location and timing of delivery of surface-derived meltwater to the ice-bed interface through moulins and supraglacial lake drainage is explained as it is applied to the Croker Bay glacial catchment of Devon Ice Cap. The formation of moulins, drainage of lakes, and the transfer of meltwater through the full ice thickness are modelled for the 2004 and 2006 ablation seasons. Through this case study the model's sensitivity to degree day factors, fracture toughness, tensile strength and crevasse width is assessed, confirming that parameters influencing the rate at which water fills a crevasse are the most significant controls on the ability of a crevasse to reach the bed. Increased surface melt production, therefore, has the potential to significantly influence the spatial and temporal transfer of meltwater through surface-to-bed connections in a warmer climate. The results and model sensitivity testing presented within this chapter have been published in Clason et al. (2012).

4.2 Introduction

Many models of ice sheet and glacier evolution base their predictions on dynamical response to perturbations in the ice shelf or ice tongue, and the grounding line for marine outlet systems, as well as the surface mass balance driven by climatic forcing. Field based studies have established that glacier and ice-sheet surface velocities can demonstrate a dynamic response to rising air temperature when surface-derived

meltwater reaches the ice-bed interface causing high subglacial water pressures, lubricating the glacier bed and promoting enhanced basal motion (Iken and Bindschadler, 1986; Zwally et al., 2002; Bingham et al., 2003; Shepherd et al., 2009; Bartholomew et al., 2010). There exists ongoing debate about the long-term significance of this effect on dynamic thinning and mass loss of glaciers and ice sheets, particularly in relation to the Greenland Ice Sheet (Parizek and Alley, 2004; van de Wal et al., 2008; Sundal et al., 2011, Bartholomew et al., 2011). Resolution of this issue requires more comprehensive temporal and spatial measurements of the association between melt and velocity from which more empirically robust physical relationships can be derived for use in ice sheet models that couple hydrology and dynamics. Both drainage of ponded meltwater (Das et al., 2008) and the direct influx of meltwater in supraglacial streams into surface crevasses or moulins are likely sources for dynamic forcing in response to supraglacial meltwater inputs. Existing coupled models of glacial hydrology and dynamics *prescribe* rather than *predict* the location of connections between the supraglacial and subglacial systems (Flowers & Clarke, 2002; Pimentel et al., 2010). Representation of the dynamic response to surficially-derived meltwater accessing the ice-bed interface is a mechanism which thus remains without physical basis in these models. To assess the long-term significance of this mechanism for ice sheet mass evolution in a changing climate it is necessary to model the temporal and spatial patterns of meltwater delivery to the ice-bed interface.

This chapter presents the application of the spatially distributed model described in chapter 3 to a glacial catchment in the Canadian High Arctic, predicting the spatial and temporal patterns of surface-derived meltwater delivery to the bed. The model structure is represented in Figure 3.1.1 of chapter 3. Each stage of the modelling routine is explained in this chapter in the context of the case study site to which it is applied, the Croker Bay catchment area of Devon Ice Cap. Total summer surface ablation is modelled across the study catchment, in this case using a simple degree-day model, and daily distributed values of melt are subsequently used to weight meltwater flow accumulation across the ice surface. Areas of surface crevassing are identified where tensile resistive stresses, calculated from strain rates derived from InSAR velocity data, exceed a threshold value of tensile strength (Figure 3.1.1, a). Following

the principles of linear elastic fracture mechanics (LEFM), a model of water-driven fracture propagation for calculation of crevasse depths (van der Veen, 2007) is used to identify where and when surface-to-bed connections form (Figure 3.1.1, b). The transfer of surface-generated meltwater to the bed through full ice-thickness crevasses and drainage of supraglacial lakes through basal fractures are modelled (Figure 3.1.1, c).

4.3 Study area

Devon Island is one of the Queen Elizabeth Islands in Nunavut, High Arctic Canada. Devon Ice Cap at c.14000 km^2 is one of the largest ice caps in the Arctic and has been the focus of extensive glacial research for nearly 50 years (Boon et al., 2010). This chapter investigates the south-west region of the ice cap, specifically the Croker Bay catchment (Figure 4.3.1), which feeds the North (NCB) and South Croker Bay (SCB) glaciers. This region was chosen due to availability of data necessary for the model. The ice surface elevation in this catchment extends from the marine calving termini of NCB and SCB glaciers up to 1853 m, approaching the ice cap summit at c.1930 m. Distinct dynamic flow regimes across the ice cap were identified from InSAR velocity data by Burgess et al. (2005). The first flow regime, regime 1, found in the upper reaches above outlet glaciers, was representative of flow through internal deformation where ice is likely frozen to the bed. Outlet glaciers including the NCB and SCB glaciers were characterised by a transition from flow regime 2, indicative of contribution by basal motion to surface velocity, possibly promoted by constraining bedrock topography, to flow regime 3, characterised by a significantly increased contribution from basal motion, possibly enhanced by meltwater reaching the bed (Figures 4.3.1 and 4.4.1.1). This transition was particularly clear at NCB glacier where velocity increased from 60 to 170 m a^{-1} along 1 km of the flowline. The study noted that supraglacial meltwater streams terminating in crevasse fields on 1960s aerial photography were coincident with this area of flow regime transition (Figure 4.4.1.1). The development of strong surface flow stripes has also been observed in this area. Both of these surface features provide evidence that the delivery of supraglacial

meltwater to the glacier bed may have a direct effect on ice velocities in these catchments. A final flow regime, regime 4, was defined, largely in the terminal reaches of glaciers, characterised by low basal friction possibly indicative of deforming subglacial sediments.

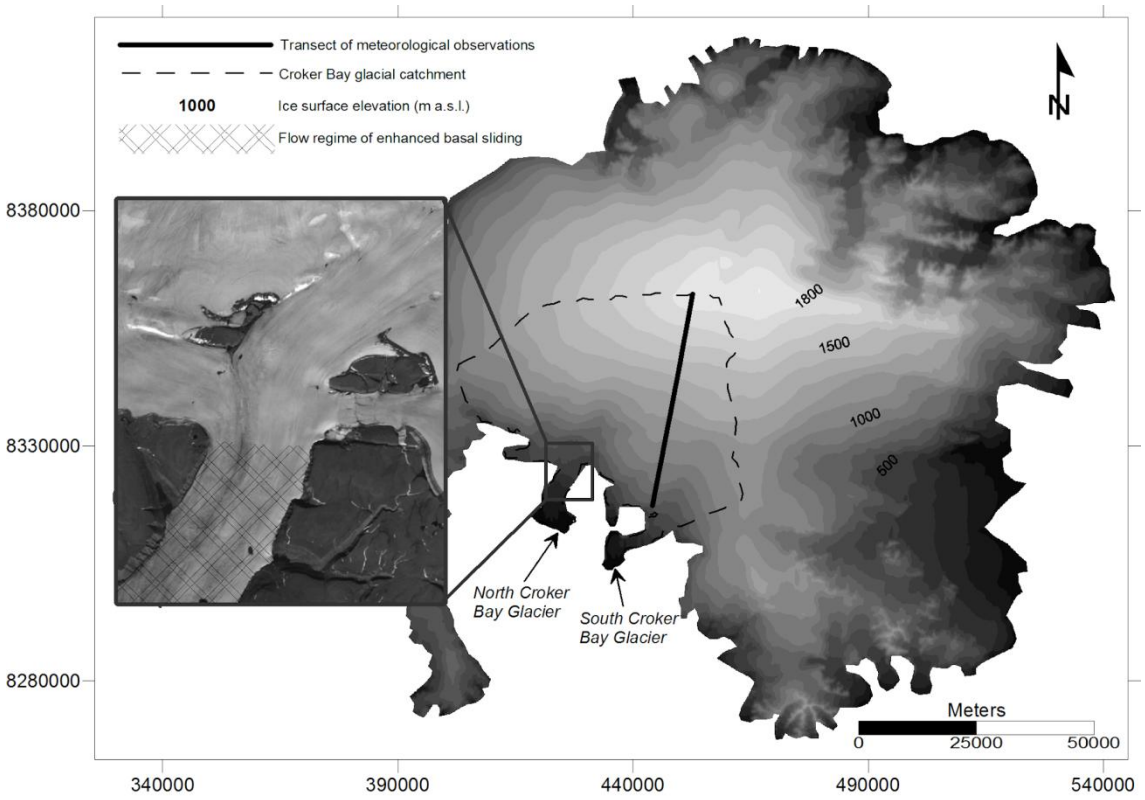

Figure 4.3.1. Devon Ice Cap ice surface elevation depicting the Croker catchment area and meteorological transect. Coordinates reference to UTM zone 17N. The insert shows the area of transition to an enhanced basal sliding flow regime from Burgess et al. (2005).

4.4 Methods

4.4.1 Melt modelling

To quantify total ice surface melt, a degree-day model is run using measured daily-averaged temperatures, as described in section 3.2.2 of chapter 3. Degree-day factors (*DDF*s) for snow and ice of 4 mm w.e. d^{-1} $°C^{-1}$ and 8 mm w.e. d^{-1} $°C^{-1}$ respectively were applied for the standard model runs. These values are representative of typical *DDF*s

for sites at high northerly latitudes as described by Hock (2003). No clear relationship could be established between accumulation and elevation at this site to justify the application of a precipitation lapse rate (Bell et al., 2008), thus the snowpack depth is set constant across the glacial catchment based on average snow depths in 2004 and 2006 respectively, measured along the meteorological transect (Figure 4.3.1). The degree-day model is applied spatially across the Croker Bay catchment, with daily mean temperature adjusted for ice surface elevation using an air temperature lapse rate of 0.0053°C m^{-1}. This lapse rate was calculated from the means of air temperatures measured at 10 minute intervals between Julian Day (JD) 136 and 235 in 2004 (Figure 4.4.2.1), at 11 sites extending from near the ice cap summit down to 478 m elevation (Bell et al., 2008) along the transect shown in Figure 4.3.1.

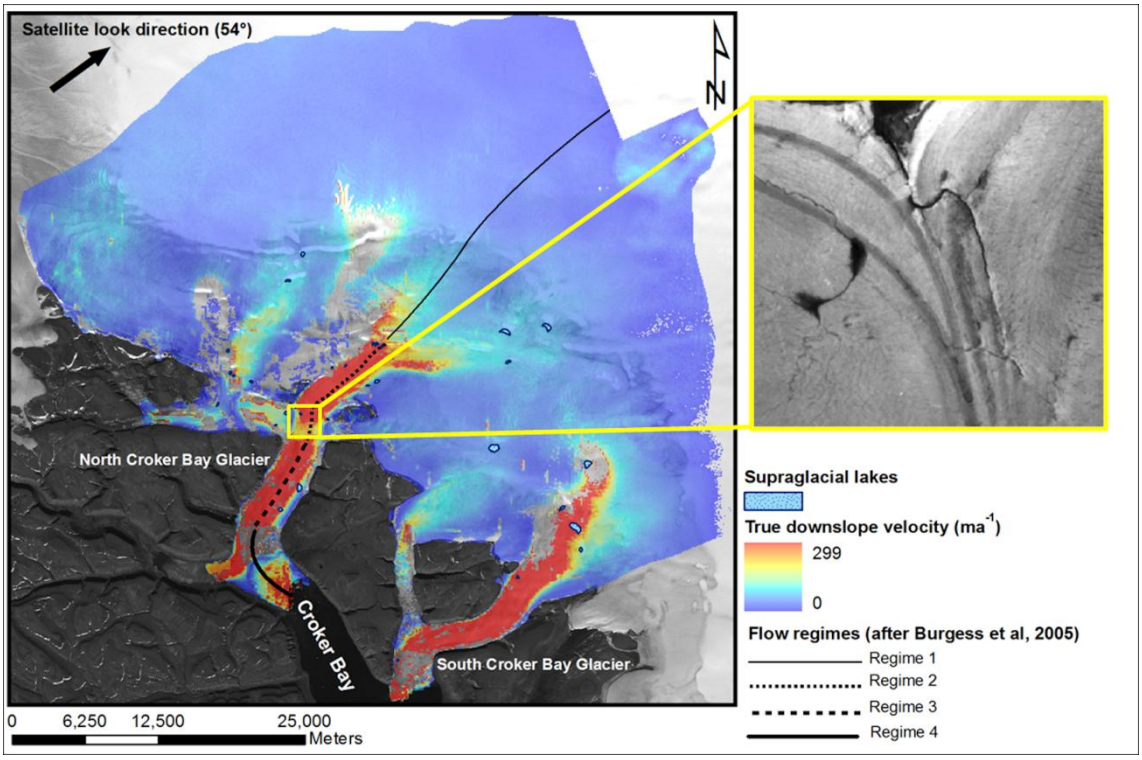

Figure 4.4.1.1. True downslope ice surface velocities, digitised supraglacial lakes and flow regimes for the Croker catchment (after Burgess et al., 2005). Flow regimes are: 1 – internal deformation, 2 – contribution from basal motion, 3 – enhanced basal motion and 4 – low basal friction. Aerial photo insert shows lake locations and streams disappearing into crevasses.

4.4.2 Meltwater routing and lake filling

The meltwater generated from degree-day modelling is subsequently used to weight flow accumulation across the catchment based on a single flow direction algorithm (Schwanghart & Kuhn, 2010). It was opted to distribute generated supraglacial meltwater across the ice surface by flow accumulation only, rather than by defining a threshold for supraglacial stream formation which would control the dendricity of stream networks. This was decided due to the spatial resolution at which the model is run (500 m), the resolution of the ice surface DEM (Dowdeswell et al., 2004) which was interpolated to 1 km grid cell sizes from a grid of transects flown 5 – 10 km apart from each other, and also the error associated with defining stream formation thresholds manually (Matsunaga et al., 2009). The uncertainty in matching observed stream networks with DEM-derived networks is particularly pronounced for glacial catchments due to the dynamic nature of the ice surface topography under varying climatic conditions, and the often transient positions of supraglacial streams, especially for ice surfaces characterised by shallow gradients. This model simplification likely results in some overestimation of available meltwater in a number of cells since meltwater flow is characterised in the form of overland flow rather than stream flow, which may be a driver of over-prediction of full ice thickness crevassing in areas of low ice thickness. Furthermore, transit time of meltwater from melt production to the destination cell, and through the snowpack where present, is not accounted for using the current approach. Whilst meltwater flow velocity would differ when in the form of overland flow in comparison to stream flow, melt generated in each cell is routed across the ice surface to reach crevasse cells instantaneously within one daily model time-step using the current approach, such that the physics of overland flow are not included in the model.

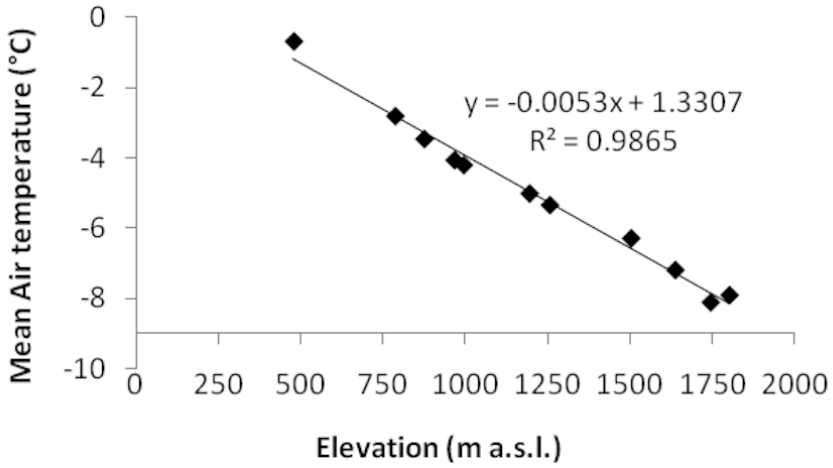

Figure 4.4.2.1. Air temperature lapse rate calculated along meteorological transect

Numerous sites of supraglacial meltwater ponding are visible on remotely sensed imagery, and drainage of these meltwater lakes into the englacial system is seen within the results of ground penetrating radar (D. Burgess, unpublished data). The flow routing component was therefore modified to additionally account for filling of supraglacial lakes. Meltwater routed into a cell containing a lake, digitised from Landsat imagery (Figure 4.4.1.1), will accumulate within that cell until the lake reaches its prescribed maximum volume, after which the lake will overtop and contribute to meltwater runoff downstream. Lake volume is determined based on a linear relationship with maximum observed lake surface area, as described in section 3.3.3 of the previous chapter.

4.4.3 Calculation of tensile stress from InSAR-derived velocity data

Interferometric synthetic aperture radar (InSAR) collected by the ERS-1 and ERS-2 satellites provided look-direction ice surface velocities for 98% of Devon Ice Cap, calculated from the pattern of interference created by Earth surface displacement between repeat-pass radar image acquisitions (Burgess et al., 2005). Images used to derive velocities for the western region of the ice cap (Figure 4.4.1.1) were obtained on the 25th and 26th April 1996. These line-of-sight velocity values were used by Burgess et al. (2005) to determine true downslope velocities. The resultant data was resolved into

'*x*' (south to north) and '*y*' (west to east) velocity components for this study. Strain rates, $\dot{\varepsilon}_{ij}$, were calculated as directional derivatives of the velocity data, $\frac{du}{dy}$, $\frac{dv}{dx}$ and $\frac{1}{2}\left(\frac{du}{dy}+\frac{dv}{dx}\right)$, for conversion to stresses. The constitutive relation for glacier ice, after Nye (1957), is applied to convert each strain rate to a stress, σ_{ij}:

$$\sigma_{ij} = B\dot{\varepsilon}_e^{(1-n)/n}\dot{\varepsilon}_{ij} \qquad (4.1)$$

Here, $\dot{\varepsilon}_e$ is the effective strain, and the flow law exponent, *n*, is 3. *B* is a viscosity parameter sensitive to ice temperature, such that *B*, and thus the 'stiffness' of the ice, will increase as temperature decreases. This parameter is related to the flow law as $B = A^{-1/n}$ (Vieli et al., 2006). For the Croker glaciers, an ice temperature of -13°C is assigned, based upon average winter sea level temperatures at NCB and ice temperatures of -12.1 to -14.7°C recorded for White Glacier, Axel Heiberg Island (Vaughan, 1993). This gives a flow law parameter value, *A*, of c.3.5x10^{-16} s^{-1} kPa^{-3} (Paterson, 1994) and a derived *B* value of 445 kPa $a^{1/3}$.

Surface tensile resistive stresses, R_{ij}, are calculated as described in section 3.4.2, using the Von Mises criteria for failure of ductile materials following Vaughan (1993). The tensile stresses are subsequently used as an input for fracture depth modelling, but also for determining the ratio of meltwater routed across the ice surface where runoff intersects a crevassed area. The value of tensile strength applied, initially set at 300 kPa, was determined by comparison of calculated surface tensile stresses with areas of surface crevassing visible on Landsat 7 panchromatic imagery of the NCB and SCB glaciers from August 2000 (background image, Figure 4.4.1.1). Where tensile stress exceeds the prescribed tensile strength, which is the maximum tensile stress that can be applied to a material before failure, the runoff ratio is set to zero, otherwise it equals 1. Thus upstream runoff is "captured" by crevasses and the flow accumulation of melt immediately downstream of a crevasse is reset to zero.

4.4.4 Crevasse depth modelling

To calculate penetration depths of individual water-filled crevasses, the method described in section 3.5.1 of chapter 3 is applied following this model, based upon LEFM, after van der Veen (2007):

$$K_I = 1.12R_{xx}\sqrt{\pi d} - 0.683\rho_i g d^{1.5} + 0.683\rho_w g b^{1.5} \qquad (4.2)$$

Surface tensile stresses, R_{xx}, calculated as described in chapter 3 using the Von Mises criterion, are used to calculate the first term in the model, and the water level in a crevasse, *b*, is determined from the meltwater accumulated in each cell having been routed across the ice surface of the Croker Bay catchment each day. The propagation depth of each crevasse in the catchment is calculated by solving for depth, *d*, each day until K_I is less than the prescribed ice fracture toughness, K_{IC}. The fracture toughness of ice, or the critical stress at which a pre-existing flaw will propagate, was prescribed initially as 150 kPa $m^{1/2}$. This was based on the average K_{IC} of 145.7 kPa $m^{1/2}$ calculated by Fischer et al. (1995) from modified ring testing of synthetic granular ice, and the zero-porosity K_{IC} of 155 kPa $m^{1/2}$ derived from crack-growth initiation experiments on Antarctic core ice by Rist et al. (1999). The water level in the crevasse, *b*, is calculated using *Q*, the rate at which water fills a crevasse, and time, *t*, such that,

$$b = Qt \qquad (4.3)$$

Here water-filling rates, *Q*, based on surface melt generated from measured temperature data are employed to investigate crevasse penetration depths and meltwater delivery to the bed throughout two ablation seasons at a daily temporal resolution. The chosen seasons, 2004 and 2006, have distinct measured air temperature records allowing model sensitivity to varying melt generation to be considered. Additionally, crevasse surface dimensions within the model are initially set at a depth-averaged width of 1 m and a length of 500 m for the standard model runs. The geometry of crevasses is a control on the level of the meltwater, *b*, in a crevasse, because accumulated daily surface meltwater is calculated as a depth of water equivalent generated across a 500 m x 500 m cell after the melt modelling and flow accumulation routines, but must be modified to converge into the prescribed surface

area of a crevasse when applied to the fracture depth calculation. Figure 4.4.4.1 depicts a simple schematic of the model as described above.

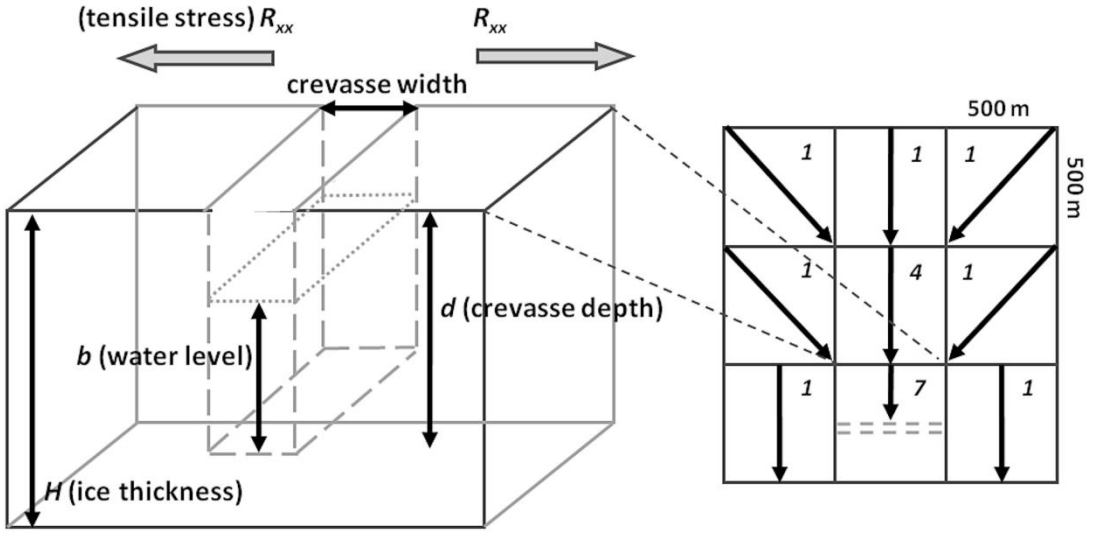

Figure 4.4.4.1. Water-filled crevasse penetration model. The supraglacial flow routing and accumulation method is depicted on the right, where numbers represent melt (water equivalent) per unit area.

The modelling routine calculates crevasse penetration depths each day for cells within the Croker catchment where R_{xx} equals or exceeds the prescribed tensile strength and thus surface crevassing can occur. Crevasse depths were calculated for each daily time step such that fracture propagation continues, and thus crevasse depth increases with time, in response to daily melt generation and inflow to the surface crevasse. The formation of moulins is predicted when calculated crevasse depths equal the ice thickness, which was measured across Devon Ice Cap by Dowdeswell et al. (2004) from airborne ice penetrating radar. The ice thickness in itself is a control on moulin formation as more melt, or more time, is required to drive a crevasse through thicker ice. Additionally, the model routine accounts for the drainage of supraglacial lakes using the method described in section 5.3.2. Lakes identified in the catchment may then drain through ice surface crevasses beneath lakes, which are assumed present beneath each lake included in the model. The meltwater delivered to the bed through both moulins and during lake drainage is quantified for each day in the model. The results which follow describe the investigation of moulin formation and lake drainage spatially and temporally for two melt seasons. The percentages of surface-derived

meltwater that are delivered to the subglacial system for the 2004 and 2006 ablation seasons are compared, and the influence of crevasse width, ice fracture toughness, tensile strength and degree-day factors evaluated.

4.5 Results

4.5.1 Initial parameters: 2004 and 2006 ablation seasons

For the 2004 season run, a temperature series recorded at 478 m elevation for JD 122-237 was applied with a prescribed spring snowpack depth of 166 mm w.e., which was an average of depths measured along the meteorological transect shown in Figure 4.3.1 (Bell et al., 2008). The temperature data series for 2006, recorded at 1414 m elevation, spanned JD 122-220 (Figure 4.5.1.1), with an initial average spring snowpack of 155 mm w.e.. By adjusting temperatures for sea-level using the calculated lapse rate, it is clear that from mid-June onwards, both the 2004 and 2006 data are typified by positive daily average temperatures (Figure 4.5.1.1); however the 2006 season reaches a maximum temperature of 9.9°C compared to a 2004 maximum of 7.5°C. 2006 is significantly warmer during the period of positive degree-days spanning JD 172-220 (late June to early August), as reflected by the respective mean temperatures for this period, of 3.8°C for 2004 and 5.8°C for 2006.

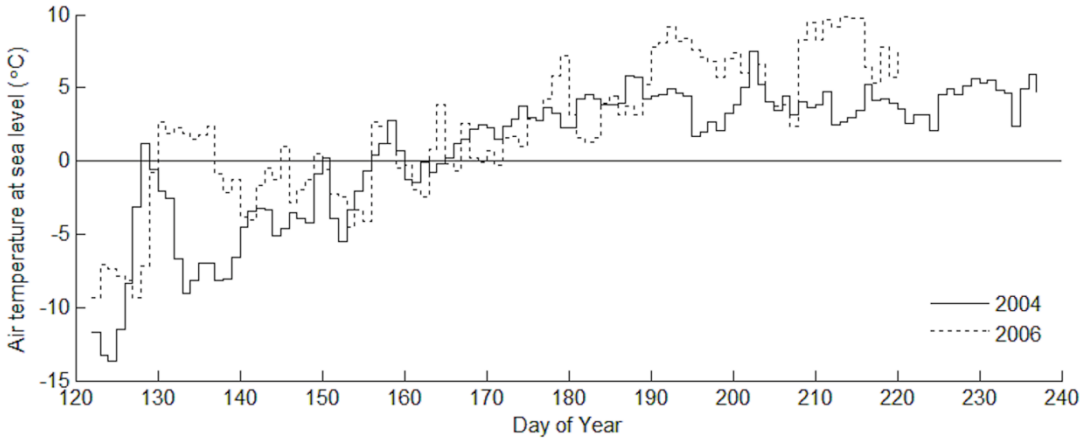

Figure 4.5.1.1. Daily average air temperature at sea level for the Croker catchment.

The temporal formation of surface-to-bed connections predicted for the 2004 and 2006 model runs using initial standard run parameters is depicted in Figure 4.5.1.2. The data show that both moulin formation and drainage of lakes occurred at higher elevations and more quickly in 2006 in comparison to 2004 when less meltwater was generated to fill crevasses and lakes. The increased availability of meltwater also resulted in a higher frequency of drainage by lakes containing a larger melt volume during 2006.

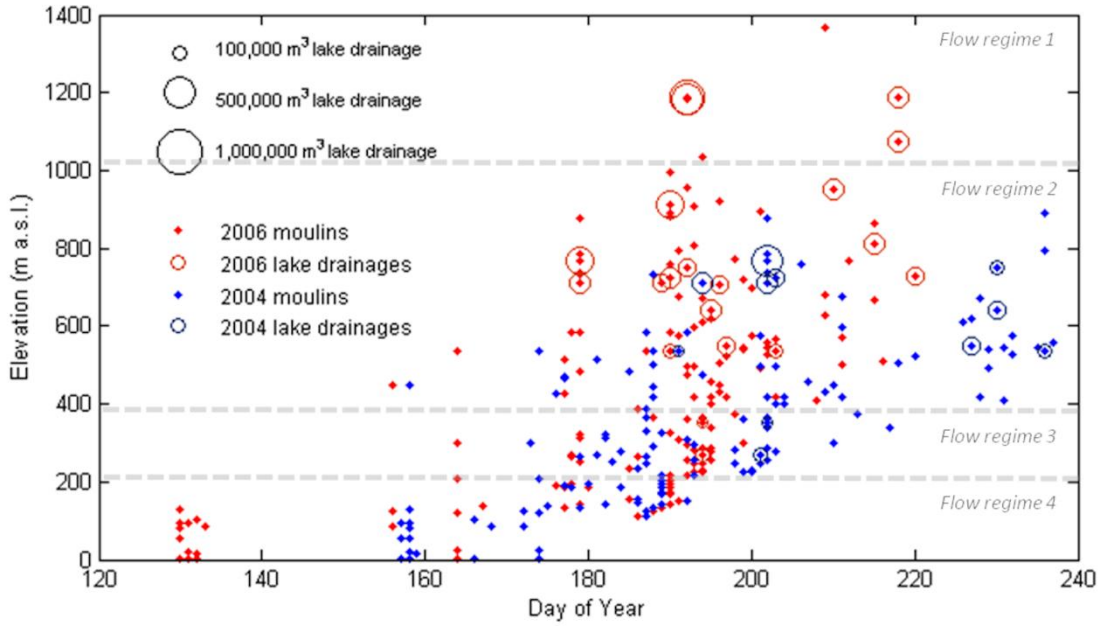

Figure 4.5.1.2. Temporal formation of surface-to-bed connections (initial parameters). Flow regime zones after Burgess et al. (2005).

Figure 4.5.1.3 shows the spatial coverage of surface-to-bed connections and illustrates that as well as forming at higher elevations, a greater number of moulins (167 vs 137 in 2004, see Table 4.6.1) and lake drainages are predicted for 2006, and cover a much larger spatial extent than in 2004. The net result is that a slightly larger percentage of generated surface melt (97.8% vs 95.2%) reaches the glacier bed in 2006 vs 2004 respectively (Table 4.6.2), and the total volume of melt delivered to the bed increases significantly from 2.6 x 10^8 m^3 in 2004 to 7.6 x 10^8 m^3 in 2006.

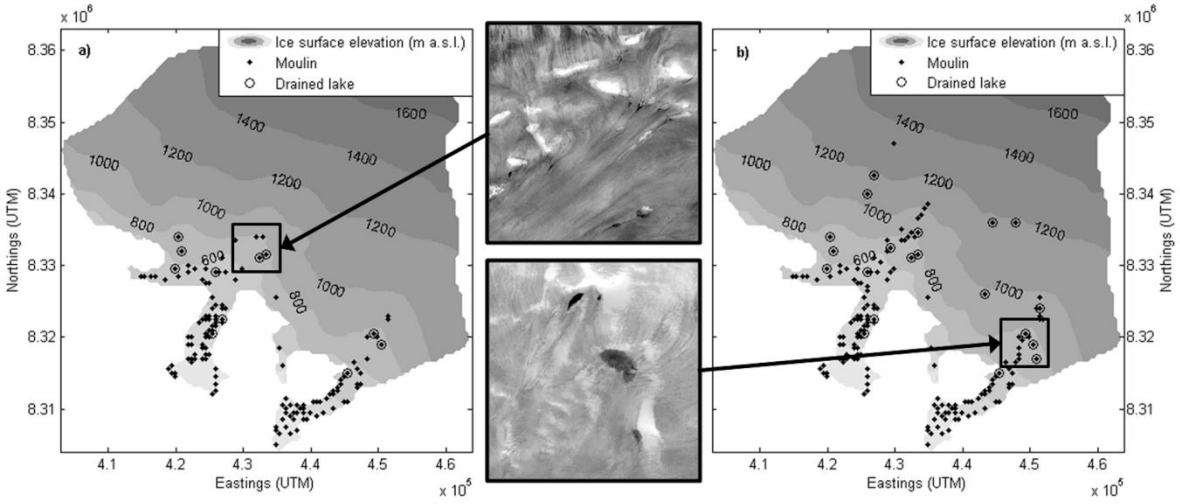

Figure 4.5.1.3. Spatial distribution of predicted surface-to-bed connection locations for a) 2004 and b) 2006. Photo inserts (Landsat) show examples of surface moulins and lake locations coincident with model predictions of surface-to-bed connections.

4.5.2 Sensitivity testing

Degree-day factors

To investigate how sensitive the model is to an almost two-fold increase in the degree-day factor for ice from Hock (2003), *DDF*s of 14 mm w.e. d^{-1} $°C^{-1}$ for ice and 3.5 mm w.e. d^{-1} $°C^{-1}$ for snow were applied for the 2004 and 2006 seasons, maintaining the initial values for the other input parameters. These *DDF*s were calculated by Mair et al. (2005) as best-fit values for the southeast and southwest quadrants of Devon Ice Cap. The results of altering the degree-day factors are shown in Figure 4.5.2.1.

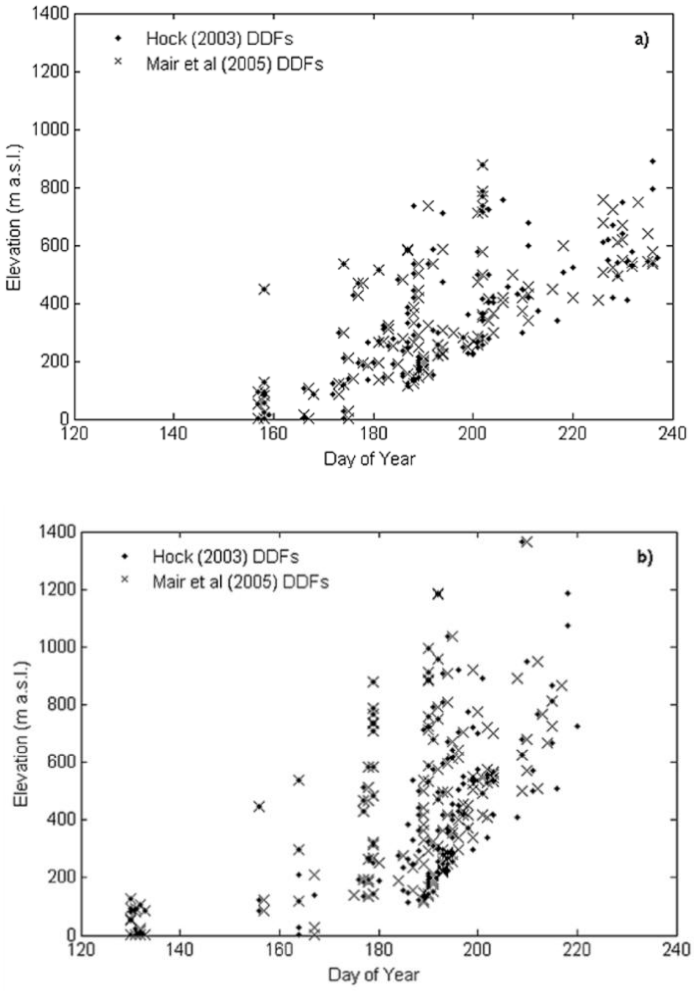

Figure 4.5.2.1. Comparison of moulin formation for ice and snow degree-day factors of 8 mm w.e. d^{-1} $°C^{-1}$ and 4 mm w.e. d^{-1} $°C^{-1}$ (Hock, 2003), and 14 w.e. mm d^{-1} $°C^{-1}$ and 3.5 w.e. mm d^{-1} $°C^{-1}$ (Mair et al., 2005): a) 2004, b) 2006.

The data suggest that the lower degree day factor for snow applied by Mair et al. (2005) results in a short temporal delay of between 1 and 3 days to the formation of moulins. The total number of surface-to-bed connections decreases slightly by 1.2% in 2006 and by 2.2% in 2004. The larger decrease in 2004 is possibly due to the longer period for which the lower *DDF* for snow is applied during the colder season. There is also a very small decrease in transfer of meltwater to the bed in comparison to the initial parameter run for both years (Table 4.6.2). Applying the Mair et al. (2005) *DDF* for ice resulted in a significant increase in the total melt generated during the melt season of 37% for 2004 and 22% for 2006. Despite this, the delayed removal of the snowpack due to the lower *DDF* for snow caused a shift in the onset of the higher melt

rate, the result of which is a limited impact on the number of surface-to-bed connections able to form. From these results it can be concluded that the model is not particularly sensitive to application of these *DDF*s, with only minimal impact on both moulin numbers and melt transfer to the bed, despite short delays in the initiation of surface-to-bed connections.

Ice fracture toughness

To investigate model sensitivity to the fracture toughness of ice, the model was run for both years using a K_{IC} value of 400 kPa $m^{1/2}$. This is the upper limit applied to modelling surface crevasse penetration by van der Veen (1998) following the results of fracture toughness testing of Fischer et al. (1995) and Rist et al. (1996). Calculated crevasse depths were not significantly different for results of 150 kPa $m^{1/2}$ and 400 kPa $m^{1/2}$ K_{IC} model runs. This was also noted by Scott et al. (2010) for crevasse-depth modelling applied to Pine Island Glacier, West Antarctica. Thus, applying a significantly higher fracture toughness value resulted in no change in either the number of moulins established, or in the percentage of surface-generated melt transferred to the ice-bed interface (Tables 4.6.1 and 4.6.2).

Tensile strength

The value of tensile strength prescribed controls the spatial distribution of cells deemed to contain initial surface fractures, and thus those cells in which crevasse propagation can occur. The initial estimation of tensile strength applied here is 300 kPa. This value is just below the 320-400 kPa estimate for White Glacier on Axel Heiberg Island, Nunavut (Vaughan, 1993), which has a similar ice temperature (-12.1 to -14.7°C) to the -13°C assigned for the Croker catchment. From studies across a wide distribution of glaciers, Vaughan (1993) presents tensile strength values ranging from around 100 up to 400 kPa. The sensitivity of the model was tested within these upper and lower bounds by applying further tensile strength values of 100, 200 and 400 kPa.

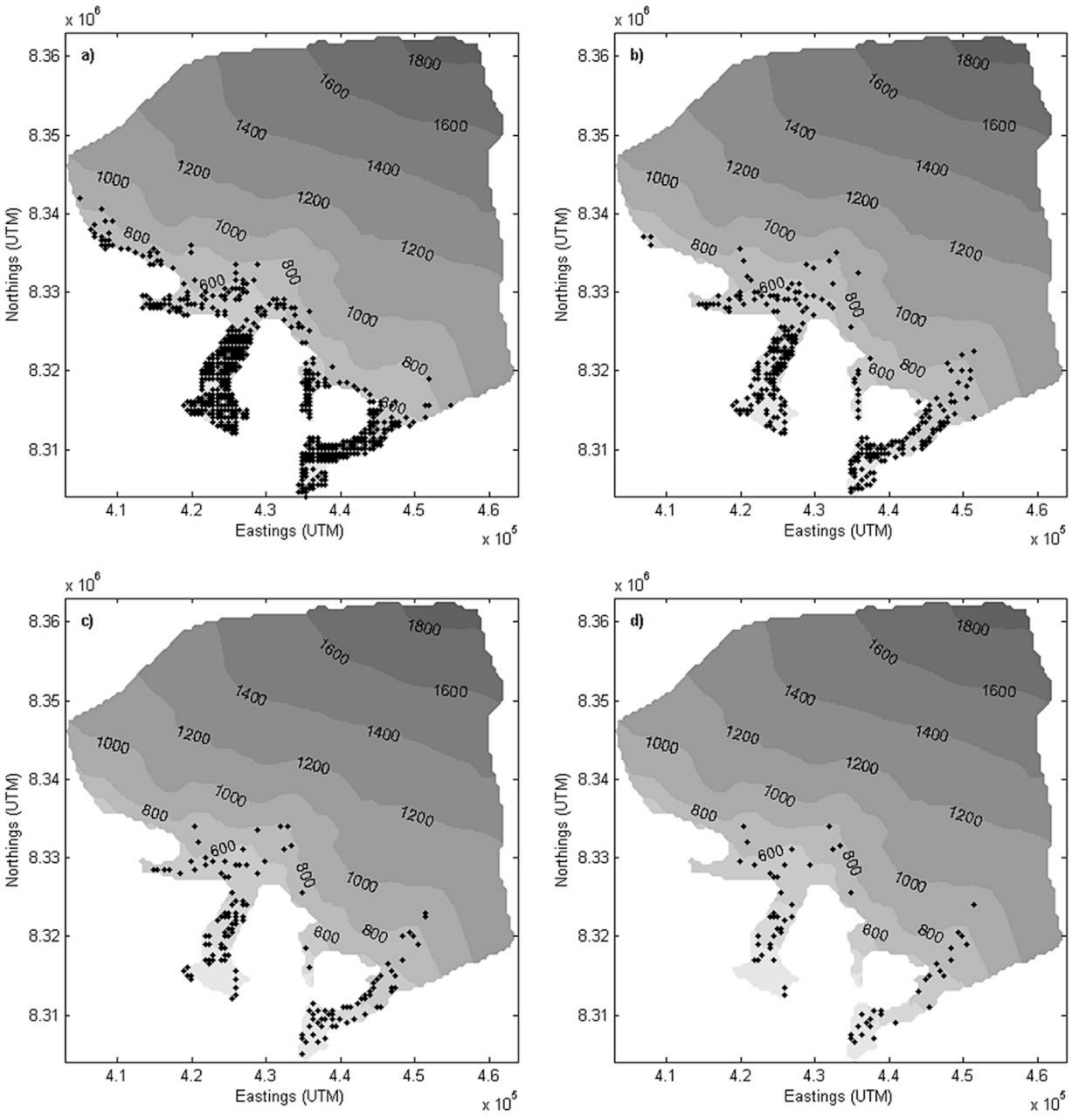

Figure 4.5.2.2. Spatial distribution of moulins in 2004 for tensile strength values of a) 100, b) 200, c) 300 and d) 400 kPa.

From the spatial distribution of moulins predicted for 2004 by the model for these scenarios (Figure 4.5.2.2), it is clear the model is highly sensitive to tensile strength. Moulin locations predicted for a 100 kPa tensile strength far exceed the number of surface crevasses and lakes visible on remotely-sensed imagery. Indeed, the total number of surface-to-bed connections predicted rises by 315.3 and 644.3% in 2004 and 2006 respectively (Table 4.6.1). The moulin numbers predicted from tensile strengths of 200 and 400 kPa differ less dramatically from the standard runs (Table 4.6.1), but the spatial extent of moulins predicted for the standard run, with a tensile strength of 300 kPa, compares best with moulin distributions evident on remotely

sensed imagery. Whilst being an important control on the potential spatial distribution of fractures penetrating the full ice thickness, and indeed the overall spatial occurrence of surface crevassing (Table 4.6.1), this parameter does not significantly affect the timing of their formation at progressively higher elevations throughout the ablation season. It should be noted that tensile strength is also an important control on the transfer of surface-generated meltwater to the ice-bed interface (Table 4.6.2). There is a significant expansion of the area containing surface fractures in the 100 kPa run, which extends the area where surface meltwater can be captured by crevasses that do not penetrate to the bed, reducing the total melt reaching the bed, and thus increasing englacial storage in crevasses that have not propagated through the full ice thickness (Table 4.6.1).

Crevasse width

The model was run for prescribed crevasse widths of 0.5, 1, 2 and 5 m, maintaining a 500 m length, to investigate model sensitivity to the meltwater head generated from different crevasse sizes. Locations of full thickness crevasses predicted for 2004 are shown in Figure 4.5.2.3 and illustrate a significant decrease in the spatial extent of moulins with increasing crevasse width.

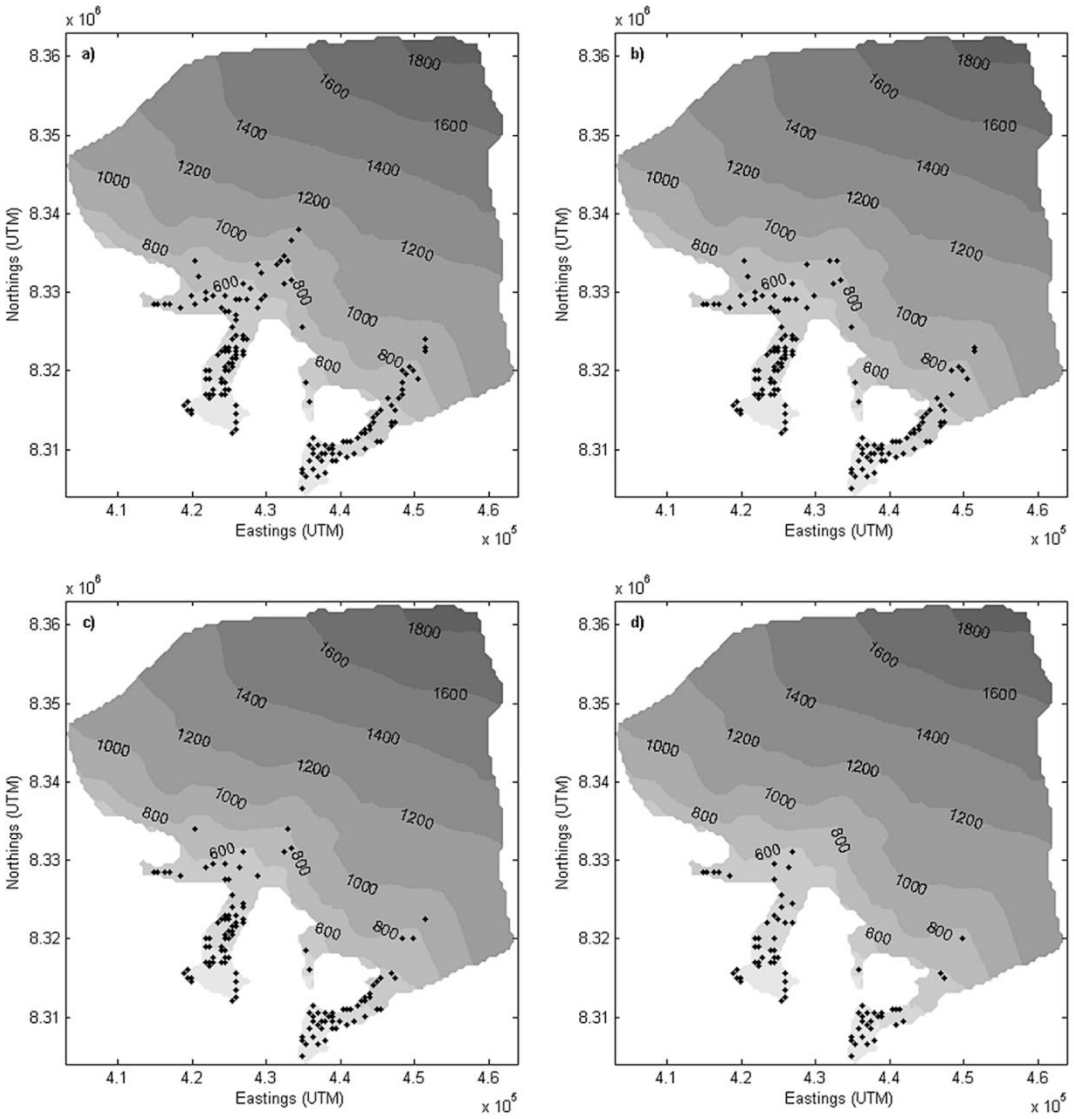

Figure 4.5.2.3. Spatial distribution of moulins in 2004 for crevasse widths of a) 0.5, b) 1, c) 2 and d) 5 m.

With narrower crevasses requiring less water inflow to maintain a high water level than for wide crevasses, propagation of crevasses can occur more rapidly and can be more easily maintained to allow formation of full-thickness fractures, or moulins (Weertman, 1973; Smith, 1976). Thus, altering crevasse width does not result in a change in the number of surface crevasses, but does affect the likelihood of those crevasses propagating through the full ice thickness to form moulins. This is demonstrated by the increasing number of crevasses not reaching the bed with increasing crevasse width (Table 4.6.1). By halving the initial width of 1 m to 0.5 m the

model predicted an increase in moulin numbers of 10.2 and 3.6% for 2004 and 2006 respectively, whilst decreasing the number of surface crevasses that do not reach the bed (Table 4.6.1). Doubling of the crevasse width to 2 m led to a decrease in moulin numbers of 16.8 and 6.6%. Altering crevasse width also resulted in a shift in the temporal formation of moulins in both years (Figure 4.5.2.4), where greater widths acted to delay the propagation of crevasses to the bed. Additionally, a larger crevasse width resulted in a decrease in the proportion of surface-derived melt delivered to the bed (Table 4.6.2) and vice versa.

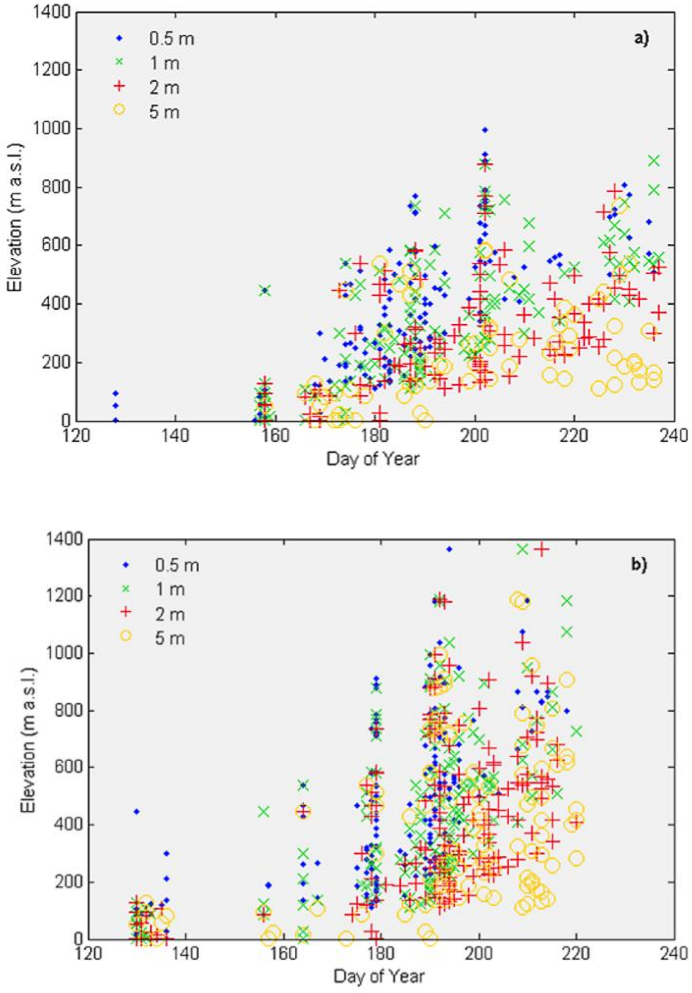

Figure 4.5.2.4. Comparison of temporal moulin formation for crevasse widths of 0.5, 1, 2 and 5 m: a) 2004, b) 2006.

4.5.3 Lake drainages

The majority of predicted surface-to-bed connections are moulins created over time by meltwater inflow to a surface fracture, while a smaller proportion are moulins that form within one day, directly beneath supraglacial lakes, when lake meltwater content reaches a critical level to drive a pre-existing surface fracture through the full ice thickness. Results of the tensile strength sensitivity tests (Table 4.6.1) suggest that decreasing the tensile strength, and thus increasing the number of surface fractures, acts to disrupt surface water inflow to lakes, reducing the potential for the formation of lakes with sufficient volume to force fracture to the bed. Altering the depth-averaged width of the crevasses also has a significant effect on the number, frequency and magnitude of lake drainages (Figure 4.5.3.1); a product of the effect of crevasse width on the crevasse meltwater level, *b*, produced for a given lake melt volume. When applying larger crevasse widths, fewer lakes drain, but they drain later in the season and typically transfer a larger volume of meltwater to the bed during each drainage event. This is due to the larger quantity of meltwater accumulated in a lake necessary to enable a wider fracture to propagate through the full ice thickness.

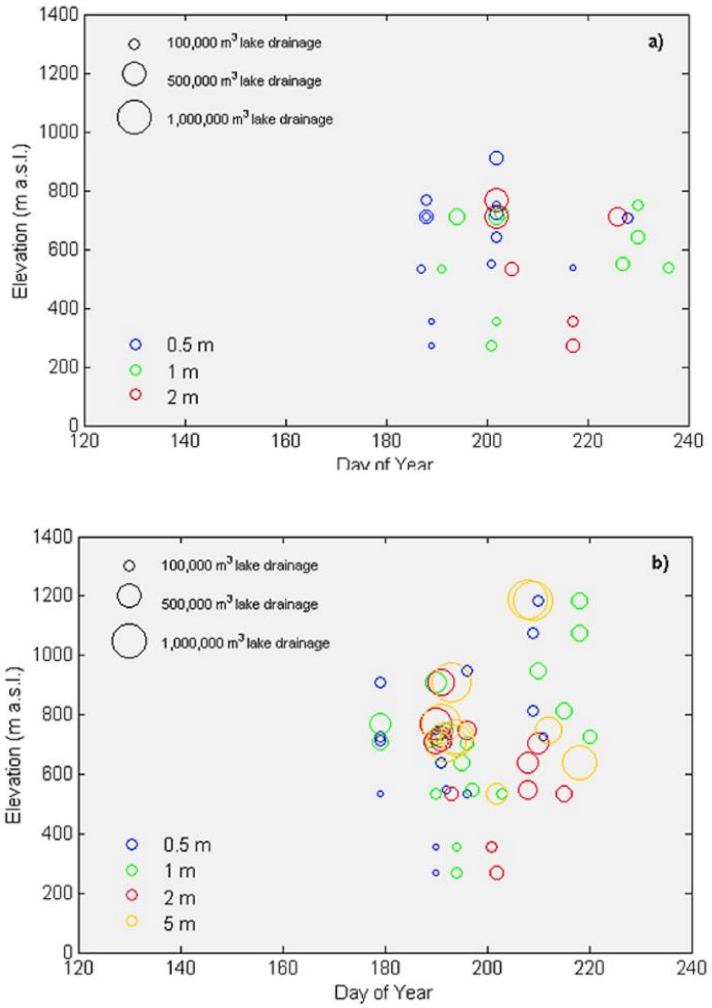

Figure 4.5.3.1. Temporal drainage of supraglacial lakes for fracture widths of 0.5, 1, 2 and 5m: a) 2004, b) 2006.

4.6 Discussion

The results of model testing described above indicate that the most important control on the spatial extent of moulins is the tensile strength (Figure 4.5.2.2, Table 4.6.1). Due to its strong controlling influence on the spatial distribution of moulins, it is imperative that the tensile strength is parameterised reliably. This is an important consideration for moulin distribution under a warming climate, due to the temperature-dependence of flow law parameter, *A*, which may rise in response to cryo-hydrologic warming (Phillips et al., 2010). Results also suggest that the delivery of surface-derived meltwater to the bed is highly sensitive to those input parameters which influence the rate at which water will fill a crevasse (Table 4.6.1). It is apparent from Table 4.6.1 that

the crevasse surface geometry is an important control on the formation of full ice-thickness crevasses when applying the van der Veen (2007) model for crevasse penetration. For both years, altering the crevasse width significantly affects the total number of surface crevasses that develop into surface-to-bed connections (Table 4.6.1). Altering the degree-day factors has a smaller effect on the numbers of moulins and drained lakes in each year. The percentage decrease in the number of surface-to-bed connections formed for the degree-day factor sensitivity test is around 1% less for 2006 than for 2004, likely due to the greater average temperature in the 2006 ablation season which reduces the duration for which the lower *DDF* for snow is applied. Results of altering the ice fracture toughness suggest that the model is highly unresponsive to changes in this parameter. Crevasse depth calculated using the LEFM model applied here is most strongly controlled by the lithostatic and water-filling stress terms, as discussed by van der Veen (2007). Thus the value of fracture toughness, although important for allowing initial fractures to develop, becomes negligible while propagation of crevasses due to meltwater influx is ongoing. Given the very small effect of fracture toughness on crevasse depth, the number of moulins predicted here is not altered by varying this input parameter.

	2004			2006		
	Total moulins (number of lake drainages)	***% change from initial run***	***Crevasses not reaching the bed***	***Total moulins (number of lake drainages)***	***% change from initial run***	***Crevasses not reaching the bed***
Initial parameters	137 (11)	-	28	167 (20)	-	7
***DDF*s: 14 (ice) and 3.5 (snow)**	134 (11)	- 2.2	31	165 (18)	-1.2	7
Fracture toughness: 400 kPa $m^{1/2}$	137 (11)	0.0	28	167 (20)	0.0	7
Tensile strength: 100 kPa	569 (4)	+ 315.3	1559	1243 (14)	+ 644.3	895
200 kPa	298 (8)	+ 117.5	149	417 (19)	+ 149.7	41
400 kPa	63 (12)	- 54.0	6	77 (20)	- 53.9	0
Crevasse width: 0.5 m	151 (13)	+ 10.2	16	173 (20)	+ 3.6	1
2 m	114 (6)	- 16.8	46	156 (15)	- 6.6	13
5 m	71 (0)	- 48.2	83	110 (10)	- 34.1	54

Table 4.6.1. Total number of surface-to-bed connections established during each model run.

Table 4.6.2 contains values of percentage transfer of surficially-derived meltwater to the bed for each model run, along with the associated percentage change from the initial parameter run. As shown for the spatial distribution of moulins, the tensile strength is the strongest control on meltwater transfer to the ice-bed interface through its influence on the locations at which surface meltwater can be captured by crevasses. This highlights the importance of establishing a reliable value for this parameter, possibly based on the close integration of field-based observations and remotely-sensed imagery. Crevasse width is also an important control on meltwater delivered to the bed. The size of crevasse surface openings controls the water level in crevasses, *b*, such that the higher the water level, the deeper a crevasse may penetrate, and the greater the number of initial surface crevasses that will have the potential to deliver meltwater to the bed. Crevasse width is unlikely to be spatially constant across a glacial catchment, thus for future applications crevasse width could be prescribed as a function of tensile stress. This may help to prevent or allow for prediction of full ice-thickness fractures, and thus meltwater delivery to the bed, in areas where crevasse dimensions may be under- or overestimated when applying a single depth-averaged crevasse geometry.

The changes in percentage transfer of surface generated melt to the bed are small in comparison to changes in moulin numbers, suggesting that while the total melt delivery to the bed does not change much in response to varying input parameters, the spatial distribution and timing of melt delivery does. This is an important consideration for models of subglacial hydrology, as the spatial distribution and volumes of meltwater reaching the bed are likely a significant control on basal water pressure. It should be emphasised that whilst changes are small within each season, the actual modelled volumes of melt delivered to the bed during 2004 and 2006 differ significantly. Larger values of percentage transfer are predicted for the warmer 2006 season (Table 4.6.2) and an almost three-fold increase in total meltwater routed from the surface to the bed is predicted in comparison to 2004. Furthermore, such enhanced drainage to the bed under scenarios of increased melt production may produce dynamic feedbacks resulting in larger tensile stresses via increased longitudinal stretching. This may result in more surface fracturing, and would suggest

that if tensile stresses were higher, less meltwater would be needed to propagate fractures through the full ice thickness. However, there would also be more crevasses present to disrupt the flow of water across the ice surface, which may in fact lead to a decrease in melt transfer to the bed.

	2004		2006	
	% transfer	*change from initial run*	*% transfer*	*change from initial run*
Initial parameters	95.2	-	97.8	-
***DDFs*: 14 (ice) and 3.5 (snow)**	94.7	-0.5	97.5	-0.3
Fracture toughness: 400 kPa $m^{1/2}$	95.2	0.0	97.8	0.0
Tensile strength: 100 kPa	85.7	-9.5	89.3	-8.5
200 kPa	96.4	+1.2	98.7	+0.9
400 kPa	95.6	+0.4	97.9	+0.1
Crevasse width: 0.5 m	95.8	+0.6	97.9	+0.1
2 m	93.6	-1.6	97.5	-0.3
5 m	88.1	-7.1	95.0	-2.8

Table 4.6.2. Percentage of surface-generated meltwater delivered to the bed during each model run.

As discussed previously, Burgess et al. (2005) identified a transition on both the NCB and SCB glaciers from a flow regime of predominantly internal deformation (regime 1) to regime 2, where basal sliding, partially controlled by subglacial topography, begins to contribute to surface velocity. Results of modelling suggest that transfer of supraglacial meltwater through moulins and during lake drainage occurs at elevations above this flow regime boundary during the 2006 ablation season, although not in 2004 when less melt was generated (Figures 4.6.1 and 4.6.2). Moulins are predicted by the standard parameter run at around 600-1000 m elevation, where the main glacier tongue opens into the ice cap. These correspond closely with sites on both aerial photography and Landsat imagery where supraglacial streams disappear into crevasses (Figure 4.5.1.3). This transition to regime 2 is coincident with the ice surface profile becoming concave-up, rather than the convex-up profile observed within flow regime

1 (Figure 4.6.1). The transition from regime 2 to regime 3, a flow regime indicative of enhanced basal sliding (Figures 4.3.1 and 4.4.1.1), occurs at around 400 m elevation. Modelling predicts that the density of moulins begins to increase significantly between 400 and 600 m elevation, directly above the boundary between flow regimes 2 and 3 (Figure 4.6.1), and remains high throughout the elevation extent of this flow regime. Meltwater delivered to the bed through moulins and lake drainages is significantly higher at these elevations, and indeed above, during 2006 (Figure 4.6.2), which may suggest increased potential for melt-induced dynamic response. Consistencies between model outputs and identified flow regimes are encouraging and indicate that the model has some success in predicting the spatial distribution of possible full-thickness fractures. Whilst field data of an appropriate temporal resolution against which to test model simulation of lake drainage events and moulin formation is not available, the model does produce results which are qualitatively realistic. This is particularly true for modelled spatial patterns of moulin formation within elevation bands, as supported by previous suggestion that meltwater reaching the bed may be a driver of increased ice surface velocities within flow regime 3.

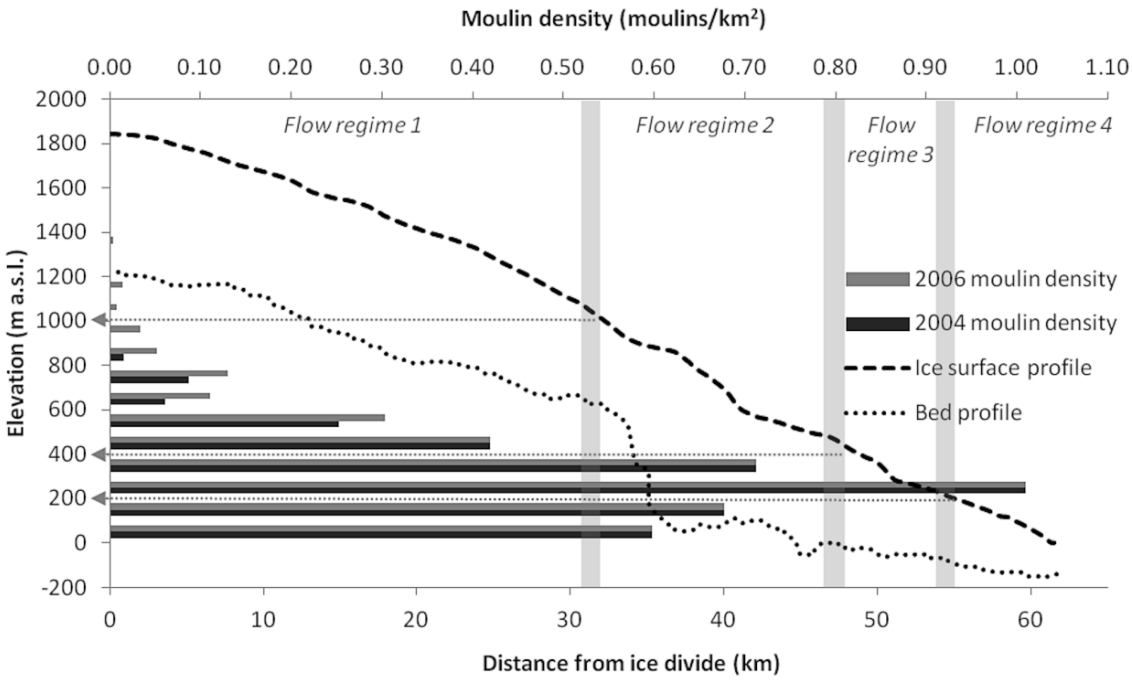

Figure 4.6.1. Density of moulins within elevation bands of 100 m. Glacier flow regime boundaries for NCB glacier (after Burgess et al., 2005) are illustrated.

The spatial resolution of model input data is a limitation, particularly for meltwater routing across the ice surface. The mountain valley terrain surrounding the Croker Bay glaciers likely results in a significant proportion of meltwater running off the ice surface, and ending up between the glacier margin and valley walls. Additional melt may be produced by preferential heating of adjacent bedrock valley walls, and twinned with water running off the glacier margin this suggests that our estimates of the percentage of supraglacial melt reaching the ice-bed interface may be too high. Furthermore the model also does not account for attenuation of meltwater within the snowpack or firn layer which may result in overestimation of meltwater available for surface flow routing, and a decrease in the time lag between melt production and moulin formation and lake drainage events. The model prediction of moulin formation around day 130 in 2006 (Figure 4.5.1.2) may be one example where early melt season snow-cover may have resulted in an increased meltwater transit time, and thus may not have given rise to moulin formation that early in the season. Future studies could improve spatial patterns and magnitudes of supraglacial meltwater pathways by incorporating attenuation and refreezing of melt in near surface snow and firn (van den Broeke et al., 2008). The transit time of meltwater through the catchment could then be better represented, particularly in areas below the snowline, and would allow for improved temporal prediction of moulin formation over the ablation season. This highlights that whilst the model produces behaviour qualitatively comparable to what is seen in reality, particularly in spatial patterns of moulin formation, better constraints on physical processes and real-time observations of drainage events would help to improve the temporal component of the model.

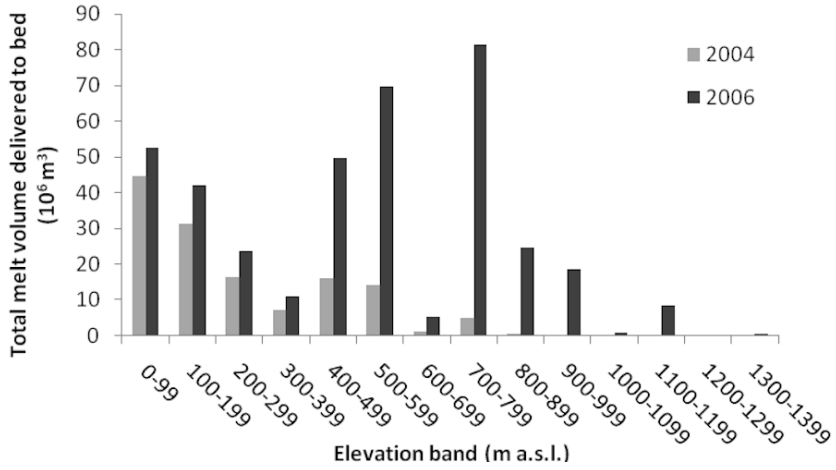

Figure 4.6.2. Total meltwater transfer through moulins and lake drainages within each 100 m elevation band.

4.7 Concluding remarks

The application of a new model designed for determining the spatial and temporal patterns of moulin formation, drainage of supraglacial lakes, and the delivery of surficially-derived meltwater to the ice-bed interface of glaciers and ice sheets, has been presented. The model has been applied to the Croker Bay catchment of Devon Island Ice Cap for the 2004 and 2006 ablation seasons and tested for sensitivity to input parameters. From model predictions, it can be concluded that accurate quantification of supraglacial meltwater is essential due to the controlling influence of crevasse water-filling levels on penetration depths. It is also clear that inaccuracies in prescribing crevasse geometry and the tensile strength of ice may lead to significant error in modelling the location and timing of surface-to-bed connection formation during the ablation season. Response to increased meltwater generation, typified by results of modelling the warmer 2006 season, highlights the potential for enhanced surface-to-bed meltwater transfer under the scenario of a warmer climate. Thus, the delivery of surficially-derived meltwater to the ice-bed interface should not be discounted as a mechanism for dynamic response to increased future ice surface melt.

Modelling surface-to-bed connections in the manner described here may have the potential to contribute towards integrating models of glacial hydrology and dynamics

in a more physically-based capacity, particularly for meltwater point inputs for models of subglacial hydrology (Pimentel et al., 2010; Schoof, 2010). The timing and quantity of meltwater reaching the ice-bed interface is an important controlling factor on water pressures at the bed and the configuration of the subglacial system (Iken & Bindschadler, 1986). Given observed velocity responses to changes in subglacial hydrology, it is important that the spatial and temporal evolution of moulin formation and lake drainage events is accounted for in integrated modelling of glacier hydrology and dynamics.

Chapter 5. Modelling the transfer of supraglacial meltwater to the bed in Leverett Glacier hydrological catchment, southwest Greenland

5.1 Abstract

Meltwater delivered to the ice-bed interface of the Greenland Ice Sheet is a driver of dynamic response through enhanced basal lubrication and changes in effective pressure. Ice surface velocities have been shown to respond directly both to meltwater production at the surface and to drainage of supraglacial lakes, suggesting efficient transfer of meltwater from the supraglacial to subglacial hydrological systems. The results of spatially-distributed modelling for prediction of moulin locations on Leverett Glacier hydrological catchment of south-west Greenland are presented here. The spatial and temporal formation of moulins is investigated for two ablation seasons, and model sensitivity to input parameters is explored. Results are compared with recorded velocities on Leverett Glacier, and modelled discharge of meltwater delivered to the bed is compared with discharge measured in the proglacial outlet. Spatial predictions of moulin formation and lake drainage, and the temporal delivery of melt to the bed through each, correspond well with sites where velocities respond to positive degree days and sites where velocity is likely responding to release of stored melt.

5.2 Introduction

The delivery of meltwater to the ice-bed interface is an important mechanism in determining the dynamic response of glaciers to atmospheric warming by establishing a direct coupling between the ice surface and the subglacial system (Alley et al., 2005). Links between subglacial water pressure and glacier velocity have been well documented (Iken & Bindschadler, 1986; Hooke et al., 1989; Mair et al., 2003; Sugiyama & Gudmundsson, 2004) , and numerous studies have presented evidence of speed-up events across alpine and arctic valley glaciers related to periods of increased

ice surface melt (e.g. Bingham et al., 2003; Anderson et al., 2004). More recently, it has been demonstrated that meltwater is capable of penetrating through many hundreds of metres of ice through full-ice thickness crevasses, or *moulins*, and through the drainage of supraglacial lakes within the ablation area of the Greenland Ice Sheet (GrIS) (Das et al., 2008). An investigation of the hydrology of Leverett Glacier catchment in south-west Greenland (Bartholomew et al., 2011a) suggested that below c.1100 m newly generated melt is transferred rapidly to the ice sheet bed through moulins driving seasonal evolution of subglacial hydrology. Above c.1100 m, surface melt was stored within supra-glacial lakes which periodically drained to the glacier bed, in a similar way to that recorded by Das et al., 2008. These mechanisms have been invoked to explain summer speed-up events across the GrIS that coincide with or follow periods of surface melting (e.g. Zwally et al., 2002; Shepherd et al., 2009; Bartholomew et al., 2010). Bartholomew et al. (2011b) recorded GPS velocity time series at 7 sites, extending from the margin of the south-west GrIS at Leverett Glacier up to c.1700 m, during the 2009 melt season. They found that the onset of velocity speed-up events occurred progressively later, further up-glacier as the melt season progresses, controlled by the onset of melt at increasingly high elevation over time.

In this chapter the spatially distributed predictive model for the formation of surface-to-bed connections, as described in chapter 3, is discussed in its application to Leverett Glacier. The spatial and temporal formation of full ice thickness crevasses and the timing of supraglacial lake drainages are modelled, and the delivery of supraglacially-generated meltwater to the ice-bed interface is quantified. The success of the model is assessed by comparing outputs which characterise the relative contribution of direct surface-to-bed melt delivery and release of stored melt throughout the 2009 melt season, against empirically derived interpretations of the temporal and spatial patterns of coupling between hydrology and dynamics (Bartholomew et al., 2011a; Bartholomew et al., 2011b). Furthermore, the modelled melt delivery to the bed is compared against measured proglacial discharge to assess the temporal accuracy of melt transferred from the ice surface to the bed by the model. The model is also run for the warmer 2010 melt season to evaluate the effect of increased melt generation on the extent of surface-to-bed connections and melt delivery.

5.3 Study area

Leverett Glacier is a land-terminating outlet glacier of the south-west GrIS, situated around 67.1°N. The hydrological catchment, as derived from a digital elevation model (DEM) produced from Interferometric Synthetic Aperture Radar (InSAR) (Palmer et al., 2011), encompasses an ice-covered area of c.1200 km^2. The catchment, which lies within the ablation zone, extends to over 50 km inland of the margin, and up to an elevation of c.1550 m (Figure 5.3.1). Meltwater within the Leverett catchment leaves the glacier through a large subglacial conduit, feeding a proglacial stream for which a peak discharge of 294 m^3 s^{-1} was recorded during the 2009 ablation season (Bartholomew et al., 2011a) and 372 m^3 s^{-1} during 2010 (Andrew Sole, personal communication).

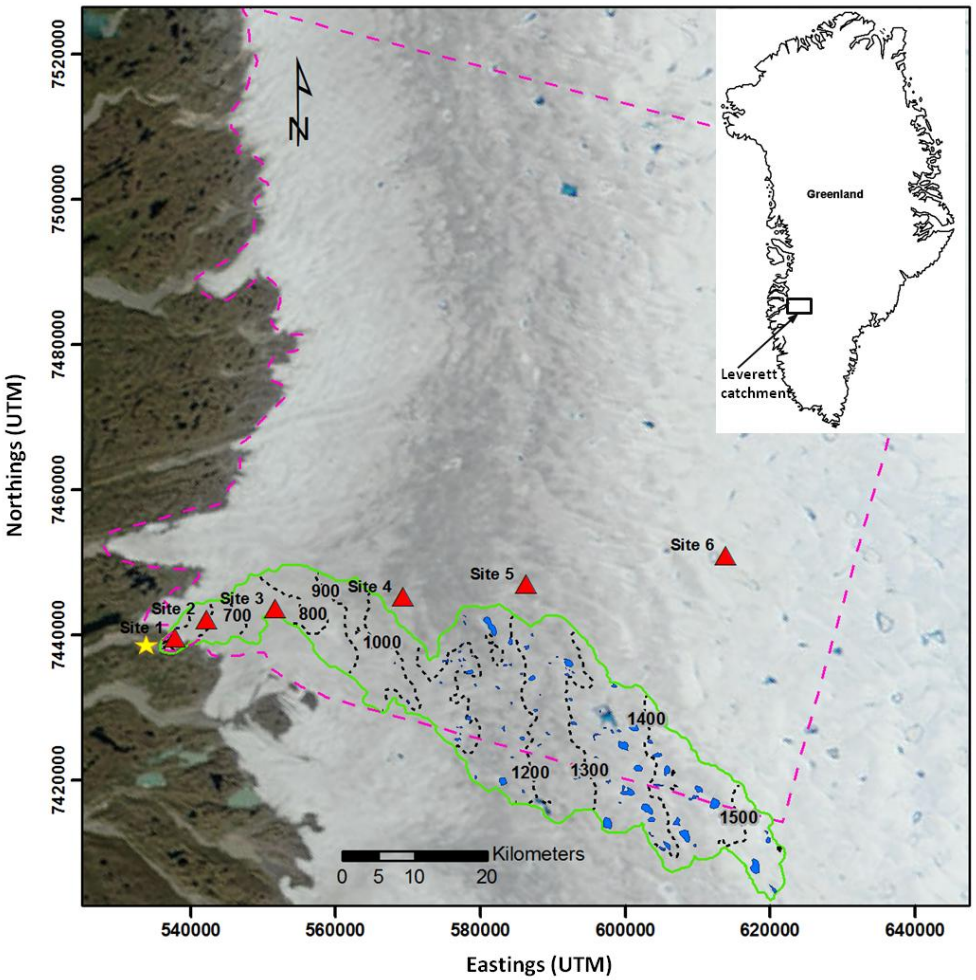

Figure 5.3.1. Leverett Glacier hydrological catchment (outlined in green). Contours show ice surface elevation; locations of meteorological data collection and GPS velocity measurements are depicted by red triangles; the location of proglacial discharge measurements is represented by the yellow star; and supraglacial lakes are highlighted in blue. The pink dotted line represents the larger area of the southwest GrIS used for moulin density testing and the background image is from MODIS (6/07/2010)

5.4 Data and methods

The modelling routine applied to the work presented in this chapter, as described in chapter 3, comprises: a simple degree-day model for generation of melt; a routine for routing of meltwater across the ice surface (Schwanghart & Kuhn, 2010) and storage of melt within supraglacial lakes; and a model for calculation of penetration depths of water-filled crevasses, after Van der Veen (2007). The model outputs discussed in this chapter include spatial and temporal information on the formation of moulins (where and when a crevasse propagates through the full ice thickness), the drainage of supraglacial lakes through crevasses underneath the lakes, and the quantity of melt delivered to the bed through each connection on each day. Further details of the methods employed here can be found in chapter 3, and in Clason et al. (2012), where the routine was applied to the Croker Bay catchment of Devon Ice Cap in High Arctic Canada and where sensitivity testing of input parameters was carried out. The findings of the Clason et al. (2012) study described in chapter 4, confirmed that the model is particularly sensitive to those variables controlling the rate at which meltwater fills a crevasse, since this is the main controlling factor on crevasse depth according to the fracture propagation model presented by van der Veen (2007). The ice tensile strength was also found to be highly significant in determining spatial patterns of moulin formation since it governs where surface crevasses are deemed to form. Importantly, model application to Devon Ice Cap concluded that increased melt generation could influence both the temporal and spatial formation of moulins, and thus produce enhanced meltwater transfer to the ice-bed interface in years typified by warmer air temperatures.

Meteorological data, used for input to degree-day modelling, were acquired at seven GPS sites from near the terminus of Leverett Glacier at 457 m (site 1, Figure 5.3.1) extending into the ice sheet interior up to 1716 m (site 7, Figure 5.3.1) (Bartholomew, 2011a). Temperature was recorded at sub-daily intervals at each site during the 2009 and 2010 melt seasons; here the focus is on the period extending from 10th May (day 130) to 16th August (day 228) for each year. An air temperature lapse rate of 5.5°C/km was calculated from the 2009 data with a strong coefficient of determination of 0.96. Degree-day factors for snow and ice (DDF_s and DDF_i) of 5.81 mm w.e. d^{-1} °C^{-1} and 7.79

mm w.e. d^{-1} °C^{-1} respectively were determined based on calibration against ablation rates recorded using surface lowering beneath ultrasonic depth gauges (UDG). Daily accumulation was recorded based on UDG measurements of surface height, and initial spring snowpack depth on 6th May 2009 was recorded at each site, resulting in an accumulation gradient of 256.6 mm w.e./km (R^2 = 0.76). Supraglacial lakes within the Leverett catchment were manually digitised in ArcGIS from Landsat 7 ETM+ imagery acquired 15th and 31st July 2009 (Figure 5.3.1), and lake surface area was used to estimate lake volume as described in chapter 3 (Figure 3.3.3.1).

Ice surface elevation for the Leverett catchment is in the form of a digital elevation model (DEM) derived from synthetic aperture radar interferometry (InSAR) twinned with airborne laser altimetry (Palmer et al., 2011). For this study the DEM was reduced in its resolution to the model spatial resolution of 500 m, and the resultant ice surface used for routing and melt-weighted flow accumulation of supraglacial meltwater. Filling and overtopping of supraglacial lakes is accounted for within the flow accumulation routine, as described in chapter 3 and as previously applied in chapter 4. For determining areas likely to contain initial surface crevassing, ice surface tensile stresses were calculated based on the Von Mises criterion, after Vaughan (1993), applying a value of 271 kPa $a^{1/3}$ for viscosity parameter, *B*, relating to an ice temperature of -5°C. An initial tensile strength of 75 kPa was prescribed based on comparison of calculated tensile stresses, as described above, with crevassing visible on satellite imagery, where the tensile strength represents the stress contour at the boundary between crevasse fields and crevasse-free areas. Tensile stresses were calculated as described in chapter 3, from a composite ice surface InSAR velocity dataset (Joughin et al., 2010), resolved into longitudinal (see Figure 5.4.1) and transverse components. Accumulated surface meltwater and the resultant surface tensile stress regime (Figure 5.4.1) were used as inputs to a model of water-filled crevasse penetration (Van der Veen, 2007). The water level within each crevasse was adjusted for a prescribed depth-averaged crevasse width of 1 m, and an ice fracture toughness of 150 kPa $m^{1/2}$ was assumed. To determine where moulins could penetrate through the full ice thickness, thus delivering meltwater to the ice-bed interface, a 5

km ice thickness dataset derived from ice penetrating radar, after Bamber et al. (2001), was applied within the modelling.

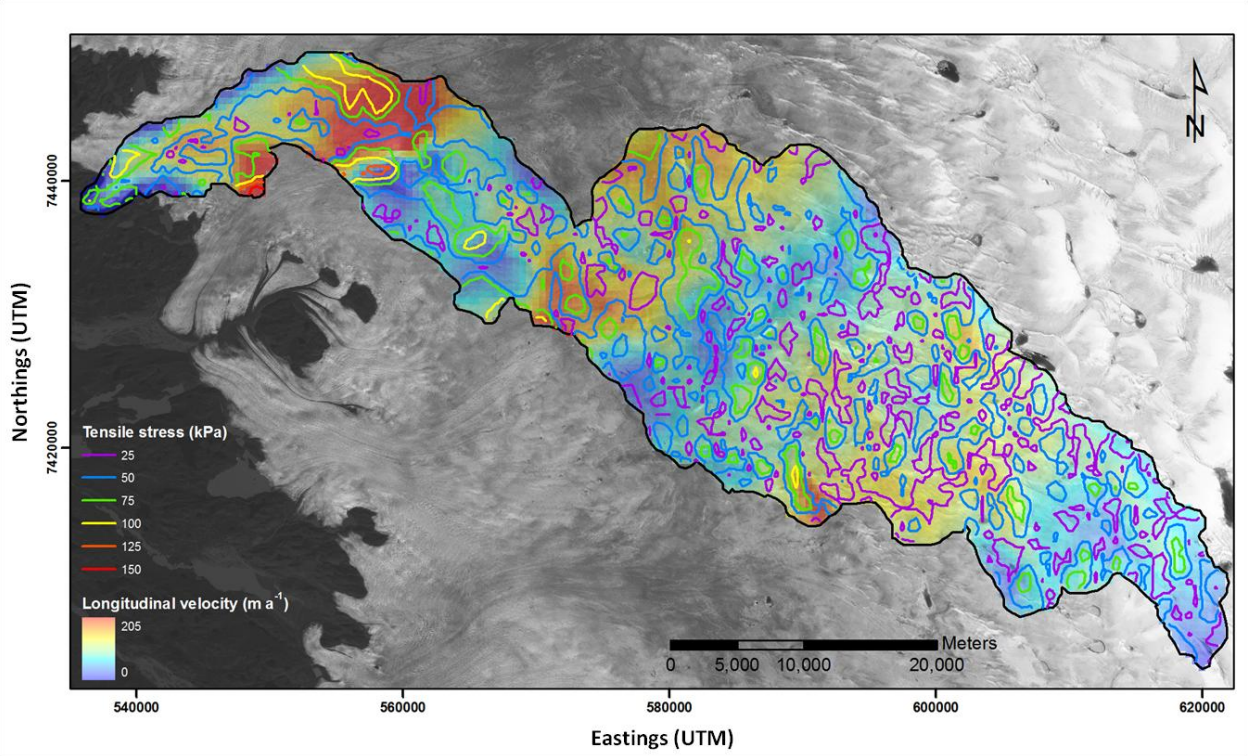

Figure 5.4.1. Longitudinally-resolved ice surface velocities from InSAR data for the Leverett catchment. Contours depict the ice surface tensile stress regime.

5.5 Results

5.5.1 2009 melt season

The model was run with initial parameters of 75 kPa tensile strength, a 1 m depth-averaged crevasse width and an ice fracture toughness of 150 kPa $m^{1/2}$, with temperature, initial snowpack depth and accumulation data recorded during the 2009 ablation season. The temporal pattern of moulins first reaching the ice-bed interface is depicted in Figure 5.5.1.1., where there is a clear trend in moulin formation which increases in elevation with time over the melt season. This is likely due to retreat of the snowline and expansion of the area experiencing melt (following Nienow et al., 1998), and also due to the larger ice thicknesses through which moulins at higher elevation must penetrate to reach the bed. No clear relationship between the

temporal distribution of moulins predicted to form through drainage of supraglacial lakes and elevation is obvious from these model outputs.

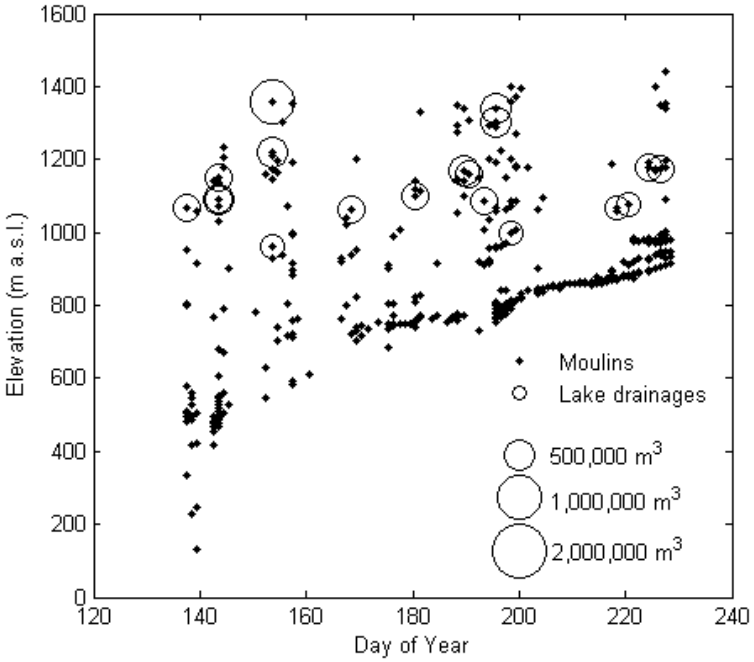

Figure 5.5.1.1. Moulin formation through the 2009 melt season with elevation.

From the spatial distribution of moulins (Figure 5.5.1.2), it can be seen that surface-to-bed connections form up to c.1400 m, delivering 93.5% of surface-generated melt to the ice-bed interface. Below 1000 m elevation there are large clusters of moulins, which may be interpreted as cells for which sufficient melt is produced to allow for full-thickness fracture propagation of a single crevasse without relying on inflow from upstream accumulated meltwater. The model sets the downstream runoff ratio to zero when routed melt is captured by a crevasse. However, at low elevations melt rates are highest and the ice is thinner, resulting in possible overestimation of moulin locations by the model in these areas.

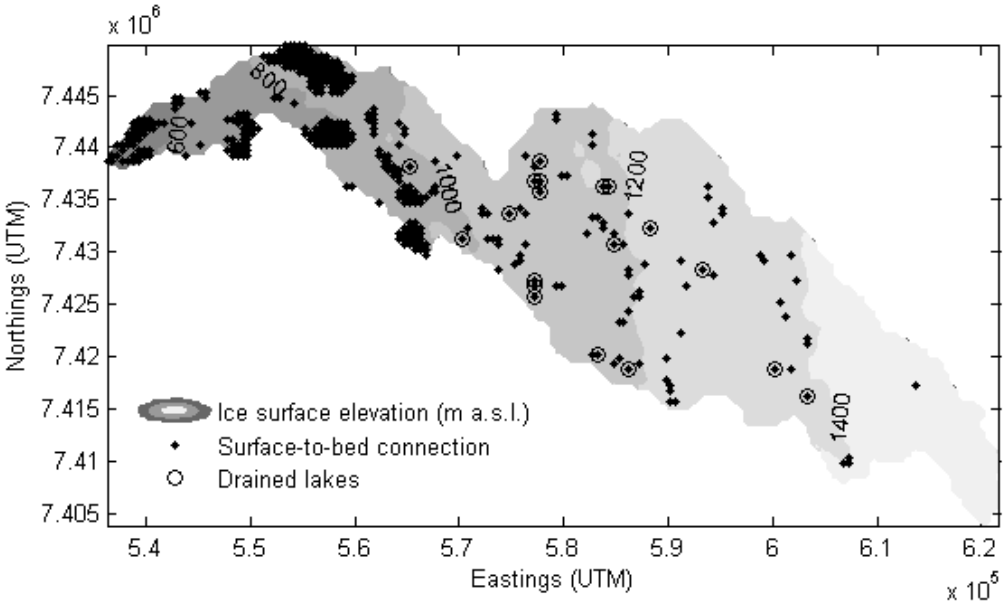

Figure 5.5.1.2. Spatial distribution of moulins and lake drainages for 2009.

5.5.2 2010 melt season

To assess model response to increased melt production in the Leverett catchment, the model was run using meteorological data from the 2010 melt season, covering the same time period as for 2009 (day 130 to day 228). During this period, daily average temperatures at site 1 were 33% higher on average during 2010 than for 2009, with a significantly warmer start to the melt season (Figure 5.5.2.1). The Arctic Report Card for 2010 (Box et al., 2010) described record temperatures and significantly increased melt days on the GrIS during this year, with temperatures highest in the west. The duration of melting was up to 50 days longer than the average in areas of the western ice sheet, and during the month of May surface temperatures were as much as 5°C higher than the 1971-2000 average according to Reanalysis data from NCEP/NCAR.

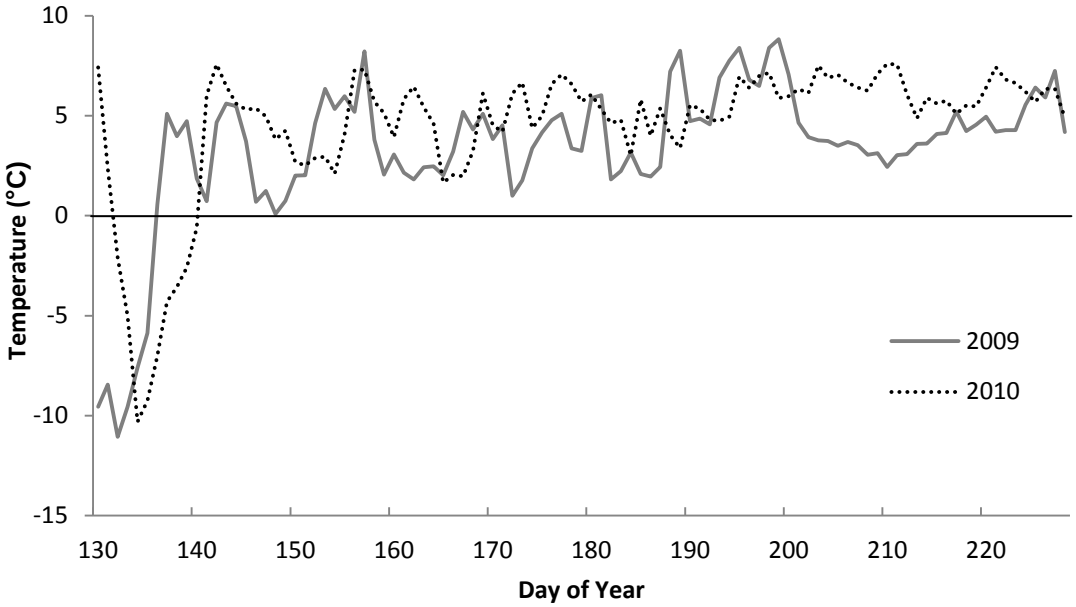

Figure 5.5.2.1. Daily average air temperatures at site 1 (457 m a.s.l.) for 2009 and 2010.

Figure 5.5.2.2 illustrates the temporal formation of surface-to-bed connections during the 2010 melt season. Moulins begin forming one week earlier in 2010 compared to the cooler 2009 season. As with the model predictions for 2009, there is a clear trend of moulin formation at increasing elevation with time into the season. Whilst drainages of supraglacial lakes are dispersed in their elevation in the early melt season, the latter part of the season is characterised by lakes draining from low to high elevation, a pattern that was not clearly visible in 2009 results.

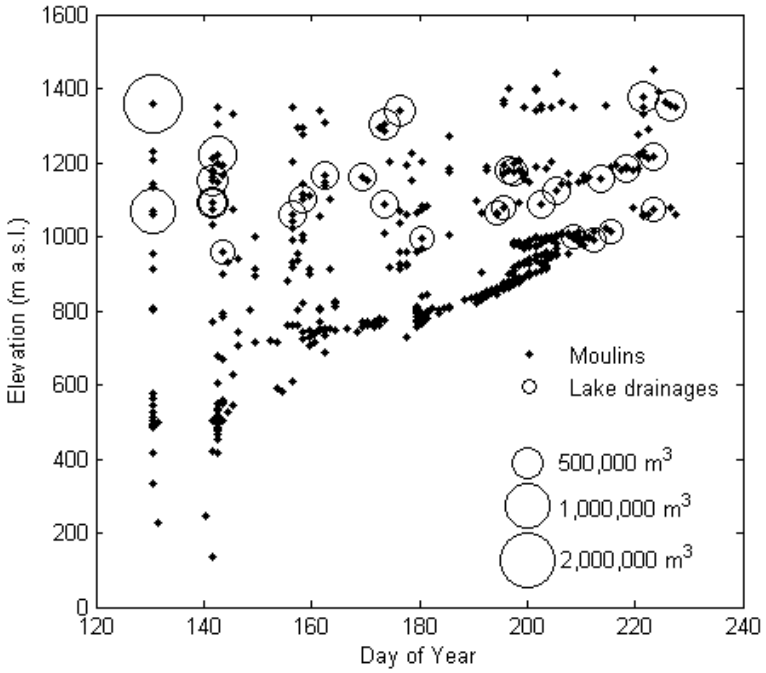

Figure 5.5.2.2. Moulin formation through the 2010 melt season with elevation.

The spatial coverage of surface-to-bed connections increases significantly in 2010 (Figure 5.5.2.3), with a rise in the number of moulins formed by full ice thickness crevasses and lake drainages of 25.6% (Table 5.5.3.1) compared to 2009. Particularly notable is an increase in moulin density above 1000 m elevation. From Figure 5.5.2.3 it is clear that lake drainages also cover a larger area of the Leverett catchment, increasing significantly in number, from 19 in 2009 to 30 in 2010 (Table 5.5.3.1). The result of increased moulin numbers and lake drainages is a 3% increase in the transfer of melt to the bed during the period of the 2010 melt season covered in the model (Table 5.5.3.1). As such, not only does the warmer 2010 melt season lead to higher absolute runoff, but it also leads to an increase in the proportion of melt that becomes runoff.

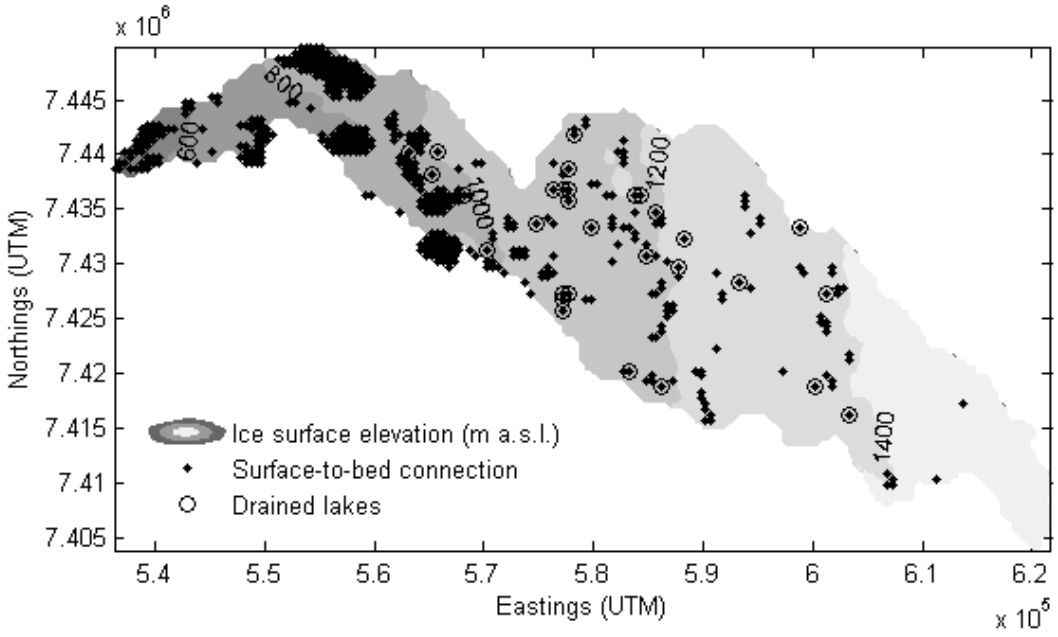

Figure 5.5.2.3. Spatial distribution of moulins and lake drainages for 2010.

5.5.3 Sensitivity testing

The model was run with a number of values for ice fracture toughness, tensile strength and crevasse width to evaluate model sensitivity to these input parameters when applied to the Leverett glacial catchment. Clason et al. (2012) review model sensitivity analysis in more detail, as applied to the Croker Bay catchment on Devon Ice Cap, and discuss the effect that altering these parameters has on the temporal formation and spatial distribution of moulins, as discussed in chapter 4. The impact of altering these three input parameters on the number of surface-to-bed connections formed, and the percentage of supraglacially-generated meltwater that is transferred from the ice surface to the ice-bed interface for this area, is now briefly discussed.

	Moulin numbers		Melt transfer	
	Total moulins (number of lake drainages)	***% change from initial run***	***% transfer***	***change from initial run***
Initial parameters (2009)	391 (19)	-	93.5	-
Fracture toughness: 400 kPa $m^{1/2}$	391 (19)	0.0	93.5	0.0
Tensile strength: 50 kPa	782 (12)	+ 100.0	77.5	- 16.0
100 kPa	125 (21)	- 68.0	96.4	+ 2.9
125 kPa	40 (22)	- 89.8	95.1	+ 1.6
Crevasse width: 0.5 m	487 (28)	+ 22.3	96.6	+ 3.1
2 m	181 (12)	- 53.7	83.8	- 9.7
5 m	100 (6)	- 74.4	75.5	- 18.0
2010 meteorological input	491 (30)	+ 25.6	96.5	+ 3.0

Table 5.5.3.1. Total number of surface-to-bed connections formed and the percentage of surface-generated meltwater delivered to the bed during each model run.

Focussing firstly on ice fracture toughness, it can be concluded that altering this parameter does not significantly affect the number of moulins formed, the number of lakes that drain, or the percentage transfer of melt from surface to bed (Table 5.5.3.1). This is in agreement with Clason et al. (2012) and Scott et al. (2010). For standard model runs, a value of tensile strength of 75 kPa was applied, based on comparison of the surface tensile stress regime with crevasse fields on Landsat imagery. Clason et al. (2012) evaluated model sensitivity to upper and lower bounds of tensile strength included in Vaughan (1993). Here, sensitivity to a narrower range of values is tested, covering possible variation in tensile strength across the catchment should ice properties such as temperature, affected by processes including cryo-hydrologic warming (Phillips et al., 2010), differ spatially. Whilst reducing tensile strength to 50 kPa results in a 100% increase in the total number of surface-to-bed connections, there is a reduction in the number of lakes draining (Table 5.5.3.1). This is due to interruption of meltwater flow across the surface caused by the increase in surface fracture density, and also explains the 16% reduction in melt transfer to the bed. Conversely, increasing the tensile strength results in a decrease in total moulins, but an increase in lake drainage events and the transfer of meltwater to the bed. This

suggests that less water is trapped englacially, and that the filling and drainage of lakes accounts for a significant proportion of melt transfer. The original depth-averaged crevasse width of 1 m was also varied within model runs. Findings suggest that reducing the width results in increased moulin numbers, lake drainages and melt transfer, whilst the opposite is true when crevasse width is increased. This reinforces that the water level within a crevasse is the most important control on the propagation rate of a water-filled crevasse (Van der Veen, 2007).

5.6 Discussion

5.6.1 2009 velocity observations

During the 2009 melt season, horizontal ice surface velocities were measured at seven GPS units, sites 1 to 7 (Figure 5.3.1), extending from Leverett Glacier at 456 m up onto the ice sheet at 1716 m elevation (Bartholomew et al., 2011b). Velocities were highest at site 2, where they exceed 300 m a^{-1} on multiple days (Figure 5.5.6.1); above this elevation velocities decrease in magnitude, until reaching site 7 where velocities vary only slightly from the subsequent winter background velocity. It is clear that the period of the melt season characterised by highest velocities begins later with increasing elevation, with high velocities recorded at sites 1 and 2 shortly after the onset of melting, and sites 5 and 6 remaining near winter background levels until much later. This is partially due to retreat of the snowline and onset of melt at increasingly high elevation, which also acts to open up surface-to-bed connections from low to high elevation (Figure 5.5.1.1). Furthermore, the periods of enhanced velocity at sites 4, 5 and 6 (all above 1061 m) are not strongly associated with high positive degree days at these sites, in contrast to sites 1, 2 and 3 (all below 800 m). This suggests that at lower elevations, velocities are responding to supraglacial melt routed quickly to the ice-bed interface through moulins, whilst at higher elevations the lack of correlation between positive degree days and velocities may be indicative of a dynamic response to release of meltwater stored in supraglacial lakes (Bartholomew et al., 2011b).

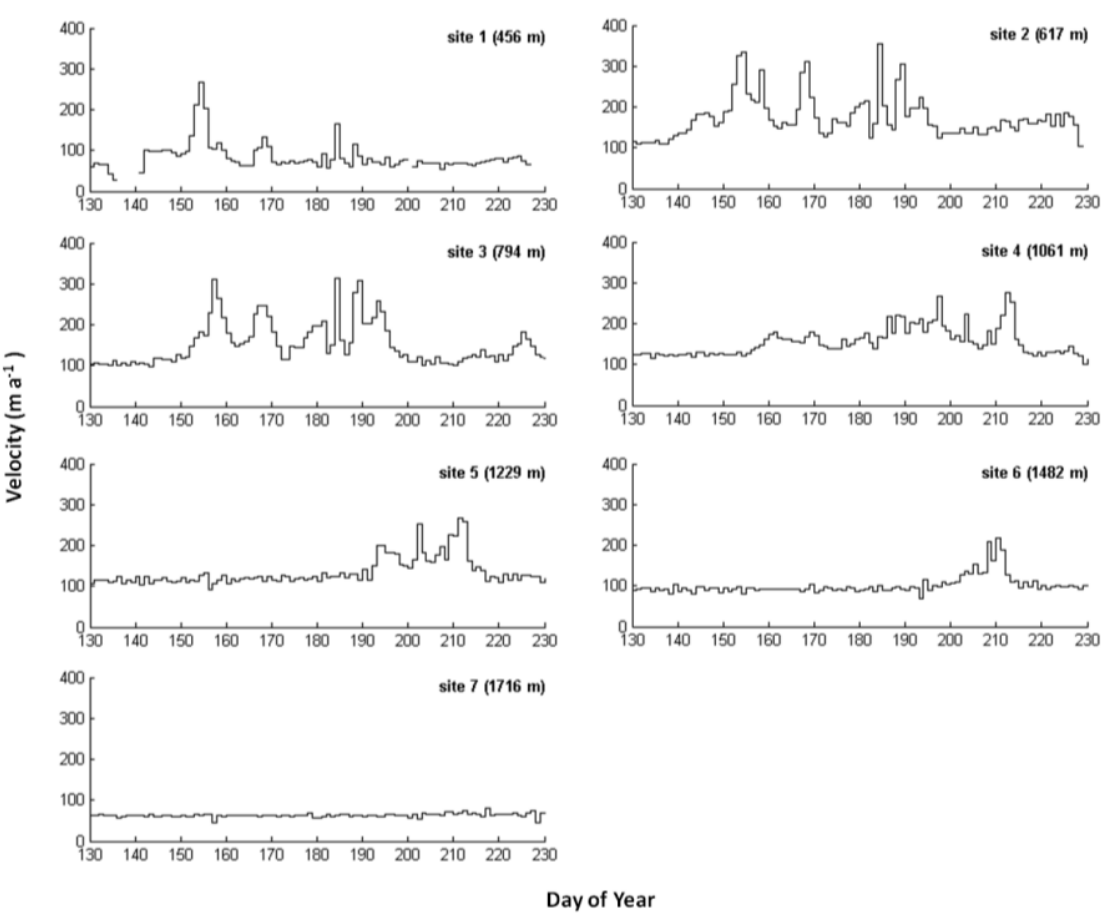

Figure 5.5.6.1. Horizontal 24-hour ice surface velocities (Bartholomew et al., 2011b) recorded by GPS at sites 1-7 during the 2009 melt season.

5.6.2 Moulin density

To assess how well the model characterises the change in the mechanism for delivery of meltwater to the bed with elevation from moulins to lake drainages, the spatial densities of modelled moulins and drained lakes and their variance with elevation was determined (Figure 5.6.2.1). During the 2009 melt season, the model predicts a marked reduction in moulin density above 1000 m. The higher density of moulins below 1000 m corresponds with the earlier onset, higher magnitude velocities recorded at GPS sites 1, 2 and 3 (Figure 5.5.6.1), and the significant drop in their density above 1000 m supports the lack of correlation between velocities and positive degree days at GPS sites 4, 5 and 6. Lake drainages begin above 750 m elevation, with the highest density of drainages occurring between 1000 m and 1250 m. Site 4 at 1061

m and site 5 at 1229 m, which exhibit the largest velocity peaks of the four sites above 1000 m, fall within the 1000-1250 m elevation band, characterised by the highest density of lake drainages.

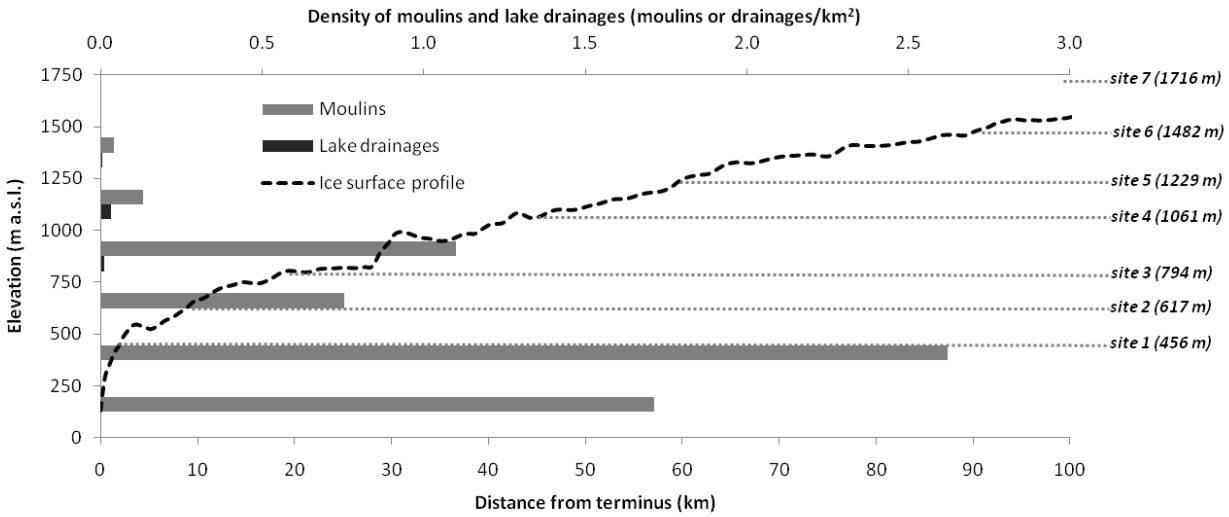

Figure 5.6.2.1. Density of moulins and lake drainages within 250 m ice surface elevation bands. Sites of GPS velocity measurements (Bartholomew et al., 2011b) are shown against the Leverett catchment ice surface profile.

However, GPS sites 4 to 7 fall outside the assumed boundary of the Leverett hydrological catchment, and thus moulin and lake drainage densities within the Leverett catchment may not be representative of those across the wider area of the southwest ice sheet margin. The model was therefore run for a larger area of the ice sheet, incorporating GPS sites 4 to 6 (Figure 5.3.1). The general pattern of change in spatial densities of moulins and lake drainages with elevation across the larger model area is similar to the smaller Leverett catchment (Figure 5.6.2.2). The density of moulins below 500 m is notably higher for the Leverett catchment; however these lower elevations occur only at the very margin of the ice sheet, where the outlet glacier termini are forming, and where large errors in the ice thickness at the margins are a likely source for discrepancy.

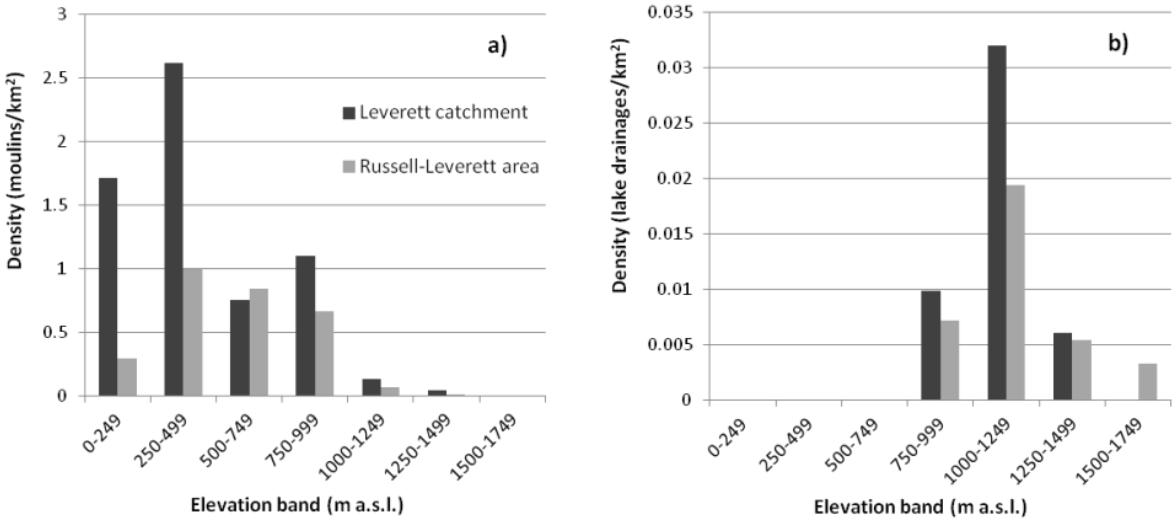

Figure 5.6.2.2. Comparison of a) moulin and b) lake drainage densities within the Leverett catchment and the wider Russell-Leverett area of the SW GrIS.

5.6.3 Melt delivery to the bed

Concentrating once again solely on the Leverett catchment, meltwater transferred to the bed each day within each elevation band was calculated to further evaluate the relative contribution of melt transferred through moulins and drained lakes (Figure 5.6.3.1). Between 0 m and 499 m elevation, there is relatively little melt delivered to the bed through moulins, most likely because the area of the Leverett catchment below 500 m is very small. The moulins formed between these elevations are required to penetrate through thinner ice (< c.300 m) than at higher elevation, and twinned with large areas of high tensile stress, this means that relatively low amounts of melt are required to force propagation of fractures to the bed. Peaks in melt delivery between 500 and 999 m match well temporally with peaks in velocity at GPS sites 2 and 3 (Figure 5.6.3.1; also c.f. Figure 5.5.6.1), as is particularly notable around days 155, 168 and 189. The pattern of melt reaching the bed between 1000 m and 1249 m is less obviously representative of the velocity response recorded at sites 4, 5 and 6; however since these higher sites are located outside of the Leverett catchment area (Figure 5.3.1), these discrepancies are understandable. Nevertheless, the period of highest modelled melt delivery to the bed between days ~187 and 201 matches well with high recorded velocities at sites 4 and 5 during this time period. There is a

significant increase in melt delivered to the bed from day 187 to 201 between 1250 m and 1500 m (Figure 5.6.3.1), the largest proportion of which is through predicted drainage of supraglacial lakes within this elevation band. The timing of velocity peaks at site 6 does not match as well with peak discharge between 1250 m and 1500 m, but this is not surprising, given model simplicity and the fact that site 6 is located c.30 km from the Leverett catchment.

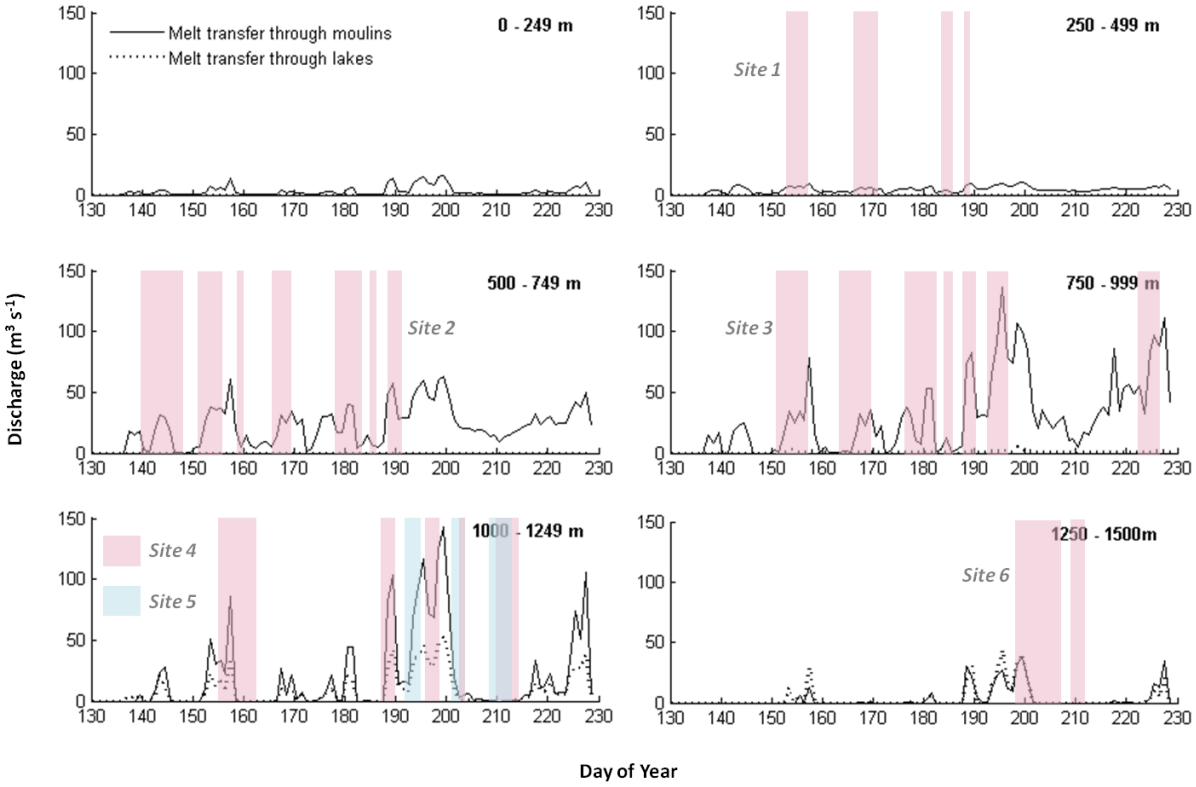

Figure 5.6.3.1. Supraglacial meltwater delivered to the bed each day through lakes and moulins within ice surface elevation bands of 250 m. Shading represents periods of accelerated ice surface velocities (after Bartholomew et al., 2011b).

Above 1000 m the model predicts that meltwater reaching the bed through drained lakes comprises a significant proportion of total melt transfer. Indeed, between 1000 m and 1249 m melt transferred through drained lakes makes up 30.7% of total melt delivered to the bed, and 50.8% of total melt delivered between 1250 m and 1500 m. Furthermore, at these highest elevations, around days 157 and 195, the relative contribution from melt delivery through drained lakes is larger than through moulins, highlighting the significance of lake drainages at high elevations. The model is therefore effective in characterising the change in relative importance of the

mechanism for delivery of meltwater to the bed with elevation. Below c.1000 m virtually all of the melt reaching the bed does so via moulins. Above c.1000 m lake drainages play a more significant role in ensuring that meltwater reaches the bed through propagation of crevasses up to 1100 m deep, and far into the ice sheet interior. A notable discrepancy in predictions of melt transfer through lake drainages is the lack of a time lag between modelled peaks in melt delivered through moulins and melt delivered through drained lakes. This suggests that the simplicity of the model does not account for the lag that may be expected for release of stored melt at higher elevations. One possible reason for this may be that the model does not fully incorporate the effect of the low tensile, or even compressive stresses found beneath and surrounding lakes, which may act to impede fracture initiation. Indeed, of the 19 lakes predicted to drain during the standard parameter model run, all but one were centred in cells characterised by tensile stresses below the prescribed tensile strength of 75 kPa; ranging 14 to 79 kPa. The exception to the lack of a time lag for lake drainage is over days 189-190, between 1250 m and 1500 m, where peak discharge through lake drainage occurs one day later due to storage of melt at the surface. Physical controls on lake drainage must be better understood for the temporal component of modelling to be improved.

5.6.4 Comparison with measured proglacial discharge

Model predictions of the total amount of meltwater reaching the ice-bed interface across the whole catchment each day were produced for both the 2009 and 2010 melt seasons. The modelled meltwater transfer was compared with daily average discharge measured in the proglacial stream during the 2009 season (Bartholomew et al., 2011a), where the pattern of rise and fall in the modelled melt delivery to the bed, although flashy in nature, follows the overall trend of the measured discharge hydrograph (Figure 5.6.4.1). Proglacial discharge measured during 2010 remained high throughout much of the ablation season due to the increased melt production in response to a season of higher air temperatures, which is seen in the model outputs, where repeated spikes in discharge of 200 $m^3 s^{-1}$ and over are predicted.

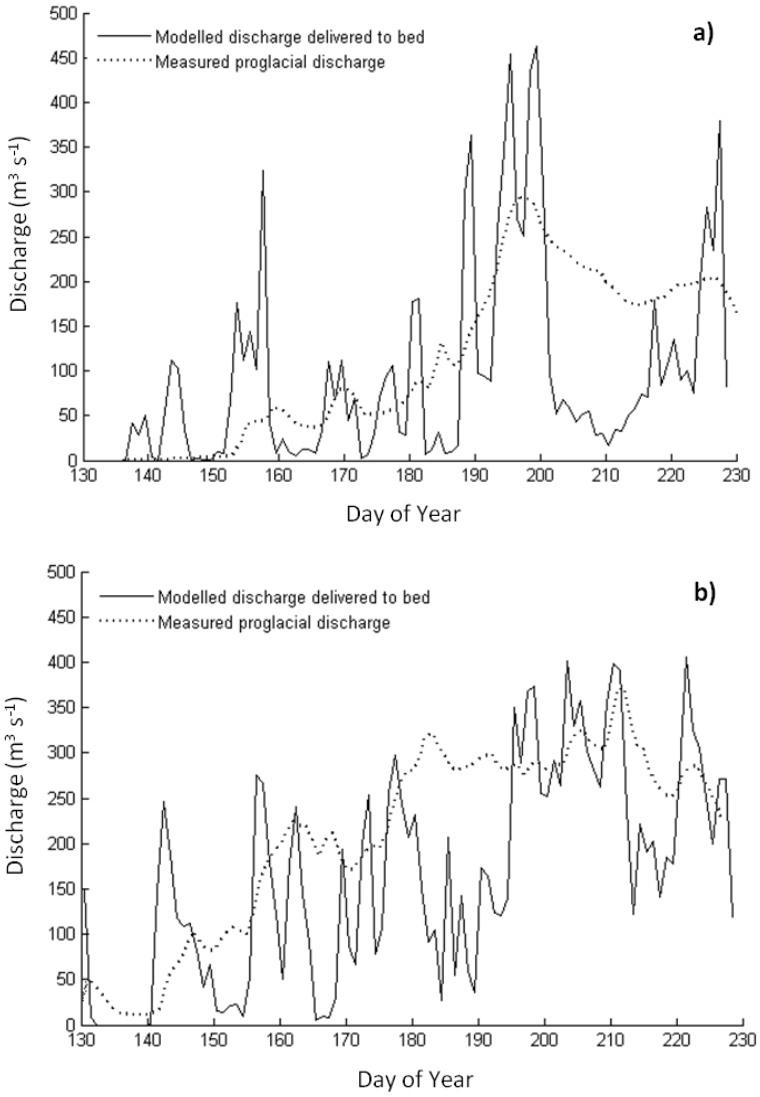

Figure 5.6.4.1. Daily average discharge measured in the proglacial stream and modelled total daily delivery of meltwater to the bed for a) 2009 and b) 2010.

The transfer of meltwater from the ice surface to the bed predicted by the model each day produces a flashy response curve in comparison to the measured average daily discharge curve for both the 2009 and 2010 melt seasons. However, this result is not unexpected, as the model does not account for subglacial drainage system configuration or transit times of meltwater from its source to the proglacial outlet. Furthermore, percolation time through snow or firn, or storage of meltwater in micro-fractures is unaccounted for due to a lack of physical basis with which to incorporate such factors within modelling. The aforementioned reasons may go some way to accounting for the discrepancies between the smooth measured discharge and flashy modelled melt delivery to the bed, which results in normalised RMS deviations

between modelled and measured discharge of 33.9% and 29.0% for 2009 and 2010 respectively. To evaluate how accurately the model was able to predict the total melt being delivered to the bed over the season, the area beneath each hydrograph was compared. For 2009 the model predicts a total of c. 799 x 10^6 m^3, 13.5 % less than total measured average daily proglacial discharge which amounts to c. 923 x 10^6 m^3. For 2010, the model does less well, predicting a total of c. 1404 x 10^6 m^3, 20.5 % less than the total of c. 1765 x 10^6 m^3 measured in the proglacial stream. Given the simplicity of the degree-day melt modelling approach, potential errors in defining the hydrological catchment, supraglacial meltwater routing, discharge measurement errors of ±15% (Bartholomew et al., 2011a), and not accounting for the transit time and storage of meltwater in snow and firn which may affect the temporal patterns of modelled discharge, such discrepancies in the area below the hydrograph are to be expected, and the results are encouraging. In addition, the match between total proglacial discharge and modelled melt delivery to the bed tells us that the model does well in assessing the total volume of meltwater stored in the englacial system during the ablation season.

5.6.5 Moulin spacing

Immediately downstream of cells containing a crevasse, as determined by the prescribed tensile strength, meltwater accumulation within the supraglacial flow routing routine is set to zero, as crevasses will entrap water routed into them from upstream. As such, the model assumes no downstream transfer of supraglacial melt following capture by crevasses, and melt must begin accumulating again in crevasse-free areas. However, clustering of predicted moulins at lower elevations suggests that below c.1000 m supraglacial melt generated within a single grid cell may be sufficient to force full-thickness penetration of a single water-filled fracture. This is due to the thinner ice in this area, the often relatively high stresses, and the increased melt production experienced at lower elevations; however it is exacerbated by underrepresentation of crevasses. With better knowledge of crevasse spacing within a glacial catchment it would be possible to distribute modelled melt such that any

melting generated within a cell is split evenly between a prescribed number of crevasses, whilst meltwater flowing into a cell from above is routed into a single locally-dominant moulin. Since the water level within a crevasse is the foremost control on propagation depth using this modelling approach (Van der Veen, 2007), by splitting intra-cell generated melt between a number of crevasses, the potential for overestimation of moulin locations may be reduced. This could be achieved in a simple, statistical fashion, by relating the density of crevasses within each cell to the tensile stress, or defining the number of crevasses in each cell through remote sensing analyses or mapping. To test this approach, and to see what *could* be implemented with sufficient knowledge of crevasse spacing in a model catchment, the model was adapted to relate the number of crevasses in each cell to the surface tensile stress regime, and was again run for the Leverett catchment with 2009 meteorological data and standard model parameters (Figure 5.6.5.1).

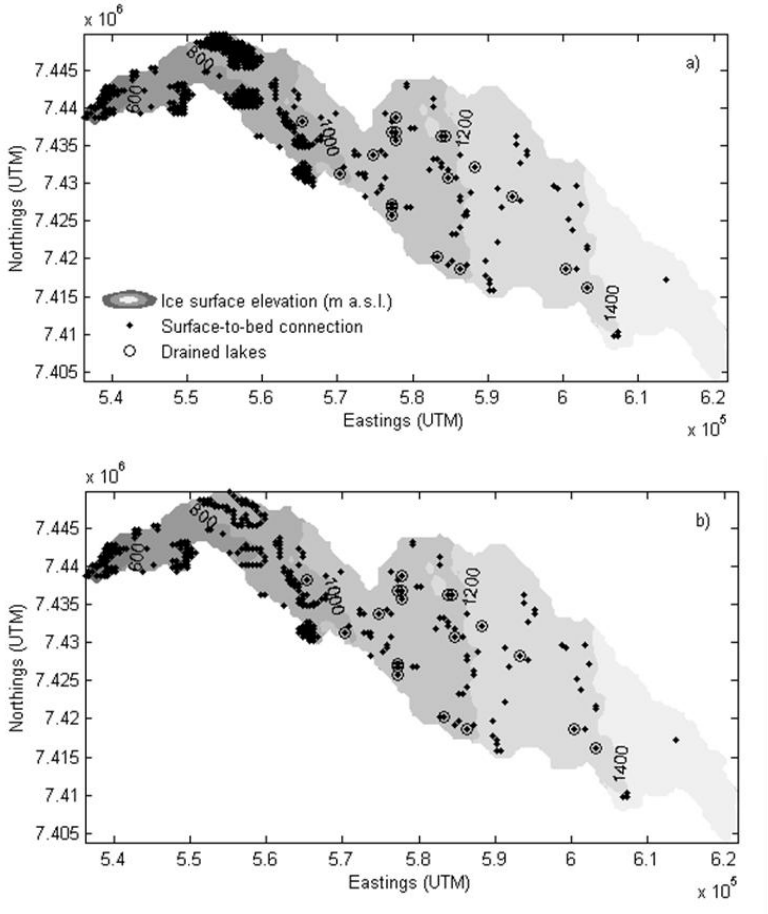

Figure 5.6.5.1. A comparison of moulin distribution for the initial 2009 model run (a) and the 2009 model run within which intra-cell crevasse spacing is incorporated (b).

One crevasse per cell was assigned where tensile stress is ≤ 100 kPa; two crevasses where tensile stress is ≤ 125 kPa; three where tensile stress is ≤ 150 kPa; and four where tensile stress is > 150 kPa. This effectively reduces the meltwater level in a crevasse in each cell, which subsequently controls crevasse penetration depth, as the crevasse opening surface area makes up a larger proportion of cell area when intra-cell crevasse numbers are higher. The proportion of a cell characterised by crevasse void space could be further controlled by allowing crevasse width to vary spatially, but this would require an even more detailed knowledge of crevasse spacing and geometry, which is limited by remotely-sensed image resolution. Whilst the number and spatial distribution of lakes remain the same, since the model continues to assume the opening of a single crevasse beneath a drained lake, it is clear that the distribution of moulins has been altered. Indeed, the total number of moulins decreased by 20.5%, resulting in a reduction in meltwater transfer to the bed of 3.9%. This decrease in moulin numbers occurs mainly within the higher tensile stress areas of the lower catchment (Figure 5.4.1), reducing clustering of moulins (Figure 5.6.5.1). The exception to this remains the clusters within c.15 km of the terminus, where the ice is no more than 400 m thick, according to the dataset applied here (Bamber et al., 2001). Temporally, the formation of moulins is almost unaffected, with the majority of moulins forming at the same time as they did in the initial run. While the spatial resolution of the Landsat imagery used in this study is restrictive in mapping the surface distribution of crevasses, or in calculating a true relation with the surface stress regime; these results highlight the importance of including crevasse spacing where it is possible, to reduce the potential for over- or indeed underestimation of moulin formation.

Modelling assumes localised dominance of a single moulin within each cell such that moulin spacing within the catchment cannot be closer than the model spatial resolution. To minimise grid-dependency, and to allow for model application at varying spatial resolution, a void ratio could be applied when observations of crevasse surface dimensions across the spatial extent of the catchment are limited or unknown. The surface area of a crevasse, A_c, may then be altered to satisfy the void ratio, e, where the total area of a cell is A_t and the ice surface area is A_i:

$$e = \frac{A_c}{A_i} = \frac{A_c}{A_t - A_c} \qquad (5.1)$$

Implementing this concept would control the cross-sectional area of a crevasse such that regardless of cell size, the same penetration depth would result in response to meltwater routed into the crevasse. Whilst total meltwater generation through degree-day modelling will change little in response to differing spatial resolution, defining the spacing of locally dominant moulins remains limited by field observations. Applying a statistical basis for crevasse and moulin spacing within different elevation bands would help to improve model predictions further. This highlights the need for mapping of the distribution of these features, as seen at the surface from field observations and remote sensing, such as the technique of image classification described by Phillips et al. (2011), to allow for a more complete modelling approach to moulin formation and meltwater transfer.

5.7 Concluding remarks

The results of applying a spatially distributed model for prediction of moulins and lake drainages to Leverett Glacier catchment of the south-western GrIS have been presented. The model predicts markedly higher spatial densities of moulins below 1000 m which is indicative of rapid delivery of daily melt to the glacier bed, a finding that is consistent with interpretations from field measurements of surface melt and velocity. Above 1000 m, modelled moulin densities decline rapidly with elevation and the model predicts that melt transfer to the bed becomes increasingly dependent on the drainage of supraglacial lakes. The increased density of predicted lake drainages is corroborated by observations of velocities recorded at higher elevation sites responding to the release of stored melt. The general patterns of behaviour reproduced by the model, in terms of sources of spatial controls on ice surface velocities, fit well with field evidence suggesting that meltwater reaches the bed through propagation of crevasses through ice of great thickness, far into the ice sheet interior.

Modelling moulin formation for the warmer 2010 season may be indicative of the potential for increased transfer of supraglacial melt, and inland expansion of the area experiencing melt delivery to the bed, during periods of increased melt generation as would be the case under a future warming climate. The result of increased melt production, such as that witnessed in 2010, may have important implications for subglacial configuration, basal water pressure, and consequently ice dynamics further inland from the terminus during warmer years. Palmer et al. (2011) suggest a close relationship between supraglacial meltwater routing, lake locations and patterns of ice surface velocity for an area of the western GrIS which includes the Leverett catchment. Localised dynamic response to meltwater delivered to the bed along such supraglacial melt pathways could lead to increased ice surface velocities and drawdown of ice from much higher elevation under a future increased melt scenario, with lakes able to drain through many hundreds of metres of ice at or above the present equilibrium line altitude (Alley et al., 2005).

There is currently a relative dearth in knowledge of the physical processes influencing the formation and propagation of moulins, and the timing and mechanisms of supraglacial lake drainage. An improved physical basis for prescribed crevasse width and spacing and for ice temperature would allow for more rigorous modelling of moulin formation. Given that we may see an increase in melt transfer to the ice-bed interface under a warmer climate as the areal extent of surface melting on the GrIS increases (Hanna et al., 2008), and that melt-induced speed-up of outlet glaciers in Greenland may become increasingly significant for mass loss, it is imperative that we continue to enhance our understanding of these processes for informing the improved coupling of hydrology and dynamics, particularly within ice sheet modelling.

Chapter 6. Discussion

6.1 Model performance

6.1.1 Comparison between research sites

Following description of model development, set-up and application in the previous chapters, this chapter will now discuss the performance of the model, model transferability, and possible future applications to which the modelling routine could contribute. The model, as described in chapter 3, was applied to two glacial catchments, contrasting in thermal regime, catchment size, geographical location and dynamic behaviour. The Croker Bay catchment of Devon Ice Cap in Arctic Canada (chapter 4) is c.2200 km^2 in area, and feeds two marine-terminating outlet glaciers, extending from sea level up to the ice divide at c.1930 m. In comparison, the c.1200 km^2 Leverett Glacier catchment of the SW Greenland Ice Sheet (chapter 5) is land-terminating, extending more than 50 km inland of the ice sheet margin up to c. 1550 m. The 10 m temperatures, or equivalent average annual temperatures, of -5°C for Leverett Glacier and -13°C for the Croker catchment, were applied for determining the stiffness parameter in the constitutive relation between strain and stress. This was subsequently used in calculation of the ice surface stress regime from InSAR velocities in the two study areas. Whilst the 10 m temperature is a somewhat approximate measure of representative annual ice temperature, assuming surface temperature does not exceed melting point (Knight, 1999), given that the crevasse depth modelling approach taken here is not integrated with depth, and with a lack of temperature data through the ice column, the temperature must be assumed constant for the full ice thickness regardless. As suggested by Figure 1.4.1.1 in the introductory chapter, the ice tensile strength varies significantly between the two study catchments, possibly because of differences in temperature at the sites. This means that whilst for Leverett Glacier surface crevasses are predicted by the model when the tensile stress exceeds 75 kPa, the standard input tensile strength, they are not predicted in the Croker catchment until the tensile stress exceeds 300 kPa. The spatial distribution of surface

crevassing and thus potential moulin locations are controlled by this, and later in this chapter model sensitivity to the prescribed tensile strength is explored further.

The sites for which the model has been applied within this study have been used in different ways to test model predictions. The Leverett Glacier benefits from a summer-long record of proglacial discharge during both 2009 and 2010; the set-up of which is described by Bartholomew et al. (2011b). This record allowed modelled daily total meltwater delivery to the bed to be evaluated against real-time field data. The record of surface velocity available for a transect of Leverett Glacier catchment (Bartholomew et al., 2011a) also provided a means of evaluation of model predictions relating to observed velocity response to meltwater input at different elevations. Indeed this velocity record, twinned with modelled quantification of melt transfer to the bed within each elevation band, could be used to investigate the relative contribution of melt transfer through surface crevasse-originating moulins and through the drainage of supraglacial lakes. The Croker Bay catchment has been the focus of a study of ice dynamic regimes, with velocity data available catchment-wide, excepting minimal areas where the look direction of the satellite produced unreliable data. The relative contribution of basal motion is discussed by Burgess et al. (2005), and was used in chapter 4 to draw inferences from the prediction of moulin formation and lake drainages in the Croker Bay catchment, regarding the possible enhancing behaviour of melt delivery on ice dynamics. Furthermore, for Devon Ice Cap, the availability of 15 m spatial resolution imagery allowed for identification and comparison of moulins and supraglacial lakes visible at the surface with those predicted by the model. However, for Leverett Glacier, surface crevasses and moulins are very hard to detect from the Landsat imagery which was used in this study to identify lakes; as such, evaluating the spatial accuracy of model predictions is much more difficult.

Whilst predicted moulin numbers are not directly comparable between the two sites, the density of moulin formation can be examined. Below 1000 m elevation, the average densities of moulins predicted by the model for the years that produced the least melt were 1.6 moulins/km^2 for Leverett Glacier during 2009, compared with a much smaller density of 0.38 moulins/km^2 for the Croker Bay catchment during 2004. Above 1000 m, there were no moulins predicted for the Croker Bay catchment during

2004, whilst the Leverett catchment contained an average density of 0.06 moulins/km^2 during 2009. These are large differences in moulin density, particularly so below 1000 m elevation where Leverett Glacier has a four times greater modelled moulin density. The reduced melt conditions and high tensile strength typified by the Croker Bay catchment are likely the controlling factors for the reduction in moulin distributions in comparison to the relatively meltwater-rich environment of the SW GrIS. In addition to moulin densities, the percentage transfer of supraglacial melt to the bed through these connections can be compared. 93.5% of melt generated on Leverett Glacier during 2009 was transferred to the bed of the catchment, with a 95.2% transfer calculated for the Croker Bay catchment during 2004. Both sites experienced an increase in percentage transfer during years typified by higher melt generation, with a 96.5% transfer during 2010 on Leverett Glacier, and 97.8% transfer during 2006 on the Croker Bay catchment. Furthermore, both sites experienced similar sensitivity in percentage melt transfer in response to varying the tensile strength and crevasse width parameters. This suggests that regardless of surface-to-bed connection numbers, the transfer of supraglacial melt to the bed of both catchments is similar, with generated melt finding pathways to the bed. Importantly, these tests suggest that in increased melt years, there is not only an increase in the absolute amount of melt delivered to the subglacial system, but also to the percentage transfer of melt. It should also be noted that the temporal formation of moulins was shown to occur earlier in the ablation season during years of higher melt production for both sites, with both sites also typified by the same pattern of increase moulin formation elevation with time into the season. In addition to any differences and similarities in model predictions for the two catchments, the sensitivity of the model in input parameters is of particular importance, as will now be explained.

6.1.2 Model sensitivities

Through evaluation of the results of model runs designed for sensitivity testing purposes, applied to both study sites, it becomes clear that the model is highly sensitive to certain input variables (chapter 4, tables 4.6.1 and 4.6.2; chapter 5, table

5.5.3.1). This is particularly true for the ice tensile strength, which controls where surface crevasses can form, and thus the spatial distribution of moulins, and for those variables controlling the rate at which a crevasse is filled with surface-generated meltwater. These results highlight the importance of constraining accurate values for model variables, and indeed for allowing spatial variation in these values where possible. Particularly important for future consideration is the spatial variation in crevasse surface geometry, since this has a strong controlling influence on both moulin numbers and the percentage of generated melt that reaches the bed. Given that crevasse size controls the rate at which a crevasse can be filled with water, and that the rate of water filling is the most important control on fracture propagation depth (van der Veen, 2007), allowing crevasse size to vary across a catchment would thus certainly increase model prediction accuracy. The major constraint in prescribing spatially-varying crevasse size is that it must be either related to some other known physical parameter or determined from field studies or remotely-sensed imagery. Whilst mapping crevasse dimensions on small alpine glaciers is possible, on glacial catchments of the sizes typified by the Croker Bay glaciers and Leverett Glacier, field surveying of crevasse sizes is problematic both in mapping representative spatial coverage and in safe access to heavily crevassed areas. Furthermore, mapping such features in the field is both costly and time and labour intensive. Digitising of crevasses from satellite or aerial imagery overcomes these issues, but suffers from the limitations imposed by the spatial resolution of the sensor. Figure 6.1.2.1 illustrates typical crevasse detail visible from satellite-acquired imagery.

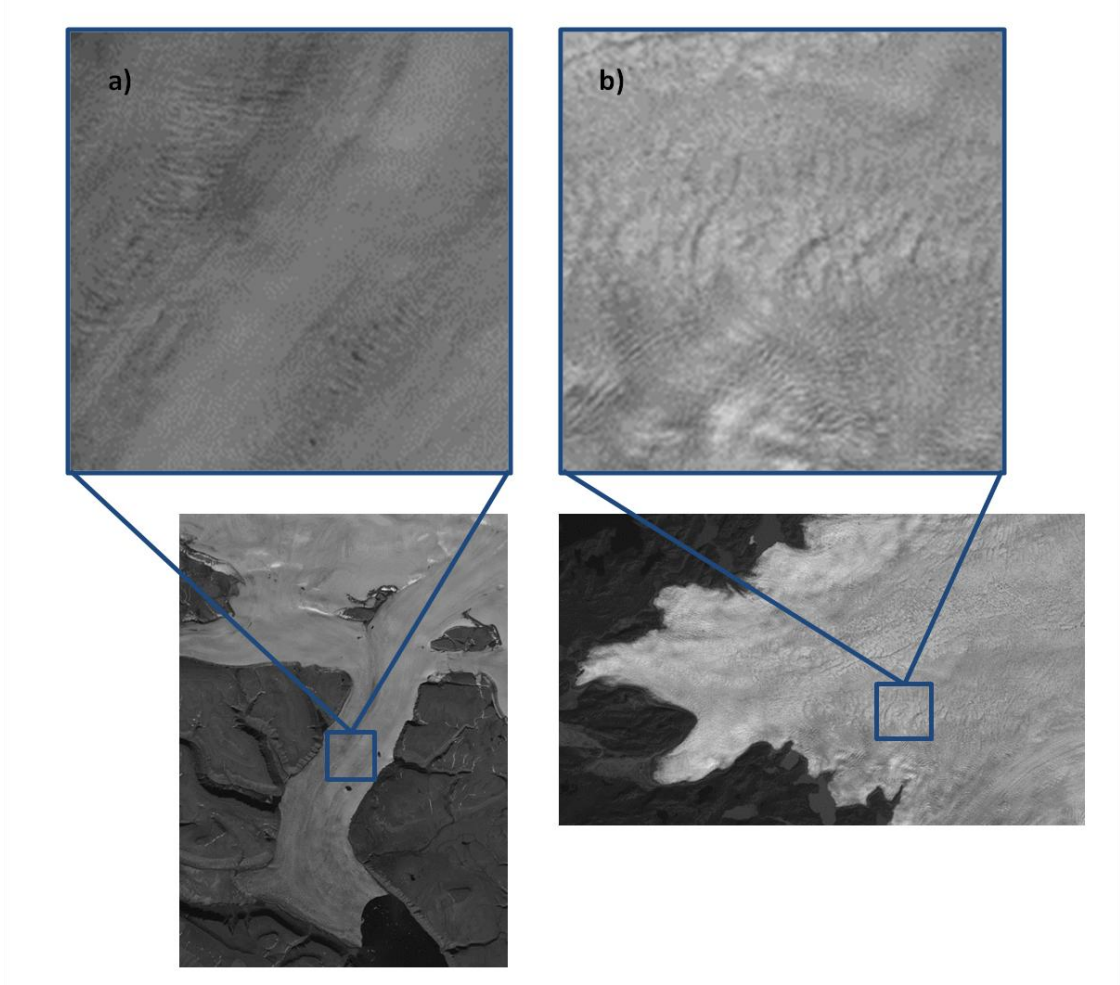

Figure 6.1.2.1. Examples of crevasses visible on Landsat imagery of the North Croker Bay (a) and Leverett (b) glaciers

Landsat 7 imagery used within this study for digitising features and analysing model spatial accuracy for Devon Ice Cap has a spatial resolution of 15 m, as the images were acquired using the panchromatic mode (band 8). Whilst transverse crevasses visible on the main North Croker bay glacier tongue can be relatively clearly identified as up to 500 m in length (Figure 6.1.2.1, a), the value assumed in model runs, it is not possible to determine their width given the resolution of the imagery. Furthermore, inland of the tongue crevasse fields are not as extensive and individual crevasse size is typically much smaller and thus indeterminable. Towards the terminus, the scene is complicated by longitudinal crevasses and heavy crevassing on the floating part of the tongue; however, given the influence of ocean-ice interaction at these lower elevations, modelling without incorporating these effects cannot produce reliable

results regardless. The images used to view surface features and digitise lakes on Leverett Glacier in SW Greenland were also acquired using Landsat 7; however these images have a spatial resolution of only 30 m, as the downloadable files were 'natural look' colour images constructed from the visible bands (1-7). From the close-up excerpt of Figure 6.1.2.1 b, the problematic nature of prescribing crevasse surface dimensions within modelling based on remotely sensed imagery of this spatial resolution becomes clear.

Perhaps even more difficult to quantify as a spatially distributed value is the ice tensile strength. Assuming that the value of this model parameter must be held constant with depth, for small glacial catchments, it may be acceptable to assume one universal value of tensile strength. Should the modelling routine be used for ice cap or ice sheet-scale applications, where this value would almost certainly in reality vary spatially, some knowledge of the 10 m temperature, or other influencing physical factors would be necessary for a number of spatially distributed points. The debate over, or perhaps lack of evidence for tensile strength being influenced in some way by ice temperature (chapter 2, Figure 2.3.1.1) is ongoing; but with relatively few investigations describing this physical property available within the scientific literature, temperature can certainly not be ruled out as a control. Results described by Vaughan (1993) following his analysis of historical field-measured strain rates did not suggest that tensile strength varied with 10 m temperature, and Petrovic (2003) in his review of previous investigations into this parameter found that ice was more sensitive to temperature when in compression than when in tension. Furthermore, with a current shortcoming in our ability to reproduce the fracture of field-sampled ice under laboratory conditions, the controlling influence of ice impurities, density and crystal size and structure cannot be realistically used to help derive spatially-varying ice tensile strength. Perhaps for future studies the 10 m temperature should be measured at intervals along the centreline of outlet glaciers and up towards the ice divide, to correctly calculate the tensile stresses, using the temperature-dependent constitutive relation, and thus determine the ice tensile strength within different areas. As Mottram & Benn (2009) also concluded from their study testing crevasse-depth models, the physical processes influencing crevassing must be properly understood

both from field and remotely sensed data if models are to be improved and incorporated into coupled models of hydrology and dynamics. In addition to sensitivity to model inputs, the sensitivity of the modelling routine to model set-up, including grid spatial resolution is of equal importance, as will be described in the following section.

6.2 Transferability

6.2.1 Spatial resolution dependence

The model, as described in chapters 4 and 5, was set at a 500 m spatial resolution for both study areas for all model runs. Due to the ice thickness at these sites, a higher spatial resolution would likely not be suitable for modelling purposes; however, to investigate how model results are affected by altering the spatial resolution, the model was run again at both 250 m and 1 km grid resolutions. This was done for both the Leverett catchment and the Croker Bay catchment, maintaining the standard parameters as described for each site in chapters 4 and 5, but altering crevasse width to equal cell width. To focus on the core component of the model and to reduce complicating factors, supraglacial lakes, as the weakest component of the modelling routine, have been removed for these tests. This allows for the effects on predicted moulin formation through water flow into surface crevasses alone to be evaluated in detail. For the Croker Bay catchment of Devon Ice Cap, running the model at a 250 m resolution results in a 139.8% increase in moulins predicted, and a 27.0% decrease in melt transfer to the bed. Running the model at a 1 km resolution results in a 77.3% decrease in the number of moulins predicted to form in comparison to the 500 m model run, but only a 1.0% increase in the percentage melt transfer from the ice surface to the bed.

From Figure 6.2.1.1 it is clear that the temporal occurrence of moulin formation does not appear to be significantly affected when the spatial resolution is reduced to 1 km; however first propagation of crevasses to the bed at low elevation occurs around 10 days later when the spatial resolution is increased to 250 m. Furthermore, the spatial

extent of moulins appears to be increased when a 1 km grid resolution is applied. These results are similar to those produced by altering the crevasse width, as depicted in chapter 4, figures 4.5.2.3 and 4.5.2.4, where moulin formation was delayed by increasing the crevasse width, also leading to a decrease in melt transfer to the bed, and vice versa. The results of altering crevasse width and altering grid spacing, where crevasse length equals the cell width, produce similar spatial and temporal patterns in moulin formation because they both control the volume of crevasse void space in a cell, and thus the level of water-filling within crevasses. Because the model currently assumes one surface crevasse per cell, by increasing the spatial resolution the water generated at the ice surface is split between more crevasses, thus slowing down fracture propagation, but increasing the number of potential sites for moulin formation. Indeed, for the 250 m resolution model run, the majority of moulins were delayed in their formation further into the melt season, reducing the amount of water that could be transferred to the bed throughout the season.

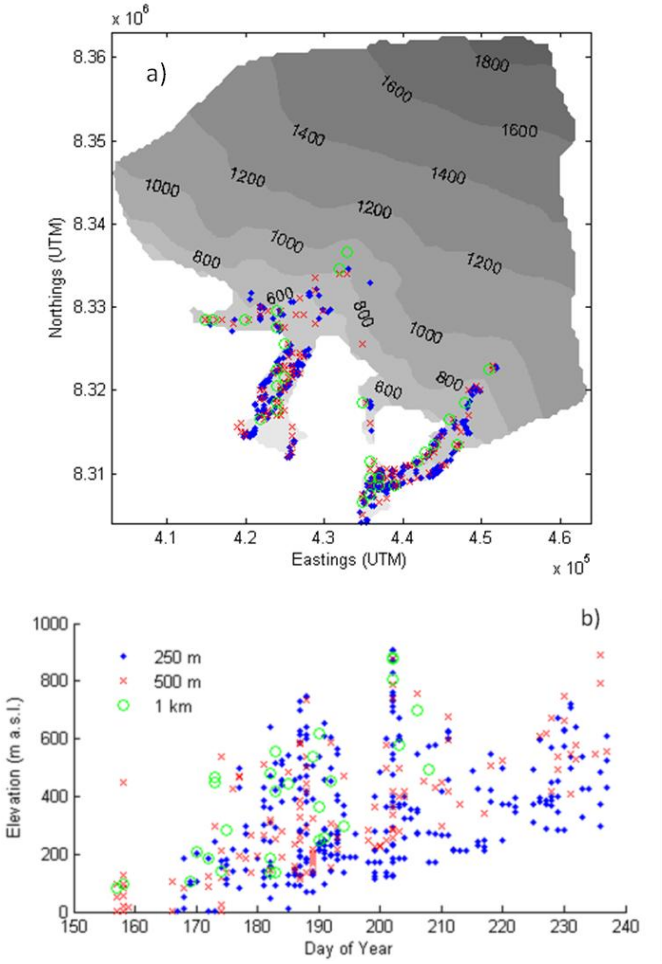

Figure 6.2.1.1. Spatial (a) and temporal (b) patterns of moulin formation predicted by modelling at 250 m, 500 m and 1 km grid resolutions for the Croker Bay catchment

When a 1 km grid spacing is applied to the Leverett catchment, the result is a 69.3% decrease in moulin numbers, and a 3.6% increase in melt delivery to the bed, possibly due to the reduction in surface crevasses which interrupt water flow across the ice surface (Figure 6.2.1.2). However, when the model is run at 250 m resolution for the Leverett catchment, it produces a 39.5% increase the in number of moulins predicted, with a 7.9% decrease in melt transfer. Temporally, there is little notable change in when crevasses propagate to the bed when the model is run either at 1 km or 250 grid resolution, excepting a very slight delay in the formation of lower elevations for the 250 m model run; likely due to the increased interruption and splitting of meltwater between crevasses which acts to slow fracture propagation.

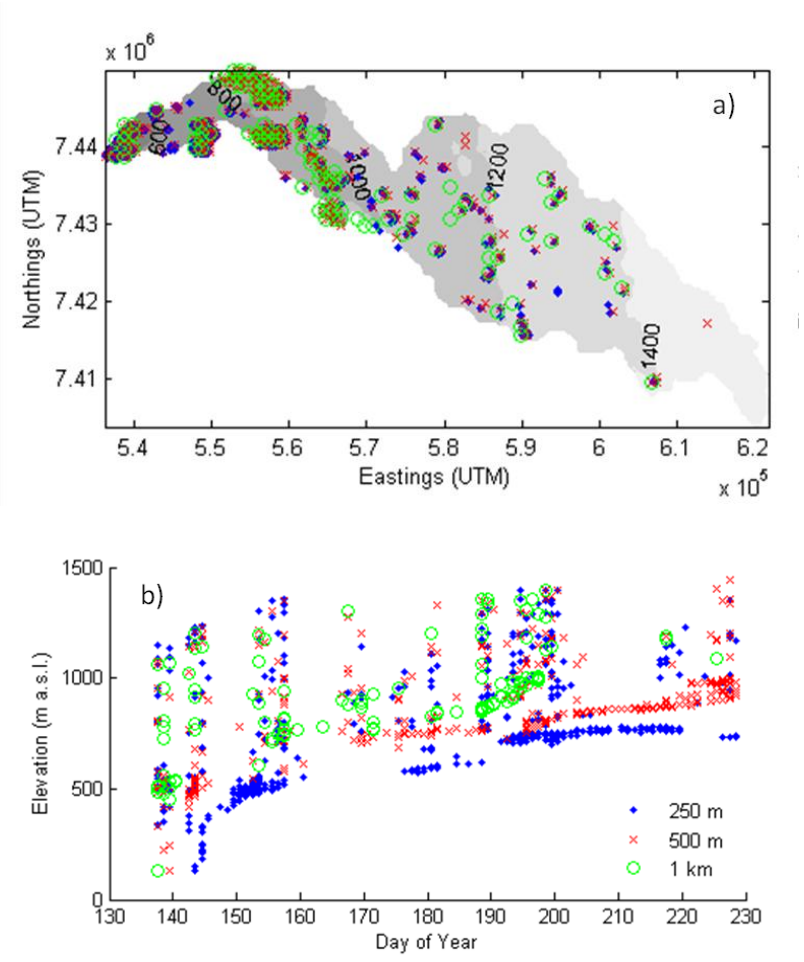

Figure 6.2.1.2. Spatial (a) and temporal (b) patterns of moulin formation predicted by modelling at 250 m, 500 m and 1 km grid resolutions for the Leverett catchment

These results show that by decreasing the spatial resolution from 500 m to 1 km, the potential for moulin formation is significantly reduced, since the model assumes only one surface crevasse per cell. This highlights that for model application at, for example, ice sheet modelling resolution, a statistical approach would have to be adopted to prescribe crevasse spacing within different elevation bands, allowing for the presence of multiple crevasses within individual cells. The proportion of a cell characterised by crevasse surface opening, controlling the meltwater level in a crevasse, could be held constant if a void ratio incorporating crevasse spacing was applied. Both the temporal and spatial patterns of moulin formation would be affected by the resultant effect on meltwater inflow to surface crevasses if this point was not addressed and variance in crevasse spacing incorporated appropriately.

6.2.2 Viability for use in different study areas

This study has shown that the model can be applied to glacial catchments significantly different in their characteristics, due to the simplicity of the compartmental model structure and the minimal data requirements. However, model application is limited in its accuracy by available observations of physical properties and surface features; namely the distribution and size of crevasses. With some knowledge of the distribution of these features from remotely sensed imagery, application to other glaciers is certainly possible. The potential for the model to be run for other outlet glaciers of Devon Ice Cap, in particular the Belcher glacier, has been noted through contact with people currently looking at the hydrology and dynamics of the ice cap (Dave Burgess; Gwenn Flowers and Martin Sharp, personal communication). Belcher glacier is an ocean-terminating glacier draining part of the north-east quadrant of the ice cap. Burgess & Sharp (2008), investigating changes in ice thickness on the ice cap, noted the presence of meltwater streams terminating in moulins and crevasse fields on the Belcher glacier. Their research suggested that flow enhanced by meltwater reaching the bed may be an influencing factor on the net ice surface lowering between 300 and 1400 m elevation, likely caused by the increased rate of ice outflow which exceeds net accumulation. Both the Belcher and Croker Bay glaciers are ocean-terminating, and as

such surface tensile stresses near the termini are influenced by both supraglacially-generated meltwater and terrestrially-derived driving stress, and basal crevassing and reduced stresses associated with marine termini. Whilst the reliability of model application to these glaciers is affected at lower elevations by the possible presence of basal crevassing, reliability of application to land-terminating glaciers is not limited in its spatial extent by these added factors. In addition to application to single Arctic and Alpine glacial catchments, the model could also be adapted for application to ice sheet modelling. This would rely on some knowledge of statistical distributions of surface features including crevasses and/or moulins, and the distribution and size of supraglacial lakes. This concept is explored further within the next section of this chapter, where possible future applications of the modelling routine are explored.

6.3 Model applications

6.3.1 Forcing models of subglacial hydrology and glacier dynamics

Recent studies, including Schoof (2010) and Hewitt (2011), have sought to constrain the formation of and switch between distributed and channelized drainage within the subglacial hydrological system. Schoof (2010), applying a model that incorporates switching between cavity-based and channelized models of subglacial configuration, investigated system response to meltwater input within an idealised subglacial drainage system. Model simulations were driven by a significant sudden increase in melt supply to the system, followed by a steady supply then a return to background values. Through these simulations he found that while a steady supply of melt would result in ice deceleration as the subglacial system, responding to water pressure, develops to become efficient; increased variation in water supply drives short-term ice acceleration as the system temporarily accommodates higher water pressures. Models for channelized and distributed drainage were presented by Hewitt (2011), where model simulations were run for a steady-state drainage system. The mechanism of channelization was investigated, concluding that a length scale in distributed systems drives the width of glacier bed for which a channel will draw its water. However, the

study did not consider the spatial variation in englacial melt transfer that may influence this spacing. Models such as these have not, thus far, included spatially distributed point-surface inputs of meltwater which have a dynamic temporal signature. Observational and modelled sources of meltwater input to the subglacial system are imperative if the behaviour and development of the subglacial system is to be truly constrained within a modelling framework.

Modelling of glacier dynamics coupled to hydrology has also advanced significantly in recent years. Pimentel et al. (2010), describing a flow-band model of ice dynamics which is coupled to hydrology, found that modelled subglacial water pressures resulted in glacier sliding significantly different from traditional pressures prescribed as a fraction of overburden pressure. Applied to Haut Glacier d'Arolla under a Little Ice Age geometry scenario, the study found that simulating increased meltwater supply to the bed produced results which although matching results of the previous EISMINT modelling project (Huybrechts et al., 1996), were not realistic in comparison to field measurements. Pimentel & Flowers (2011) further explored hydrological-dynamic coupling by applying a flow-band model that allows for switching between distributed and channelized flow. When applied to an alpine-type glacier the model qualitatively replicated both diurnal and seasonal changes in dynamics, and, notably, the 'spring event'. Despite these advances, coupled models of glacial hydrology and dynamics often lack a basis in real-time observations or physically-based modelling of hydrological inputs from real data; instead remaining largely theoretical, based on hypothetical data sets and idealistic glacial catchments. Whilst the model presented in this thesis is spatially distributed, a model of a similar construction could be developed to prescribe temporal records of average meltwater inputs across elevation bands to flow-band models of ice dynamics.

6.3.2 Incorporating supraglacially-derived hydrology into ice sheet models

Ice sheet modelling, particularly in response to future climate scenarios, does not at present fully incorporate distributed surface-derived meltwater inputs to the

subglacial system, or indeed incorporate the full influence of subglacial hydrology on dynamic response. Some models, including Arnold & Sharp (1992; 2002) included hydrological influence on dynamics in modelling the evolution of past ice sheets; however these models were one and two dimensional. Schoof (2010) highlighted the importance of incorporating surface-derived melt inputs through his subglacial modelling work. He stated that by not including subglacial processes which respond to diurnal melt cycles rather than mean melt alone, the evolution of past ice sheets cannot be simulated appropriately, and that the same is true for present day and future ice sheet models. A recent report on implementation of glacial hydrology within land ice models further stressed the need for inclusion of both the locations and timing of meltwater inputs, necessary to drive realistic simulation of subglacial hydrological system evolution (Price et al., 2011a). Furthermore the report highlighted a need for improved observations, including the distribution of important sub-grid scale features including crevasses, moulins and supraglacial lakes (Price et al., 2011b). Section 6.2.1 of this chapter explored the effect of altering model grid resolution on model results. The results of testing sensitivity to grid resolution further highlighted the importance of having some knowledge of the density of surface crevasses at different elevations.

To address this, remote sensing-based analysis such as image classification could be applied to determine where crevasses, or even moulins, are visible at the ice surface, as was described by Phillips et al. (2011). Whilst this does not tell us anything about how far those surface features penetrate through the ice column, it would provide a basis for a statistical approach to incorporation of supra-to-subglacial connections within ice sheet models. Ice sheet modelling is generally restricted to operating at a spatial resolution determined by the ice thickness. With knowledge of crevasse distribution or moulin densities, higher resolution modelling could be applied at the margins and outlet glaciers to account for the more dynamic nature of hydrology pathways and more extensive crevassing in these regions, whilst allowing for coarser resolution modelling for the ice sheet interior, as typified by current ice sheet models. Figure 6.3.2.1 illustrates conceptually how this model could be implemented within larger land ice models. It depicts an example section of the GrIS, split into grid resolutions of 500 m below 1000 m elevation, and 5 km above. Modelled moulin

densities, calculated from running the model for the wider Russell-Leverett area in chapter 5, are shown for each 250 m elevation band, and meltwater flow accumulation at 500 m and 5 km spatial resolution is depicted to illustrate how supraglacial hydrology could be incorporated at varying resolutions, allowing for higher resolution modelling at the margin.

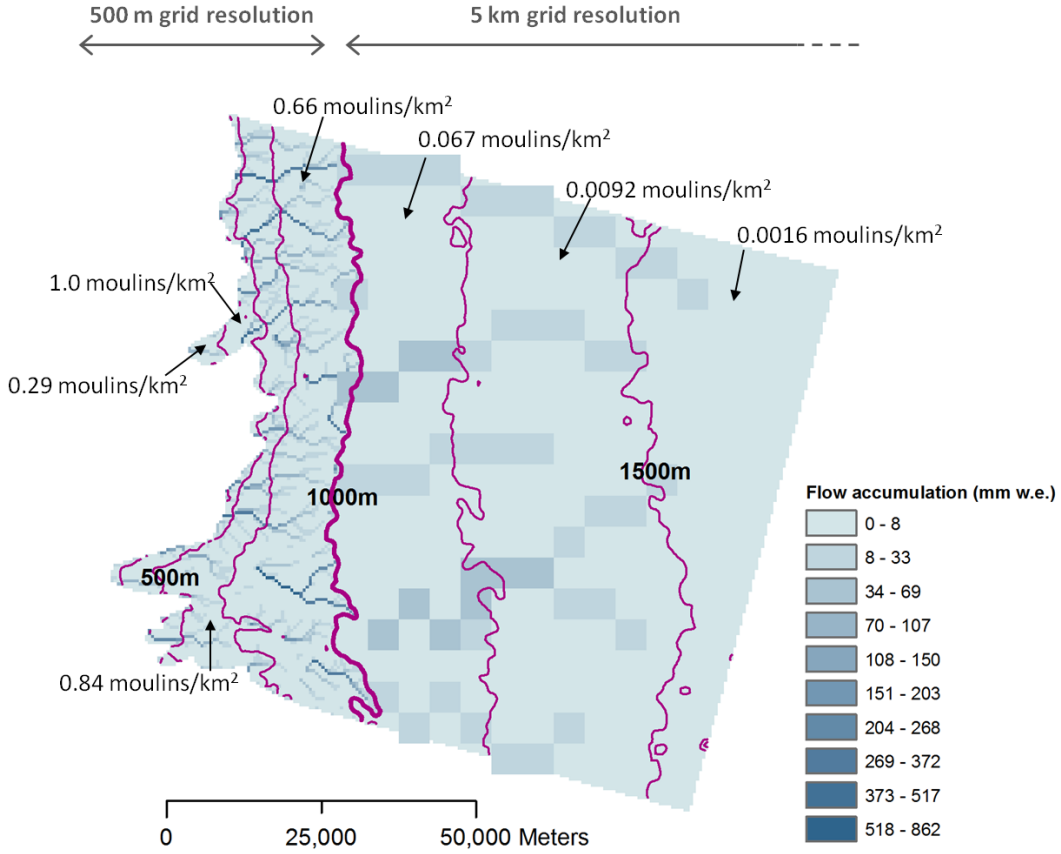

Figure 6.3.2.1. Conceptual illustration of possible model implementation within wider ice sheet modelling. Regional excerpt shown here extends northwards from 67°N on the SW GrIS

To highlight the importance of sufficient inclusion of connections between the supraglacial and subglacial systems within ice sheet modelling, Figure 6.3.2.2 illustrates how the densities of moulins could be influenced by future increased air temperatures. For this model run, the A1B mean June, July and August air temperature projection for the Arctic region, a rise of 2.1°C, as described in the IPCC Fourth Assessment Report (IPCC, 2007), was applied to the 2009 measured temperatures for Leverett Glacier. This scenario projects how air temperatures may change by the end of the 21st Century

based on average projections from 21 global climate models and with greenhouse gas emissions reflecting a world of rapid economic growth, the population reaching a ceiling of 9 billion, and with emphasis on both fossil-fuel and renewable energy resources.

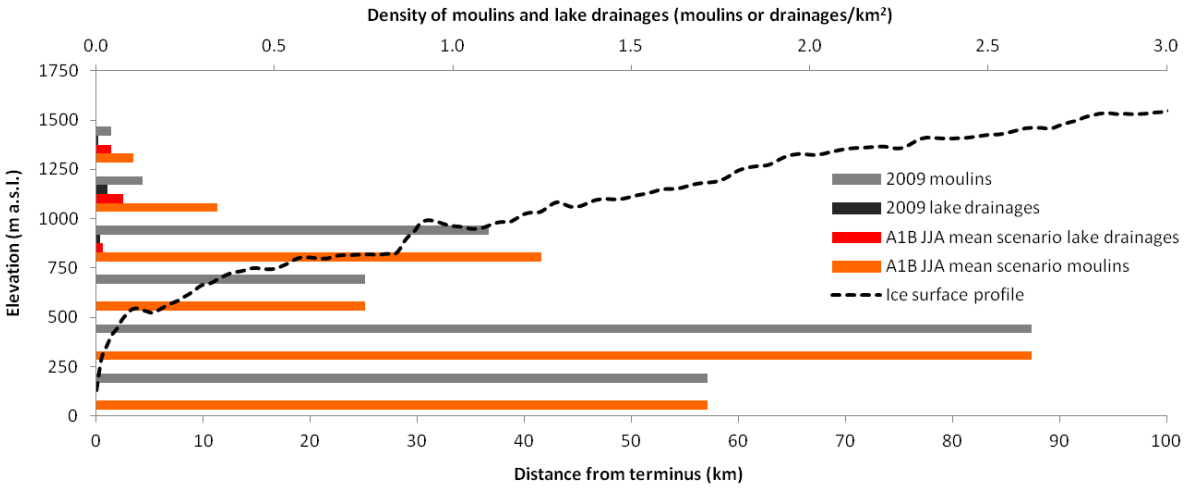

Figure 6.3.2.2. Density of moulins and lake drainages within 250 m ice surface elevation bands for Leverett Glacier for model runs with measured 2009 temperatures and the A1B JJA mean increased temperature scenario of 2.1°C

The results of running the model for an increased future temperature scenario show that the density of moulins at higher elevations, in this case above 750 m, may increase. Furthermore, the occurrence of lake drainages could also increase, resulting in a more widespread delivery of melt to the bed through large ice thicknesses at high elevations. Below 750 m no change is observed due to the smaller ice thicknesses and higher melt production resulting in all possible crevasses experiencing sufficient melt-filling to drive them to the bed. This is likely an overestimation due to underrepresentation of crevasses towards the terminus. In addition to a significant increase in absolute moulin numbers (+47.3%) and densities, and increased occurrence of lake drainages (+194.7%), applying this scenario also resulted in an increase of 4.6% in the transfer of surface-derived melt to the bed, and a temporal shift in moulin formation, with moulins at higher elevation forming much earlier than for the standard 2009 model run (Figure 6.3.2.3). These factors may have important implications for ice dynamics. Thus, in light of future increased melt scenarios, incorporating the spatial

and temporal transfer of surface-derived melt to the bed is imperative if ice sheet models are to fully consider the behaviour and development of the subglacial system, and the consequent ice velocity responses that drive ice sheet change evolution and its contribution to eustatic sea level change.

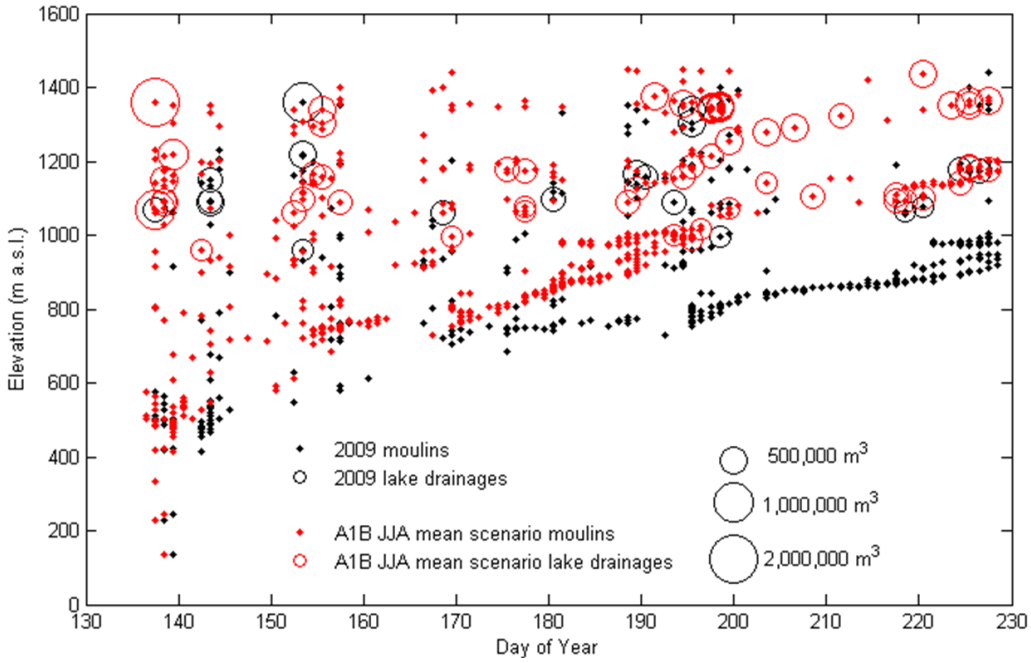

Figure 6.3.2.3. Comparison of moulin formation and lake drainages for Leverett Glacier for model runs with measured 2009 temperatures and an increased temperature scenario (A1B JJA mean of 2.1°C)

6.3.3 Hydrology applications

In addition to incorporation in glacier and ice sheet modelling studies, this model may also be useful for terrestrial hydrological applications. With glacial meltwater being increasingly considered as a source of hydropower from proglacial output, having a predictive capability for modelling meltwater delivery to the subglacial system could be useful for hydropower companies. Studies of Greenland's hydroelectric power potential date back over three decades, with papers including Partl (1978) assessing resources available for the development of hydropower schemes. The Partl (1978) study, which based its findings on available climatological data, concluded that power generation may be restricted to summer months in the east of Greenland due to lack of storage reservoirs, but for year-round power generation in the southwest,

meltwater could be stored within natural lakes. However, this study did not have the data or modelling capacity to consider meltwater transit times from melt generation to proglacial discharge, controlled by such factors as pathways of melt delivery to the bed and evolution of the subglacial system. Recently there has been interest in the link between hydropower potential and the evolution of the Greenland Ice Sheet, including a study of the Amitsulôq ice cap by Ahlstrøm et al. (2007). An R^2 correlation of 0.93 was calculated between specific summer balance and discharge, highlighting the controlling influence of glacial meltwater for the hydro-catchment discharge. Whilst melt from ablation, or the specific summer balance, is tied closely with proglacial discharge, this does not fully account for the temporal delivery of generated melt to the subglacial hydrological system, or indeed the shape of the resultant hydrograph.

The model described in this thesis produces outputs including the volume of melt delivered to the ice-bed interface. This can be expressed as the total daily melt delivered to the bed across the whole glacial catchment, as was discussed in detail in chapter 5 where applied to the Leverett catchment. The delivery of melt to the bed could also be expressed as melt delivered through individual moulins or sites of lakes draining to the bed, or the total melt delivery within defined elevation bands. Furthermore, the temporal resolution of the model could be increased, where sufficient meteorological data are available, to investigate diurnal or even hourly fluctuations in melt delivery. Mottram et al. (2009), as part of a feasibility study for a hydroelectric power project for Ilulissat in west Greenland, applied a hydrological model to delineate basins, model drainage pathways and ultimately predict discharge into ice-marginal lakes in the region. They highlight that modelling, including defining drainage basins, is complicated by features of the englacial system. Indeed, the simplified hydrological model they apply assumes instant transfer of 100 % of meltwater to the bed to overcome this, subsequently assuming water flow direction governed by water flow potential. Such modelling studies, although restricted by available data, would be improved in their predictions of discharge into storage lakes for hydropower if timing of moulin formation and lake drainage events was incorporated to give a better idea of when peak proglacial discharge might occur. This further highlights the need to better model supraglacial storage of meltwater,

including the temporal effect this has on delaying melt delivery to the bed, as was also described as a shortcoming of the model described in this thesis. Furthermore, given the difficulties in defining drainage basin boundaries, a predictive capability for spatial distribution of moulins would help to delineate these basins by providing a better idea of access points to the englacial system. This thesis has shown that both spatial and temporal patterns of moulin formation are affected by increased melt scenarios in warmer years. Given that that both drainage basin extent and the temporal discharge record are likely affected by this, further thought on better incorporation of englacial hydrology within hydrological modelling is certainly warranted.

Chapter 7. Conclusions

The response of glaciers and ice sheets to future climatic scenarios, and how the evolution of land ice will drive changes in eustatic sea level, remains an area of research with many unknowns, and considerable advances to be made in our understanding. The development of coupled models of glacial hydrology with ice dynamics is a key component in working towards a more comprehensive understanding of glacial system response to melt generation within ice sheet models. Whilst recent advances in the modelling of subglacial drainage systems are an encouraging step towards the incorporation of hydrology in larger scale ice sheet models, the dynamic response to changing subglacial water pressure cannot be fully understood or modelled without appropriate inclusion of meltwater inputs to the system. The englacial hydrological system remains perhaps the most poorly understood, and certainly the least researched area of glacial hydrology; yet it is the efficiency of this system, and the temporal and spatial patterns of melt delivery from the surface to the ice-bed interface, that drive subglacial system evolution. In light of this, and in light of an increasing need to improve our predictions of ice sheet evolution in a warming climate, it is imperative that the englacial system, in its capacity as a link between the ice surface and the bed, receives the focus it requires.

A new model for the transfer of meltwater from the ice surface to the ice-bed interface has been presented within this thesis. The modelling routine consists of three main components, the first of which is a spatially-distributed model for melt production, based upon a simple degree-day modelling approach. The second model component simulates the routing and flow accumulation of meltwater across the ice surface, including storage and over-spilling of supraglacial lakes. The final component is a model of fracture penetration depth for water-filled crevasses. This component, which calculates crevasse depth based chiefly on meltwater transfer into surface crevasses and the tensile stress of the ice, predicts where and when surface crevasses become full ice thickness moulins, and where supraglacial lakes can force fracture to the bed through their drainage. Results of model application to two glacial catchments differing in their physical characteristics: Leverett Glacier in south Greenland, and the

Croker Bay catchment of Devon Ice Cap, have been presented. These results focussed on the spatial patterns and density of moulin formation, and on the temporal formation of surface-to-bed connections and quantification of meltwater delivery to the bed through these connections.

Through model application to these two sites, it can be concluded that:

- Under scenarios of increased meltwater production, there is an increase in the number of moulins and the number of lakes that drain within a melt season. Furthermore, enhanced meltwater production at high elevation results in increased density of lake drainage at these elevations, contributing to an increase in melt transfer from the ice surface to the bed.
- Melt transfer through lakes contributes a much larger percentage to total melt transfer above 1000 m elevation than below, for Leverett Glacier, and the density of lake drainages at high elevation is predicted to increase under a future warming climate scenario.
- The model is particularly sensitive to those factors which influence the rate of meltwater filling in crevasses; including crevasse size and increased air temperatures. Additionally, the importance of knowledge of the spatial variation in crevasse surface size and ice tensile strength has been highlighted through sensitivity tests.

In addition to these main conclusions, it has also been shown that the model can provide a first estimate of temporal changes in meltwater delivery to the bed, having been compared with some success to measured proglacial discharge. This research has shown that significant changes in the spatial and temporal patterns of meltwater transfer to the subglacial system may be expected under differing climatic conditions, an important consideration for input to models of evolution of the subglacial drainage system and its consequent influence on ice dynamics.

The model presented here is a new approach to representing the supraglacial and englacial systems, predicting moulin formation in a framework that is both spatially distributed and temporally varying. As such, it would benefit from further development. The sensitivity that the model has been shown to have to certain

parameters attests to this, and also to the need to better parameterise model inputs. To that end, there is certainly an argument to support more extensive field and remotely-sensed observations of those physical factors to which the model is sensitive. The factors most important to better parameterise, based on the sensitivity tests conducted within the scope of this thesis, are the ice tensile strength and crevasse surface dimensions. Furthermore, model sensitivity to spatial resolution must be further considered for incorporation at a larger scale. Results of sensitivity testing to spatial resolution showed that whilst the temporal formation of moulins is largely unaffected by modelling at a lower resolution, the number of moulins may be underestimated since the model currently assumes only one moulin per cell. For implementation within ice sheet modelling, future model development may be geared towards a statistical approach to determining the spatial distribution of surface features whilst allowing for variation in spatial resolution, as governed by the data and computational cost limitations of ice sheet and land ice models.

For future developments in englacial research, and for incorporation of glacial hydrology within models of ice dynamics, better modelling of potential pathways for direct delivery of melt from the surface to the bed is imperative. Methods for mapping and modelling surface crevasses and supraglacial lake evolution, which ultimately provide the entry pathways for meltwater to the englacial system, are in particular need of improvement. The prediction of lake drainage events, arguably the weakest model component, would certainly benefit from incorporation of more rigorous physical constraints, particularly to more accurately predict the timing of these drainages. This is limited by our current understanding of the processes governing supraglacial lake drainages, especially those occurring through propagation of lake-bottom fractures. The complexities of the stress regime in lake locations may suggest that simple models of crevasse penetration, as presented here, cannot incorporate the factors influencing when and how a lake will drain through a crevasse. What we do know is that many of these lakes contain enough water to drive fracture to the bed; indeed, more than 1000 lakes, containing up to 98% of the water stored in lakes on the central west margin of the GrIS, could drain through 1 to 1.5 km of ice to the bed according to one study (Krawczynski et al., 2009). Whilst patterns of drainage

migrating from low to high elevation have been observed on the GrIS, the physical controls on their drainage are not fully understood. The model does not account for temporal changes in the surface stress regime, which may be the reason for a lack of a clear pattern of lake drainage from low to high elevation, due to the upward propagation of increased longitudinal stresses with retreat of the snow/firn line. Furthermore, the mechanics of how sufficient water can drive this drainage within low tensile and compressive stress regimes must be further investigated if lake drainage is to be incorporated adequately within coupled models of glacial hydrology and dynamics.

This study has presented a new method for potential incorporation of the timing and spatial patterns of moulin formation within glacier and ice sheet models. Furthermore the study has investigated the quantitative controls on moulin formation within a modelling framework, identifying those glacial features and physical parameters which require better understanding for future modelling work. With evidence for increasing air temperatures, particularly in the Arctic (IPCC, 2007; Box et al., 2010), and with model predictions within this study suggesting both an increase in absolute volume and percentage transfer of melt delivered to the bed under increased melt scenarios, and an increased density of surface-to-bed connections at high elevation, the need to incorporate the temporal and spatial delivery of meltwater to the bed is imperative. Knowledge of processes involved in the coupling between glacial hydrology and dynamics has come a long way since the true importance of this coupling was highlighted by studies such as Iken & Bindschadler (1986). In light of this, improving our ability to model glacier dynamics, including inputs from the hydrological system, is imperative. In light of a future warming climate scenario, and associated increased melt production, hydrology must be appropriately incorporated into ice sheet models in order to improve estimates of future ice sheet evolution and consequent sea level change.

References

Ahlstrøm, A.P., Bøggild, C.E., Oleson, O.B., Petersen, D. & Mohr, J.J., (2007), Mass balance of the Amitsulôq ice cap, West Greenland, *IAHS-AISH Publication*, 318, 107-115

Alley, R.B., Clark, P.U., Huybrechts, P. & Joughin, I., (2005a), Ice-Sheet and Sea-Level Changes, *Science*, 320, 456-460

Alley, R.B., Dupont, T.K., Parizek, B.R. & Anandakrishnan, S., (2005b), Access of surface meltwater to beds of sub-freezing glaciers: preliminary insights, *Annals of Glaciology*, 40, 8-14

Anderson, R.S., Anderson, S.P., MacGregor, K. R., Waddington, E.D., O'Neel, S., Riihimaki, C.A. & Loso, M.G., (2004), Strong feedbacks between hydrology and sliding of a small alpine glacier, *Journal of Geophysical Research*, 109, F03005

Arnold, N. & Sharp, M., (1992), Influence of glacier hydrology on the dynamics of a large Quaternary ice sheet, *Journal of Quaternary Science*, 7 (2), 109-124

Arnold, N.S., Willis, I.C., Sharp, M.J., Richards, K.S. & Lawson, W.J., (1996), A distributed surface energy balance model for a small valley glacier. I. Development and testing for Haut Glacier, d'Arolla, Valais, Switzerland, *Journal of Glaciology*, 42 (140), 77-89

Arnold, N., Richards, K., Willis, I. & Sharp, M., (1998), Initial results from a distributed, physically based model of glacier hydrology, *Hydrological Processes*, 12, 191-219

Arnold, N. & Sharp, M., (2002), Flow variability in the Scandinavian ice sheet: modelling the coupling between ice sheet flow and hydrology, *Quaternary Science Reviews*, 21, 485-502

Bamber, J.L., Layberry, R.L. & Gogineni, S.P., (2001), A new ice thickness and bed data set for the Greenland ice sheet: 1. Measurement, data reduction, and errors, *Journal of Geophysical Research*, 106 (D24), 33, 773-33, 780

Bamber, J.L., Alley, R.B. & Joughin, I., (2007), Rapid response of modern day ice sheets to external forcing, *Earth and Planetary Science Letters*, 257, 1-13

Bartholomaus, T.C., Anderson, R.S. & Anderson, S.P., (2011), Growth and collapse of the distributed subglacial hydrologic system of Kennicott Glacier, Alaska, USA, and its effects on basal motion, *Journal of Glaciology*, 57 (206), 985-1002

Bartholomew, I., Nienow, P., Mair, D., Hubbard, A., King, M.A. & Sole, A., (2010), Seasonal evolution of subglacial drainage and acceleration in a Greenland outlet glacier, *Nature Geoscience*, 3, 408-411

Bartholomew, I.D., Nienow, P., Sole, A., Mair, D., Cowton, T., King, M.A. & Palmer, S., (2011a), Seasonal variations in Greenland Ice Sheet motion: Inland extent and behaviour at higher elevations, *Earth and Planetary Science Letters*, 307 (3-4), 271-278

Bartholomew, I., Nienow, P., Sole, A., Mair, D., Cowton, T., Palmer, S. & Wadham, J., (2011b), Supraglacial forcing of subglacial drainage in the ablation zone of the Greenland ice sheet, *Geophysical Research Letters*, 38, L08502

Bell, C., Mair, D., Burgess, D., Sharp, M., Demuth, M., Cawkwell, F., Bingham, R. & Wadham, J., (2008), Spatial and temporal variability in the snowpack of a High Arctic ice cap: implications for mass-change measurements, *Annals of Glaciology*, 48, 159-170

Benn, D.I., Hulton, N.R.J. & Mottram, R.H., (2007a), 'Calving laws', 'sliding laws' and the stability of tidewater glaciers, *Annals of Glaciology*, 46, 123-130

Benn, D.I., Warren, C.R. & Mottram, R.H., (2007b), Calving processes and the dynamics of calving glaciers, *Earth-Science Reviews*, 82, 143-179

Bingham, R.G., Nienow, P.W. & Sharp, M.J., (2003), Intra-annual and intra-seasonal flow dynamics of a High Arctic polythermal valley glacier, *Annals of Glaciology*, 37, 181-188

Boon, S. & Sharp, M., (2003), The role of hydrologically-driven ice fracture in drainage system evolution on an Arctic glacier, *Geophysical Research Letters*, 30, CRY 1-1 – 1-4

Boon, S., Burgess, D.O., Koerner, R.M. & Sharp, M.J., (2010), Forty-seven Years of Research on the Devon Island Ice Cap, Arctic Canada, *Arctic*, 63 (1), 13-29

Box, J.E. & Ski, K., (2007), Remote sounding of Greenland supraglacial melt lakes: implications for subglacial hydraulics, *Journal of Glaciology*, 53 (181), 257-265

Box, J.E., Cappelen, J., Decker, D., Fettweis, X., Mote, T., Tedesco, M. & van de Wal, R.S.W., (2010), Greenland, *Arctic Report Card 2010*, http://www.arctic.noaa.gov/reportcard.

Braithwaite, R.J., (1995), Positive degree-day factors for ablation on the Greenland ice sheet studied by energy-balance modelling, *Journal of Glaciology*, 41 (137), 153-160

Braithwaite, R.J. & Raper, S.C.B., (2007), Glaciological conditions in seven contrasting regions estimated with the degree-day model, *Annals of Glaciology*, 46, 297-302

Brock, B.W., & Arnold, N.S., (2000), A spreadsheet-based (Microsoft Excel) point surface energy balance model for glacier and snow melt studies, *Earth Surface Processes and Landforms,* 25, 649-658

Brock, B.W., Willis, I.C., Sharp, M.J. & Arnold, N.S., (2000), Modelling seasonal and spatial variations in the surface energy balance of Haut Glacier d'Arolla, Switzerland, *Annals of Glaciology*, 31, 53-62

Burgess, D.O. & Sharp, M.J., (2004), Recent changes in the areal extent of the Devon Ice Cap, Nunavut, Canada, *Arctic, Antarctic, and Alpine Research*, 36 (2), 261-271

Burgess, D.O., Sharp, M.J., Mair, D.W.F., Dowdeswell, J.A. & Benham, T.J., (2005), Flow dynamics and iceberg calving rates of Devon Ice Cap, Nunavut, Canada, *Journal of Glaciology,* 51 (173), 219-230

Burgess, D. & Sharp, M., (2008), Recent changes in thickness of the Devon Island ice cap, Canada, *Journal of Geophysical Research*, 113, B07204

Catania, G.A., Neumann, T.A. & Price, S.F., (2008), Characterizing englacial drainage in the ablation zone of the Greenland ice sheet, *Journal of Glaciology*, 54 (187), 567-578

Clason et al., C.C., Mair, D.W.F., Burgess, D.O. & Nienow, P.W., (2012), Modelling the delivery of supraglacial meltwater to the ice-bed interface: application to the southwest Devon Ice Cap, Nunavut, Canada, *Journal of Glaciology*, 58 (208), 361-374

Colgan, W., Davis, J. & Sharp, M., (2008), Is the high-elevation region of Devon Ice Cap thicknening?, *Journal of Glaciology*, 54 (186), 428-436

Corfee-Morlot, J., Malsin, M. & Burgess, J., (2007), Global warming in the public sphere, *Philosophical Transactions of the Royal Society A*, 365, 2741-2776

Dadic, R., Corripio, J.G. & Burlando, P., (2008), Mass-balance estimates for Haut Glacier d'Arolla, Switzerland, from 2000 to 2006 using DEMs and and distributed mass-balance modelling, *Annals of Glaciology,* 49, 22-26

Das, S.B., Joughin, I., Behn, M.D., Howat, I.M., King, M.A., Lizarralde, D. & Bhatia, M.P., (2008), Fracture Propagation to the Base of the Greenland Ice Sheet During Supraglacial Lake Drainage, *Science*, 320, 778-781

Dowdeswell, J.A. & Drewry, D.J., (1989), The dynamics of Austfonna, Nordaustlandet, Svalbard: surface velocities, mass balance, and subglacial meltwater, *Annals of Glaciology*, 12, 37-45

Dowdeswell, J.A., Benham, T.J., Gorman, M.R., Burgess, D. & Sharp, M.J., (2004), Form and flow of the Devon Island Ice Cap, Canadian Arctic, *Journal of Geophysical Research,* 109, F02002

Fischer, M.P., Alley, R.B. and Engelder, T., (1995), Fracture toughness of ice and firn determined from the modified ring test, *Journal of Glaciology*, 41 (138), 383-394

Flowers, G.E. & Clarke, G.K.C., (2002), A multicomponent coupled model of glacier hydrology 2. Application to Trapridge Glacier, Yukon, Canada, *Journal of Geophysical Research B: Solid Earth*, 107 (11), ECV 9-1 – 9-17

Gulley, J.D., Benn, D.I., Screaton, E. & Martin, J., (2009), Mechanisms of englacial conduit formation and their implications for subglacial recharge, *Quaternary Science Reviews*, 28, 1984-1999

Hambrey, M.J. & Muller, F., (1978), Structures and ice deformation in the White Glacier, Axel Heiberg Island, NW Territories, Canada, *Journal of Glaciology*, 20 (82), 215-228

Hanna, E., Huybrechts, P., Steffen, K., Cappelen, J., Huff, R., Shuman, C., Irvine-Fynn, T., Wise, S. & Griffiths, M., (2008), Increased runoff from melt from the Greenland Ice Sheet: a response to global warming, *Journal of Climate*, 21 (2), 331-341

Harper, J.T., Humphrey, N.F. & Pfeffer, W.T., (1998), Crevasse patterns and the strain-rate tensor: a high-resolution comparison, *Journal of Glaciology*, 44 (146), 68-76

Hewitt, I.J., (2011), Modelling distributed and channelized subglacial drainage: the spacing of channels, *Journal of Glaciology*, 57 (202), 302-314

Hock, R., (2003), Temperature index melt modelling in mountain areas, *Journal of Hydrology*, 282, 104-115

Hock, R., (2005), Glacier melt: a review of processes and their modelling, *Progress in Physical Geography*, 29 (3), 362-391

Holdsworth, G., (1975), *Deformation and flow of Barnes Ice Cap, Baffin Island*, Ottawa, Environment Canada Inland Water Directorate (Scientific Series 52)

Holmlund, P., (1988), Internal geometry and evolution of moulins, Storglaciären, Sweden, *Journal of Glaciology*, 34 (117), 242-248

Hooke, R. LeB., Calla, P., Holmund, P., Nilsson, M. & Stroeven, A., (1989), A 3 year record of seasonal variations in surface velocity, Storglaciären, Sweden, *Journal of Glaciology*, 35 (120), 235-247

Hubbard, A. & Hubbard, B., (2000), The potential contribution of high-resolution glacier flow modeling to structural glaciology, *Geological Society Special Publication*, 176, 135-146

Huggel, C., Kääb, A., Haeberli, W. & Krummenacher, B., (2003), Regional-scale GIS-models for assessment of hazards from glacier lake outbursts: evaluation and application in the Swiss Alps, *Natural Hazards and Earth System Sciences*, 3, 647-662

Huintjes, E., Li, H., Sauter, T., Li, Z. & Schneider, C., (2010), Degree-day modelling of the surface mass balance of Urumqi Glacier No. 1, Tien Shan, China, *The Cryosphere Discussions*, 4 (1), 207-232

Huybrechts, P., Payne, T. & The EISMINT Intercomparison Group, (1996), The EISMINT benchmarks for testing ice-sheet models, *Annals of Glaciology*, 23, 1-12

Iken, A. & Bindschadler, R.A., (1986), Combined measurements of subglacial water pressure and surface velocity of Findelengletscher, Switzerland: Conclusions about drainage system and sliding mechanism, *Journal of Glaciology*, 32 (110), 101-119

IPCC, (2007), Solomon, S., Qin, D., Manning, M., Chen, Z., Marquis, M., Averyt, K.B., Tignor, M. & Miller, H.L., (eds.), *Climate Change 2007: The Physical Science Basis. Contribution of Working Group I to the Fourth Assessment Report of the Intergovernmental Panel on Climate Change*, Cambridge University Press, Cambridge, United Kingdom

Irvine-Fynn, T.D.L., Hodson, A.J., Moorman, B.J., Vatne, G. & Hubbard, A.L., (2011), Polythermal Glacier Hydrology: A review, *Reviews of Geophysics*, 49, RG4002

Jansson, P., (1995), Water pressure and basal sliding on Storglaciären, northern Sweden, *Journal of Glaciology*, 41 (138), 232-240

Jóhannesson, T., Sigurdsson, O., Laumann, T. & Kennett, M., (1995), Degree-day glacier mass-balance modeling with application to glaciers in Iceland, Norway and Greenland, *Journal of Glaciology*, 41(138), 345-358

Joughin, I., Das, S.B., King, M.A., Smith, B.E., Howat, I.M. & Moon, T., (2008), Seasonal Speedup Along the Western Flank of the Greenland Ice Sheet, *Science*, 320, 781-783

Joughin, I., Smith, B.E., Howat, I.M., Scambos, T. & Moon, T., (2010), Greenland flow variability from ice-sheet-wide velocity mapping, *Journal of Glaciology*, 56 (197), 415-430.

Kamb, B., (1987), Glacier surge mechanism based on linked cavity configuration of the basal water conduit system, *Journal of Geophysical Research*, 92 (B9), 9083-9100

Kehle, R.O., (1964), Deformation of the Ross Ice Shelf, Antarctica, *Geological Society of America Bulletin*, 75, 259-286

Knight, P.G., (1999), *Glaciers*, Routledge

Krabill, W., Thomas, R., Jezek, K., Kuivinen, K. & Manizade, S., (1995), Greenland ice sheet thickness changes measured by laser altimetry, *Geophysical Research Letters*, 22 (17), 2341-2344

Krawczynski, M.J., Behn, M.D., Das, S.B. & Joughin, I., (2009), Constraints on the lake volume required for hydro-fracture through ice sheets, *Geophysical Research Letters*, 36, L10501

Lillesand, T.M., Kiefer, R.W. & Chipman, J.W., (2004), *Remote Sensing and Image Interpretation, 5th Edition,* John Wiley & Sons, Inc.

Luthje, M., Pedersen, L.T., Reeh, N. & Greuell, W., (2006), Modelling the evolution of supraglacial lakes on the West Greenland ice-sheet margin, *Journal of Glaciology*, 52 (179), 608-618

Mair, D., Nienow, P., Willis, I. & Sharp, M., (2001), Spatial patterns of glacier motion during a high-velocity event: Haut Glacier d'Arolla, Switzerland, *Journal of Glaciology*, 47 (156), 9-20

Mair, D.W.F., Sharp, M.J. & Willis, I.C., (2002), Evidence for basal cavity opening from analysis of surface uplift during a high-velocity event: Haut Glacier d'Arolla, Switzerland, *Journal of Glaciology*, 48 (161), 208-216

Mair, D., Willis, I., Fischer, U.H., Hubbard, B., Nienow, P. & Hubbard, A., (2003), Hydrological controls on patterns of surface, internal and basal motion during three "spring events": Haut Glacier d'Arolla, Switzerland, *Journal of Glaciology*, 49 (167), 555-567

Mair, D., Burgess, D. & Sharp, M., (2005), Thirty-seven year mass balance of Devon Ice Cap, Nunavut, Canada, determined by shallow ice coring and melt modelling, *Journal of Geophysical Research,* 110, FO1011

Matsunaga, K., Nakaya, T., & Sugai, T., (2009), Simple DEM-Based Methods to Delineate Channel Networks for Hydrogeomorphological Mapping, *Transactions in GIS*, 13 (1), 87-103

McGrath, D., Colgan, W., Steffen, K., Lauffenburger, P. & Balog, J., (2011), Assessing the summer water budget of a moulin basin in the Sermeq Avannarleq ablation region, Greenland ice sheet, *Journal of Glaciology*, 57 (205), 954-964

McMillan, M., Nienow, P., Shepherd, A., Benham, T. & Sole, A., (2007), Seasonal evolution of supra-glacial lakes on the Greenland Ice Sheet, *Earth and Planetary Science Letters*, 262, 484-492

Meier, M.F., (1960), Mode of flow of Saskatchewan Glacier, Alberta, Canada, *United States Geological Survey Professional Paper*, 351

Molander, C.W., Photogrammetry, in Maune, D.F. (Ed.), (2001), *Digital Elevation Model Technologies and Applications: The DEM Users Manual*, American Society for Photogrammetry and Remote Sensing

Mottram, R.H. & Benn, D.I., (2009), Testing crevasse-depth models: a field study at Breiðamerkurjökull, Iceland, *Journal of Glaciology*, 55 (192), 746-752

Mottram, R., Nielsen, C., Ahlstrøm, A.P., Reeh, N., Kristensen, S.S., Christensen, E.L., Forsberg, R. & Stenseng, L., (2009), A new regional high-resolution map of basal and surface topography for the Greenland ice-sheet margin at Paakitsoq, West Greenland, *Annals of Glaciology*, 50 (51), 105-111

Müller, F. & Iken, A., (1973), Velocity fluctuations and water regime of Arctic valley glaciers, *International Association of Hydrological Sciences Publication*, 95, 165-182

Nath, P.C. & Vaughan, D.G., (2003), Subsurface crevasse formation in glaciers and ice sheets, *Journal of Geophysical Research*, 108, B1, 2020

Nienow, P., Sharp, M. & Willis, I., (1998), Seasonal changes in the morphology of the subglacial drainage system, Haut Glacier d'Arolla, Switzerland, *Earth Surface Processes and Landforms*, 23, 825-843

Nienow, P., Sharp, M., Boon, S., Bingham, R. & Heppenstall, K., (c.2001), Supraglacial drainage processes on High Arctic Glaciers: implications for subglacial hydrology and glacier dynamics, *(unpublished)*

Nye, J.F., (1955), Comments on Dr. Loewe's letter and notes on crevasses, *Journal of Glaciology,* 2 (17), 512-514

Nye, J.F., (1957), The distribution of stress and velocity in glaciers and ice sheets, *Proceedings of the Royal Society of London, Series A,* 239 (1216), 113-133

Palmer, S., Shepherd, A., Nienow, P. & Joughin, I., (2011), Seasonal speedup of the Greenland Ice Sheet linked to routing of surface water, *Earth and Planetary Science Letters*, 302 (3-4), 423-428

Parizek, B.R. & Alley, R.B., (2004), Implications of increased Greenland surface melt under global-warming scenarios: ice-sheet simulations, *Quaternary Science Reviews*, 23, 1013-1027

Partl, R., (1978), Power from glaciers: the hydropower potential of Greenland's glacial waters, *Energy*, 3, 543-573

Paterson, W.S.B., (1994), *The Physics of Glaciers, 3rd Edition*, Butterworth-Heinemann, Oxford

Pellicciotti, F., Brock, B., Strasser, U., Burlando, P., Funk, M. & Corripio, J., (2005), An enhanced temperature-index glacier melt model including the shortwave radiation balance: development and testing for Haut Glacier d'Arolla, Switzerland, *Journal of Glaciology*, 51 (175), 573-588

Petrovic, J.J., (2003), Review: Mechanical properties of ice and snow, *Journal of Materials Science*, 38, 1-6

Phillips, T., Rajaram, H. & Steffen, K., (2010), Cryo-hydrologic warming: A potential mechanism for rapid thermal response of ice sheets, *Geophysical Research Letters*, 37, L20503

Phillips, T. Leyk, S., Rajaram, H., Colgan, W., Abdalati, W., McGrath, D. & Steffen, K., (2011), Modeling moulin distribution on Sermeq Avannarleq glacier using ASTER and WorldView imagery and fuzzy set theory, *Remote Sensing of Environment*, 115, 2292-2301

Pimentel, S., Flowers, G.E. & Schoof, C.G., (2010), A hydrologically coupled higher-order flow-band model of ice dynamics with a Coulomb friction sliding law, *Journal of Geophysical Research*, 115, F04023

Pimentel, S. & Flowers, G.E., (2011), A numerical study of hydrologically driven glacier dynamics and subglacial flooding, *Proceedings of the Royal Society A,* 467 (2126), 537-558

Price, S.F., Payne, A.J., Catania, G.A. & Neumann, T.A., (2008), Seasonal acceleration of inland ice via longitudinal coupling to marginal ice, *Journal of Glaciology*, 54 (185), 213-219

Price, S., Flowers, G., Schoof, C. & Creyts, T., (2011a), Improving hydrology in land ice models, *A workshop on implementing land ice hydrology in the Community Ice Sheet Model, Boulder, Colorado, January 13, 2011*

Price, S., Flowers, G. & Schoof, C., (2011b), Improving Hydrology in Land Ice Models, *Eos*, 92 (19)

Raymond, C. F., Benedict, R.J., Harrison, W.D., Echelmeyer, K.A. & Sturm, M., (1995), Hydrological discharges and motion of Fels and Black Rapids Glaciers, Alaska, U.S.A.: implications for the structure of their drainage systems, *Journal of Glaciology*, 41 (138), 290-304

Rignot, E., Braaten, D., Gogineni, P., Krabill, W.B. & McConnell, J.R., (2004), Rapid ice discharge from southeast Greenland glaciers, *Geophysical Research Letters*, 31, L10410

Rignot, E. & Kanagaratnam, P., (2006), Changes in the Velocity Structure of the Greenland Ice Sheet, *Science*, 311, 986-990

Rist, M.A., Sammonds, P.R., Murrell, S.A.F., Meredith, P.G., Oerter, H. & Doake, C.S.M., (1996), Experimental fracture and mechanical properties of Antarctic ice: preliminary results, *Annals of Glaciology*, 23, 284-292

Rist, M.A., Sammonds, P.R., Murrell, S.A.F., Meredith, P.G., Doake, C.S.M., Oerter, H. & Matsuki, K., (1999), Experimental and theoretical fracture mechanics applied to Antarctic ice fracture and surface crevassing, *Journal of Geophysical Research*, 104 (B2), 2973-2986

Scambos, T.A., Hulbe, C., Fahnestock, M. & Bohlander, J., (2000), The link between climate warming and break-up of ice shelves in the Antarctic Peninsula, *Journal of Glaciology*, 46 (154), 516-530

Schoof, C., (2010), Ice sheet acceleration driven by melt supply variability, *Nature*, 468, 803-306

Scott, J.B.T., Smith, A.M., Bingham, R.G. & Vaughan, D.G., (2010), Crevasses triggered on Pine Island Glacier , West Antarctica, by drilling through an exceptional melt layer, *Annals of Glaciology*, 51 (55), 65-70

Schwanghart, W. & Kuhn, N.J., (2010), TopoToolbox: A set of Matlab functions for topographic analysis, *Environmental Modelling & Software*, 25, 770-781

Selmes, N., Murray, T. & James, T.D., (2011), Fast draining lakes on the Greenland Ice Sheet, *Geophysical Research Letters*, 38, L15501

Shepherd, A. & Wingham, D., (2007), Recent Sea-Level Contributions of the Antarctic and Greenland Ice Sheets, *Science*, 315, 1529-1532

Shepherd, A. Du, Z., Benham, T.J., Dowdeswell, J.A. & Morris, E.M., (2007), Mass balance of Devon Ice Cap, Canadian Arctic, *Annals of Glaciology*, 46, 249-254

Shepherd, A., Hubbard, A., Nienow, P., King, M., McMillan, M. & Joughin, I., (2009), Greenland ice sheet motion coupled with daily melting in the late summer, *Geophysical Research letters*, 36, L01501

Smith, R.A., (1976), The application of fracture mechanics to the problem of crevasse penetration, *Journal of Glaciology*, 17 (76), 223-228

Sneed, W.A. & Hamilton, G.S., (2007), Evolution of melt pond volume on the surface of the Greenland Ice Sheet, *Geophysical Research* Letters, 34, L03501

Sole, A., Payne, T., Bamber, J., Nienow, P. & Krabill, W., (2008), Testing hypotheses of the cause of peripheral thinning of the Greenland Ice Sheet: is land-terminating ice thinning at anomalously high rates?, *The Cryosphere Discussions*, 2, 673-710

Sole, A.J., Mair, D.W.F., Nienow, P.W., Bartholomew, I.D., King, M.A., Burke, M.J. & Joughin, I., (2011), Seasonal speedup of a Greenland marine-terminating outlet glacier forced by surface melt-induced changes in subglacial hydrology, *Journal of Geophysical Research*, 116, F03014

Sundal, A.V., Shepherd, A., Nienow, P., Hanna, E., Palmer, S. & Huybrechts, P., (2009), Evolution of supra-glacial lakes across the Greenland Ice Sheet, *Remote Sensing of Environment*, 113 (10), 2164-2171

Sundal, A.V., Shepherd, A., Nienow, P., Hanna, E., Palmer, S. & Huybrechts, P., (2011), Melt-induced speed-up of Greenland ice sheet offset by efficient subglacial drainage, *Nature*, 469, 521-524

Sugiyama, S. & Gudmundsson, G.H, (2004), Short-term variations in glacier flow controlled by subglacial water pressure at Lauteraargletscher, Bernese Alps, Switzerland, *Journal of Glaciology*, 50 (170), 353-362

Sugiyama, S., Bauder, A., Weiss, P. & Funk, M., (2007), Reversal of ice motion during the outburst of a glacier-dammed lake on Gornergletscher , Switzerland, *Journal of Glaciology*, 53 (181), 172-180

Thomas, R., Frederick, E., Krabill, W., Manizade, S. & Martin, C., (2009), Recent changes on Greenland outlet glaciers, *Journal of Glaciology*, 55 (189), 147-162

van den Broeke, M., Smeets, P. Ettema, J., van der Veen, C., van de Wal, R. & Oerlemans, J., (2008), Partitioning of melt energy and meltwater fluxes in the ablation zone of the west Greenland ice sheet, *The Cryosphere,* 2, 179-189

van de Wal, R.S.W., Boot, W., van den Broeke, M.R., Smeets, C.J.P.P., Reijmer, C.H., Donker, J.J.A. & Oerlemans, J., (2008), Large and Rapid Melt-Induced Changes in the Ablation Zone of the Greenland Ice Sheet, *Science*, 321, 111-113

van der Veen, C.J., (1998), Fracture mechanics approach to penetration of surface crevasses on glaciers, *Cold Regions Science and Technology*, 27, 31-47

van der Veen, C.J., (2007), Fracture propagation as means of rapidly transferring surface meltwater to the base of glaciers, *Geophysical Research Letters*, 34, L01501

Vaughan, D.G., (1993), Relating the occurrence of crevasses to surface strain rates, *Journal of Glaciology*, 39 (132), 255-266

Vaughan, D.G., (2008), West Antarctice Ice Sheet collapse – the fall and rise of a paradigm, *Climate Change*, 91, 65-79

Vieli, A., Payne, A.J., Du, Z. & Shepherd, A., (2006), Numerical modelling and data assimilation of the Larsen B ice shelf, Antarctic Peninsula, *Philosophical Transactions of the Royal Society, Series A,* 364, 1815-1839

Weertman, J., (1973), Can a water-filled crevasse reach the bottom surface of a glacier?, *IASH publication*, 95, 139-145

Weiss, J., (2004), Subcritical crack propagation as a mechanism of crevasse formation and iceberg calving¸ *Journal of Glaciology*, 50 (168), 109-115

Willis, I.C., Arnold, N.S. & Brock, B.W., (2002), Effect of snowpack removal on energy balance, melt and runoff in a small supraglacial catchment, *Hydrological Processes*, 16, 2721-2749

Wilson, J.P., Lam, C.S. & Deng, Y., (2007), Comparison of the performance of flow-routing algorithms used in GIS-based hydrologic analysis, *Hydrological Processes*, 21, 1026-1044

WMO, (1986), Intercomparison of models for snowmelt runoff, *Operational Hydrology Report 23*, WMO No. 646

Zumberge, J.H., Giovenetto, M., Kehle, R. & Reid, J., (1960), Deformation of the Ross Ice Shelf, near the Bay of Whales, Antarctica, *IGY Glaciological Report,* 3

Zwally, J.H., Abdalati, W., Herring, T., Larson, K., Saba, J. & Steffen, K., (2002), Surface Melt-Induced Acceleration of Greenland Ice Sheet Flow, *Science*, 297, 218-222

Zwally, H.J., Giovinetto, M.B., Li, J., Cornejo, H.G., Beckley, M.A., Brenner, A.C., Saba, J.L. & Yi, D., (2005), Mass changes of the Greenland and Antarctic ice sheets and shelves and contributions to sea-level rise: 1992-2002, *Journal of Glaciology*, 51 (175), 509-527

Appendix 1. Modelling routine Matlab code

```
%This model predicts full ice-thickness crevasses, lake filling and
%drainage and quantifies meltwater delivery to the bed. Crevasses and
%lakes transfer their total accumulated melt fill to the bed when
%connections are made and subsequent days of melt inflow are also
%routed to the bed.

%*********************************************************************

%input variables

met_elev = 457; %elevation (m a.s.l.) of met station/temperature
sensor
temp_lapse = 0.0055; %air temperature lapse rate (degC/m)
DDF_i = 7.79; %Degree-day factor for ice (mm w.e. d degC)
DDF_s = 5.81; %Degree-day factor for snow (mm w.e. d degC)
Pi = 918; %density of ice
Pw = 1000; %density of freshwater
P_s = 0.3; %density of new snow (g/cm3)
g = 9.81; %acceleration due to gravity
t = 24; %time in hours (24 because daily time-step)
Kic = 150000; %fracture toughness (Pa m^1/2)
TS = 75000; %tensile strength (Pa)
cell_width = 500; %width of each grid cell
crev_width = 1; %width of crevasses
crev_length = 500; %length of crevasses

%*********************************************************************

%meteorological data
metdata = xlsread('Lev_met_input09.xlsx','A2:C100'); %reads met data
JD = metdata(:,1); %reads julian days
temp = metdata(:,2); %reads average temperature data (degC)
precip = metdata(:,3); %reads daily total precipitation data (mm)

%ice surface elevation data (m)
[dem,X,Y] = rasterread('SP_DEM_LEV.asc'); %reads DEM ASCII
DEM = dem(:); %matrix -> vector
surface_nans = isnan(DEM);
SIZ = length(DEM);
size_days = length(JD);
surf_elev = zeros(1,SIZ)';

for loop = 1:length(DEM); %replace nans in DEM with zeros
    if surface_nans(loop) == 1;
        surf_elev(loop,:) = 0;
    else
        surf_elev(loop,:) = DEM(loop);
    end
end

%*********************************************************************
```

```
%adjusts initial snowpack across the catchment with accumulation
%gradient

s_depth = 0; %starting snowpack depth at met station (mm w.e.)
snow_elev = 454; %elevation of snow depth measurement (m a.s.l.)
accum_grad = 0.2566; %snow accumulation gradient (mm w.e./m)

grad_elev = zeros(SIZ,1);
snow_depth = zeros(SIZ,1);

for a = 1:length(surf_elev);

    %adjusts snow depth for elevation using accumulation gradient
    if surf_elev(a) < snow_elev;
        grad_elev(a,:) = (snow_elev-surf_elev(a))*accum_grad;
    elseif surf_elev(a) > snow_elev;
        grad_elev(a,:) = (surf_elev(a)-snow_elev)*accum_grad;
    end

    if surf_elev(a) == snow_elev;
        snow_depth(a,:) = s_depth;
    elseif surf_elev(a) < snow_elev;
        snow_depth(a,:) = s_depth - grad_elev(a);
    elseif surf_elev(a) > snow_elev;
        snow_depth(a,:) = s_depth + grad_elev(a);
    end

    if snow_depth(a,:) <= 0;
        snow_depth(a,:) = 0;
    else
        snow_depth(a,:) = snow_depth(a);
    end
end

clear grad_elev;

%**********************************************************************

%tensile stress data (kPa)
[tensile] = rasterread('tensile_stresses_LEV.asc');
Rxx_pa = tensile*1000; %convert kPa to Pa
Rxx = Rxx_pa(:); %matrix -> vector
RR = Rxx_pa < TS;%assign a runoff ratio of zero where melt meets cell
%>= tensile strength (1 if "no crevasse")

%ice thickness data (m)
[h] = rasterread('ice_thickness_LEV.asc');
H = h(:); %matrix -> vector

%lake data
[lakes] = rasterread('lake_volume_LEV.asc'); %reads lake volume (10^6
%m^3)
LV = lakes*1000000000/(cell_width*cell_width); %convert 10^6 m^3 to mm
LV_vector = LV(:);

%georeference data
eastings = X(:);
northings = Y(:);
```

```
%assigns 1s to areas outside the ice surface boundary
ice_limits = isnan(DEM);

%no melting across the catchment until after day 1 calculation
melt_start = 0;

%*********************************************************************

%pre-allocate space for model outputs
SIZE = size(LV);
LVactual = zeros(SIZE);
lapse_elev = zeros(SIZ,1);
temp_elev = zeros(SIZ,1);
pos_temp = zeros(SIZ,1);
snow = zeros(SIZ,1);
precip_snow = zeros(SIZ,1);
snow_total = zeros(SIZ,size_days);
daily_melt = zeros(SIZ,1);
cumu_melt = zeros(SIZ,size_days);
dmax = zeros(SIZ,1);
b_lake = zeros(SIZ,1);
B_lake = zeros(SIZ,1);
Ki_lake = zeros(SIZ,1);
crevasse_depth = zeros(SIZ,1);
full_crevasses = zeros(SIZ,size_days);
drained_lakes = zeros(SIZ,size_days);
lake_drainage_events= zeros(SIZ,size_days);
melt_to_bed = zeros(SIZ,size_days);
b = zeros(SIZ,size_days);
B = zeros(SIZ,1);
moulin = zeros(SIZ,size_days);
total_daily_melt_delivery = zeros(1,size_days);
melt_delivery_volume = zeros(1,size_days);
melt_delivery_discharge = zeros(1,size_days);
tot_melt = zeros(1,size_days);

%*********************************************************************

%model begins calculating melt, crevasse depths and lake filling/
%drainage for each time step from here

%loops through days
for i = 1:length(temp);
    disp(['calculating melt, fracture depth and lake filling/drainage
for day ', num2str(i)]);

    %loops through each DEM cell
    for j = 1:length(surf_elev);


%*********************************************************************

        %Degree-day melt model component

        %adjusts temperature for changing elevation using lapse rate
        if surf_elev(j) < met_elev;
            lapse_elev(j) = (met_elev-surf_elev(j))*temp_lapse;
        elseif surf_elev(j) > met_elev;
            lapse_elev(j) = (surf_elev(j)-met_elev)*temp_lapse;
```

```
        end

        if surf_elev(j) == met_elev;
            temp_elev(j) = temp(i);
        elseif surf_elev(j) < met_elev;
            temp_elev(j) = temp(i) + lapse_elev(j);
        elseif surf_elev(j) > met_elev;
            temp_elev(j) = temp(i) - lapse_elev(j);
        end

        %sets daily average temperatures to zero when below 0degC
        if temp_elev(j) >= 0;
            pos_temp(j) = temp_elev(j);
        elseif temp_elev(j) < 0;
            pos_temp(j) = 0;
        end

        if ice_limits(j) == 1;
            pos_temp(j) = 0;
        end

      %determines whether precipitation is falling as snow or is rain
      and neglected (when above 1degC)
        if temp_elev(j) <= 1;
            snow(j) = precip(i)*P_s; %converts snow in mm to mm w.e.
            precip_snow(j) = snow(j);
        else
            snow(j) = 0;
            precip_snow(j) = snow(j);
        end

        %adds fallen snow to initial snowpack
        if i == 1;
            snow_total(j,i) = snow_depth(j) + precip_snow(j);
        else
            snow_total(j,i) = snow_total(j,i-1) + precip_snow(j);
        end

        %calculates daily melt
        if i == 1;
            if snow_total(j,i) == 0;
                cumu_melt(j,i) = melt_start
+(pos_temp(j)*DDF_i);%apply DDF for ice when no snow cover
                daily_melt(j) = cumu_melt(j,i);
            else
                cumu_melt(j,i) = melt_start
+(pos_temp(j)*DDF_s);%apply DDF for snow when snowpack not depleted
                daily_melt(j) = cumu_melt(j,i);
            end
        else
            if cumu_melt(j,i-1) > snow_total(j,i);
                cumu_melt(j,i) = cumu_melt(j,i-1)+(pos_temp(j)*DDF_i);
                daily_melt(j) = cumu_melt(j,i)-cumu_melt(j,i-1);
            else
                cumu_melt(j,i) = cumu_melt(j,i-1)+(pos_temp(j)*DDF_s);
                daily_melt(j) = cumu_melt(j,i)-cumu_melt(j,i-1);
            end
        end

    end
```

```
    %creates an xyz file of E, N and melt for each day
    melt_xyz(:,1)=eastings;
    melt_xyz(:,2)=northings;
    melt_xyz(:,3)=daily_melt;

    %converts xyz melt values into grid format
    xyz = melt_xyz;
    xyz = sortrows(xyz,[1 -2]); %sort the rows by easting and then
%northing
    height = sum(xyz(:,1)==xyz(1,1)); %grid height
    width = sum(xyz(:,2)==xyz(1,2)); %grid width
    melt_grid = reshape(xyz(:,3),height,width);


%*********************************************************************

    %Melt routing and accumulation component, including filling of
%lakes

    %calculates weighted flow accumulation
    W0 = melt_grid; %daily melt input for weighting
    cs  = abs(Y(2)-Y(1)); %cell size
    siz = size(dem); %matrix dimensions
    dem = fillsinks(dem); %fills sinks in DEM
    Ms = flowdir(X,Y,dem,'type','single'); %single flow direction
%algorithm
    [As, LVactual] = flowaccwithlakes(Ms,W0,RR,LV,LVactual);
%calculates flow accumulation and filling of lakes
    LV_percent_fill= 100*(LVactual./LV); %fill percentage of lake
%maximum volume

    %rate of crevasse filling for input to fracture model (m/hr)
    q = (As/t)/1000;
    Q = q(:);

    %lake filling for drainage of lakes through fractures (m/hr)
    q_lake = (LVactual/t)/1000;
    Q_lake = q_lake(:);

    %converts runoff ratio matrix to vector(this will be modified as
%lakes
    %drain, adding to cells through which water is no long routed)
    RR = RR(:);


%*********************************************************************

    %Fracture depth model and lake drainage component and melt
%delivery to the bed

    %(Where solving for Ki or Ki_lake on LHS, a simple LEFM model
%(after Van der Veen, 2007) for calculating depths of water-filled
%crevassesis applied. The first term on RHS is the stress intentsity
%factor (Ki1)associated with a tensile stress, term two (Ki2)
%represents the lithostatic stress in ice with density Pi, and the
%third term (Ki3)represents the effect of water pressure).

    for I = 1:length(surf_elev);
```

```
%*****************************************************************

        %lake drainage component

        %runs fracture model for lake drainage only for cells where
%lakes
        %are present
        if LV_vector(I) > 0;

            %fracture depth is equal to ice thickness
            dmax(I) = H(I);

            %melt fill in lakes converted to melt head (m)
            b_lake(I) = Q_lake(I)*t;

            %adjusts fill for cell size and crevasse dimensions
            B_lake(I) =
(b_lake(I)*(cell_width*cell_width))/(crev_width*crev_length);

            %this is solved when B_lake is suffient for Ki > Kic for
%depth equal to ice thickness
            Ki_lake(I) = (1.12*(Rxx(I)*(sqrt(pi*dmax(I)))))-
(0.683*(Pi*(g*(dmax(I)^1.5))))+(0.683*(Pw*(g*(B_lake(I)^1.5))));

            if i == 1;
                %no drainage if Ki not greater than Kic on first day
                if Ki_lake(I) < Kic;
                    crevasse_depth(I) = 0;
                    drained_lakes(I,i) = 0;
                    lake_drainage_events(I,i) = 0;
                    melt_to_bed(I,i) = 0;
                    RR(I) = Rxx(I) < TS;
                    %accumulated lake fill transfered to bed and lake
%cell added to runoff ratio grid if lake drains
                elseif Ki_lake(I) >= Kic;
                    crevasse_depth(I) = dmax(I);
                    drained_lakes(I,i) = 1;
                    lake_drainage_events(I,i) = 1;
                    melt_to_bed(I,i) = ((Q_lake(I))*t)*1000;
%(converted back to mm w.e)
                    RR(I) = drained_lakes(I,i) == 0;
                end
            else
                %registers that a lake has previously drained and
%continues to route daily melt input to the bed
                if drained_lakes(I,i-1) == 1;
                    crevasse_depth(I) = dmax(I);
                    drained_lakes(I,i) = 1;
                    lake_drainage_events(I,i) = 0;
                    melt_to_bed(I,i) = ((Q(I))*t)*1000; %(converted
%back to mm w.e)
                    RR(I) = drained_lakes(I,i) == 0;
                    %no drainage if Ki still not greater than Kic
                elseif Ki_lake(I) < Kic;
                    crevasse_depth(I) = 0;
                    drained_lakes(I,i) = 0;
                    lake_drainage_events(I,i) = 0;
                    melt_to_bed(I,i) = 0;
```

```
                    RR(I) = Rxx(I) < TS;
                    %accumulated lake fill transfered to bed and lake
%cell added to runoff ratio grid when lake drains
                elseif Ki_lake(I) >= Kic;
                    crevasse_depth(I) = dmax(I);
                    drained_lakes(I,i) = 1;
                    lake_drainage_events(I,i) = 1;
                    melt_to_bed(I,i) = ((Q_lake(I))*t)*1000;
%(converted back to mm w.e)
                    RR(I) = drained_lakes(I,i) == 0;
                end
            end

            %where lakes are not present fracture model runs as normal
        else %LV_vector(I) == 0

            dmax(I) = 0;
            b_lake(I) = 0;
            B_lake(I) = 0;
            Ki_lake(I) = 0;
            drained_lakes(I,i) = 0;
            RR(I) = Rxx(I) < TS;


%************************************************************

            %component for water-filled crevasse depth calculation and
%melt transfer

            %calculates crevasse depths only if tensile stress >=
%tensile
            %strength (initial surface fracture present)
            if Rxx(I) >= TS;

                d_start = 1e-7; %initial fracture depth value above
%zero to ensure initiation
                d_increment = 1; %increment of crevasse depth
                d = d_start; %starting crevasse depth
                Ki = 1+Kic;  %starts at a value greater than Kic so
%while loop is run at least once

                %continues iterating through values of depth (thus,
%crevasse propagates as long as Ki > fracture toughness)until %Ki is
%equal to or less than the fracture toughness
                while (Ki > Kic);

                    %total depth of water in 1x1 after 24 hours
%(converted from rate of filling 'Q')
                    B(I) = Q(I)*t;

                    if i == 1;
                        %depth of water in crevasse on day 1 (adjusted
%for cell size and crevasse dimensions)
                        b(I,i) =
(B(I)*(cell_width*cell_width))/(crev_width*crev_length);
                    else
                        %cumulative depth of water head
                        b(I,i) = b(I,i-
1)+((B(I)*(cell_width*cell_width))/(crev_width*crev_length));
                    end
```

```
                    %continually solved for increasing values of depth
%until Ki <= Kic
                    Ki = (1.12*(Rxx(I)*(sqrt(pi*d))))-
(0.683*(Pi*(g*(d^1.5))))+(0.683*(Pw*(g*(b(I,i)^1.5))));

                    d = d + d_increment;
                end

                crevasse_depth(I) = d;

                %crevasse depth is zero for all cells with tensile
%stress < tensile strength
            else %Rxx(I) < TS
                crevasse_depth(I) = 0;
            end

            %melt is delivered to the bed when crevasse depth >= ice
%thickness
            if i == 1;
                if crevasse_depth(I) < H(I);
                    full_crevasses(I,i) = 0;
                    melt_to_bed(I,i) = 0;
                else %crevasse_depth(I) >= H(I)
                    full_crevasses(I,i) = 1;
                    %if crevasse reaches bed on day 1, first day of
%melt fill is routed to the bed
                    melt_to_bed(I,i) = ((Q(I))*t)*1000; %(converted
%back to mm w.e)
                end
            else
                if full_crevasses(I,i-1) == 1;
                    full_crevasses(I,i) = 1;
                    %if crevasse reached bed on a previous day, melt
%is transfered to bed on all subsequent days
                    melt_to_bed(I,i) = ((Q(I))*t)*1000;
                elseif crevasse_depth(I) >= H(I);
                    full_crevasses(I,i) = 1;
                    %when crevasse first reaches bed, all accumulated
%melt content drains
                    melt_to_bed(I,i) =
(b(I,i)*((crev_width*crev_length)/(cell_width*cell_width)))*1000;
                else %crevasse_depth(I) < H(I)
                    full_crevasses(I,i) = 0;
                    melt_to_bed(I,i) = 0;
                end
            end

        end


%*****************************************************************

        %'moulin' denotes any surface-to-bed connection (whether
%through lake drainage or a full ice thickness crevasse). A connection
%is formed when melt is first delivered to the bed and persists
%throughout the remainder of the modelled ablation season.

        if i == 1;
            if   melt_to_bed(I,i) == 0;
```

```
                moulin(I,i) = 0;
            else moulin(I,i) = 1;
            end
        else
            if   moulin(I,i-1) == 1;
                moulin(I,i) = 1;
            elseif melt_to_bed(I,i) == 0;
                moulin(I,i) = 0;
            else moulin(I,i) = 1;
            end
            if ice_limits(I) == 1;
                moulin(I,i) = 0;
            end
        end
    end


%*****************************************************************
*

    %reshapes runoff ratios to grid format (updated with any drained
%lakes)
    RR = reshape(RR,SIZE);

    %total melt generated at surface each day (mm w.e./day)
    tot_melt(i) = sum(daily_melt);

    %total meltwater (mm w.e./day) delivered to the bed through
%connections each day
    total_daily_melt_delivery(i) = sum(melt_to_bed(:,i));

    %convert melt to bed from specific discharge (mm w.e./day) to
%actual discharge (cumecs)
    melt_delivery_volume(i) =
(total_daily_melt_delivery(i)/1000)*(cell_width*cell_width); %converts
%from mm to m^3
    melt_delivery_discharge(i) = (melt_delivery_volume(i)/86400);
%convert to m^3/s

end

%total melt generated at surface over whole time period
total_generated_melt = sum(tot_melt);

%total meltwater delivered to the ice-bed interface over the whole
%time period
total_melt_to_bed = sum(total_daily_melt_delivery);

%percentage of surface melt reaching the bed over whole time period
percent_melt_to_bed = (total_melt_to_bed/total_generated_melt)*100;


%*****************************************************************

%data conversion for plotting and grid display


%creates an xyz file of E, N and moulin (all connections) formation
moulin_xyz(:,1)= eastings;
```

```
moulin_xyz(:,2)= northings;
moulin_xyz(:,3)= moulin(:,i);

%converts xyz locations of moulins (all connections) into grid format
xyzm = moulin_xyz;
xyzm = sortrows(xyzm,[1 -2]); %sort the rows by easting and then
%northing
heightm = sum(xyzm(:,1)==xyzm(1,1)); %grid height
widthm = sum(xyzm(:,2)==xyzm(1,2)); %grid width
moulin_grid = reshape(xyzm(:,3),heightm,widthm); %changes to grid
%format

%creates an xyz file of E, N and lake drainage
drainage_xyz(:,1)= eastings;
drainage_xyz(:,2)= northings;
drainage_xyz(:,3)= drained_lakes(:,i);

%converts xyz locations of total drainage events into grid format
xyzm = drainage_xyz;
xyzm = sortrows(xyzm,[1 -2]); %sort the rows by easting and then
%northing
heightm = sum(xyzm(:,1)==xyzm(1,1)); %grid height
widthm = sum(xyzm(:,2)==xyzm(1,2)); %grid width
drainage_grid = reshape(xyzm(:,3),heightm,widthm); %changes to grid
%format
```

Appendix 2. List of symbols

Symbol	Description (units)
a	Water level below the ice surface (m)
A	Temperature dependent flow law parameter (s^{-1} kPa^{-3})
A_c	Internal surface area of crevasse (m^2)
A_i	Ice surface area (m^2)
A_t	Total cell area (m^2)
α	Angle between azimuth and average flow direction (°)
b	Water level within a crevasse (m)
b_i	Depth below the ice surface (m)
B	Stiffness parameter (kPa $a^{1/3}$)
d	Crevasse depth (m)
$DDF_{i/s}$	Degree-day factor for ice/snow (mm w.e. d^{-1} °C^{-1})
e	Void ratio
$\dot{\varepsilon}_e$	Effective strain rate (s^{-1})
$\dot{\varepsilon}_{xx}$	Longitudinal strain rate (s^{-1})
$\dot{\varepsilon}_{xy}$	Shear strain rate (s^{-1})
$\dot{\varepsilon}_{yy}$	Transverse strain rate (s^{-1})
$\dot{\varepsilon}_{zz}$	Vertical strain rate (s^{-1})
g	Gravitational acceleration (9.81 m s^{-2})
H	Ice thickness (m)
K_I	Stress intensity factor (MPa $m^{1/2}$)
K_{IC}	Ice fracture toughness (kPa $m^{1/2}$)
M_t	Total daily melt (mm w.e.)
n	Glen's 'n' exponent
N	Number of days

ρ_i	Density of ice (918 kg m^{-3})
ρ_w	Density of water (1000 kg m^{-3})
Q	Rate at which water fills a crevasse (m hr)
R_{xx}	Tensile stress (Pa)
σ_{xx}	Longitudinal stress (Pa)
σ_{yy}	Transverse stress (Pa)
σ_v	Von Mises stress (Pa)
σ_1/σ_3	Principal, or 'maximum and minimum', stresses (Pa)
t	Time (hrs)
T_t	Mean temperature (°C)
τ_{xy}	Shear stress (Pa)
V_u	Measured velocity (m s^{-1})
V_x	Longitudinal velocity component (m s^{-1})
V_y	Transverse velocity component (m s^{-1})